Development and Characterization of Decellularized Rabbit Tracheal Cartilage Matrix for Use in Tissue Engineering

by

Paul Hong

Submitted in partial fulfillment of the requirements
for the degree of Master of Science

at
Dalhousie University
Halifax, Nova Scotia
August 2016

TABLE OF CONTENTS

LIST OF TABLES

LIST OF FIGURES

ABSTRACT

Reconstruction of large upper airway defects requires replacement tissue. Unfortunately, there is no widely available tracheal tissue substitute that can be used at this time. To overcome this limitation, tissue engineering approaches have been used to generate tracheal grafts. The objective of this study was to decellularize and characterize rabbit tracheal tissue with the aim of generating an extracellular matrix scaffold for tracheal tissue engineering.

Rabbit tracheal tissue was subjected to novel decellularization treatments. The decellularization processes involved cycles of modified enzymatic-detergent treatments. For characterization, decellularized and fresh specimens underwent histological, biochemical, and mechanical analyses. Scanning electron microscopy and biocompatibility assay were also performed.

The decellularization treatments resulted in significant reduction of genetic/cellular material. The glycosaminoglycan content of the extracellular matrix was not significantly altered in most cases. The effectiveness of decellularization was also confirmed on histological, immunohistochemical, and scanning electron microscopic analyses. Mechanical testing results showed that the tensile parameters were largely maintained after decellularization. Contact cytotoxicity assay showed that the decellularized extracellular matrix was biocompatible.

Overall, the decellularization treatments resulted in significant reduction of genetic/cellular material while preserving the underlying extracellular matrix structure. The tracheal extracellular matrix generated by decellularization has potential to be a viable scaffold material in tracheal tissue engineering.

LIST OF ABBREVIATIONS USED

2D	Two-Dimensional
3D	Three-Dimensional
α-Gal	Galactose-Alpah-1,3-Galactose
bFGF	Basic Fibroblast Growth Factor
BMSC	Bone Marrow Mesenchymal Stromal Cells
C-R	Crown-Rump
$CaCl_2$	Calcium Chloride
DEM	Detergent-Enzymatic Method
DMEM	Dulbecco's Modified Eagle Medium
DNA	Deoxyribonucleic Acid
ECM	Extracellular Matrix
EDTA	Ethylenediaminotetraacetic Acid
ESC	Embryonic Stem Cell
iPSC	Inducible Pluripotent Stem Cell
FBS	Fetal Bovine Serum
GAG	Glycosaminoglycan
H&E	Hematoxylin and Eosin
HEK	Human Embryonic Kidney
HEPES	4-(2-Hydroxyethyl)-1-Piperazineethanesulfonic Acid
HLA	Human Leukocyte Antigen
HRP	Horseradish Peroxidase
KCl	Potassium Chloride
KH_2PO_4	Potassium Phosphate
$MgCl_2$	Magnesium Chloride
$MgSO_4$	Magnesium Sulfate
MHC	Major Histocompatibility Complex
MSC	Mesenchymal Stem Cell
NaCl	Sodium Chloride
$NaHCO_3$	Sodium Bicarbonate
Na_2HPO_4	Sodium Phosphate
PBS	Phosphate Buffered Saline
PCU	Poly(Carbonateurea) Urethane
PCP	Porcine Cartilage Powder
Pen/Strep	Penicillin and Streptomycin
PGA	Polyglycolic Acid
PMSF	Phenylmethylsulfonyl Fluoride
POSS	Polyhedral Oligomeric Silsesquioxane
RNA	Ribonucleic Acid
rpm	Revolutions Per Minute
SDS	Sodium Dodecyl Sulfate
SEM	Scanning Electron Microscopy
TnBP	Tributyl Phosphate
TGF-β	Transforming Growth Factor-β
VEGF	Vascular Endothelial Growth Factor

ACKNOWLEDGEMENTS

I would like to express my gratitude to my supervisor Dr. Manohar Bance, whose guidance and friendship was essential to my growth as a researcher. I would like to thank my Supervisory Committee, Dr. Paul F. Gratzer and Dr. Kazue Semba for their mentorship and advice. Also, I thank my external examiner Dr. Boris Kablar for his support and valuable feedback on this thesis project.

I wish to express my gratitude to Dr. Samuel Veres for this help with the mechanical testing. The technical assistance of Karl Conlan and Melvin Kwok is also gratefully acknowledged. Finally, I would like to thank my family and my wife for their continuous support, encouragement, and understanding.

CHAPTER 1: INTRODUCTION

Trachea is a vital component of the upper airway. The two main functions of the trachea include airway passageway for ventilation and trapping and expelling unwanted inhaled substances via the mucociliary blanket that lines the tracheal lumen. When a large portion of the trachea is diseased or stenotic, replacement tissue may be required to reconstruct this crucial organ.

1.1 Embryology of the Human Trachea

There are two main developmental periods during the prenatal phase of human tracheal embryogenesis: the embryonic and fetal periods. The embryonic period is divided into 23 stages according to the Carnegie system defined by specific morphologic criteria. The laryngotracheal or respiratory diverticulum appears between the 4^{th} and 6^{th} pharyngeal arches (O'Rahilly and Boyden, 1973). At day 20, the laryngotracheal diverticulum, from which the respiratory system originates from, is positioned medially. At day 26, two lung buds arise from the laryngotracheal diverticulum, which then migrates caudally (tracheal bifurcation) into the mesenchyme ventral to the foregut. On day 28, the trachea and lung buds become more apparent as the respiratory tract, esophagus, and tracheoesophageal septum elongates. The respiratory and digestive tracts, separated by the tracheoesophageal septum, start developing independently at this time. As the fetal period begins [30 mm crown-rump (C-R) stage], the chondrocytes become identifiable within the rings of the trachea. The paries membranaceus shows primordium of the trachealis muscle, which contains spindle-shaped myoblasts with elongated nuclei. The epiglottis, thyroid cartilage, and the tracheal wall (hyaline cartilaginous rings) are better defined. A few days later (42-50 mm C-R stages), the circular trachealis muscle

becomes more noticeable but the tracheal glands are not yet identifiable in the submucosa. At 62 mm C-R stage, the circular muscle fibers of the trachealis muscle are attached to the inner surfaces of the cartilages; some longitudinal muscle fibers are also identifiable posterior to the circular layer. Both muscular layers are well defined at the 100 mm C-R stage. The elastic fibers, tracheal glands, and lymphocytes are still not observed in the submucosa or lamina propria; eventually, they become defined during the post-natal period (O'Rahilly and Tucker, 1973; O'Rahilly and Müller, 1984).

1.2 Anatomy and Function of the Human Trachea

The upper airway starts at the nasal cavity and extends down to the inferior limit of the trachea where it bifurcates into right and left main stem bronchi. Superiorly, the trachea is attached to the cricoid cartilage at the level of the 6^{th} cervical vertebra and ends at the level of the T4-T5 intervertebral disc in the thorax. The average length of the adult human trachea is 11-12 cm (Manoukian, 1997). The trachea not only functions as the 'windpipe' or a conduit for air movement and ventilation, but it also serves other roles such as trapping inhaled foreign dust/microorganisms and expelling them as phlegm via the mucociliary blanket and the ciliated respiratory epithelium (Neville and Bolanowski, 1979).

The trachea is composed of cartilaginous rings and membranous soft tissue (Figure 1.1). A cross section of the trachea can be described as ovoid with horseshoe-shaped incomplete cartilage rings positioned anterolaterally and membranous part completing the ring posteriorly, which is supported by the trachealis muscle (Wanner, 1979). The cartilage in the trachea is hyaline in nature and there are approximately 15-20 cartilaginous rings joined together by fibrous tissue and smooth muscle (Neville and Bolanowski, 1979). Some of the cartilage rings can be fused, either partially or

completely, with each other. Cartilage of the trachea provides the anterolateral rigidity but also provides flexibility; the posterior surface of the trachea is capable of allowing esophageal dilatation (i.e. passage of liquid or food). Perichondrium overlies the cartilage and is tightly adherent, and it is continuous with a thin sheet of connective tissue that forms the fibrous membrane between rings of cartilage (Wanner, 1979).

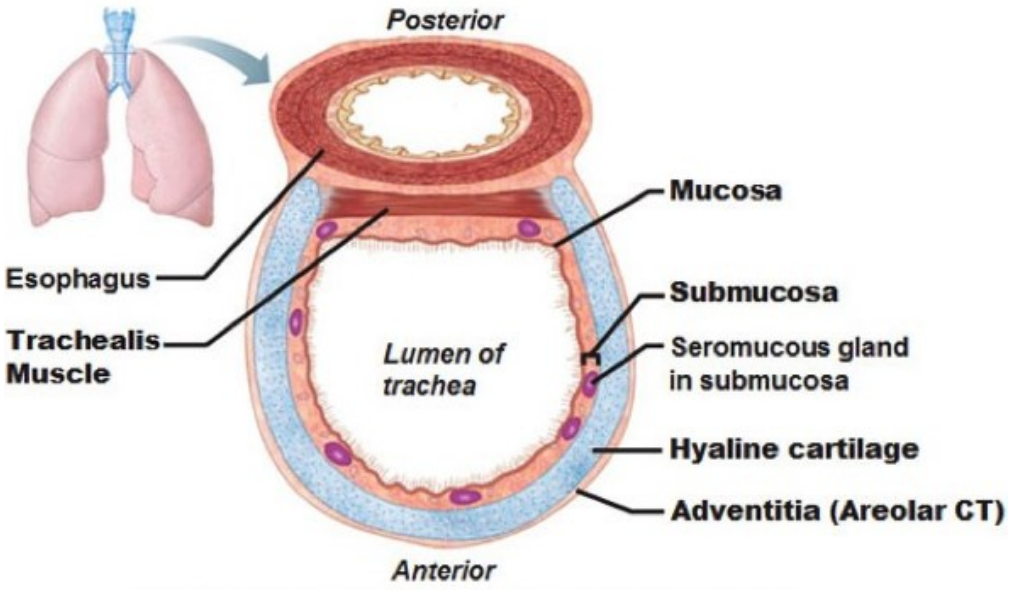

Figure 1.1. Cross section of the trachea and esophagus. Figure adapted from https://www.studyblue.com/notes/note/n/chapter-22/deck/3076552.

In the cervical region, the trachea is covered anteriorly by the infrahyoid muscles and the isthmus of the thyroid gland; the great vessels of the neck are found on the lateral aspect, while the esophagus is positioned posteriorly. The recurrent laryngeal nerve lies in the tracheoesophageal groove. In the thorax, trachea lies in the superior mediastinum, and is crossed anteriorly by the innominate artery, the aortic arch, and the left brachiocephalic vein (Horsfield, 1974).

The main function of the trachea is to serve as a channel for ventilation. Other related functions include clearing secretions, and warming, humidifying, and filtering the inspired air. The microanatomy of the tracheal lining consists of a pseudostratified ciliated columnar epithelium interposed with goblet cells, basal cells, and neuroendocrine cells. The submucosa contains elastin, submucous glands, and smooth muscles (Basbaum and Finkbeiner, 1988; Brigger and Boseley, 2012).

The blood supply to the trachea arises from the inferior thyroid, subclavian, innominate, supreme intercostal, internal thoracic, and superior and middle bronchial arteries (Horsfield, 1974). The arterial blood vessels come together to form networks along the lateral aspect of the trachea (transverse segmental blood supply). These blood vessels interconnect and feed the submucosal capillary network, which is highly arborized beneath the endotracheal mucosa. Venous drainage is through small tracheal veins that are connected to the inferior thyroid veins (venous plexus on the anterior surface of the thyroid gland isthmus), which drain into left and right descending veins. The descending veins enter their respective brachiocephalic veins (Horsfield, 1974).

Lymphatic drainage of the trachea involves pretracheal, paratracheal, and tracheobronchial groups of lymph nodes. The recurrent laryngeal nerve and the sympathetic nerve fibers, mostly from middle cervical ganglion, provide both sensory and motor innervation to the trachea (Riquet et al. 2002).

1.3 Clinical Problem

Upper airway obstruction can result from various tracheal lesions. Most common congenital lesions of the trachea include subglottic or tracheal stenosis, laryngotracheal clefts, and tracheomalacia (Prokakis et al. 2014; Mulliken and Grillo, 1968). Acquired causes of tracheal stenosis include iatrogenic trauma due to prolonged intubation or

tracheostomy, malignancy (e.g. head and neck or chest tumors invading the trachea), and connective tissue diseases that can cause chronic chondritis or perichondritis (Rubikas et al. 2014; Cotton, 1991).

If the tracheal disease is non-malignant, limited to the endotrachea, and does not involve a long-segment, endoscopic procedures may be able to manage the condition. For example, a thin subglottic stenosis (Figure 1.2) can be treated with endoscopic balloon dilatation procedure (Maresh et al. 2014). This avoids open surgery, which can be associated with more complications and slower recovery.

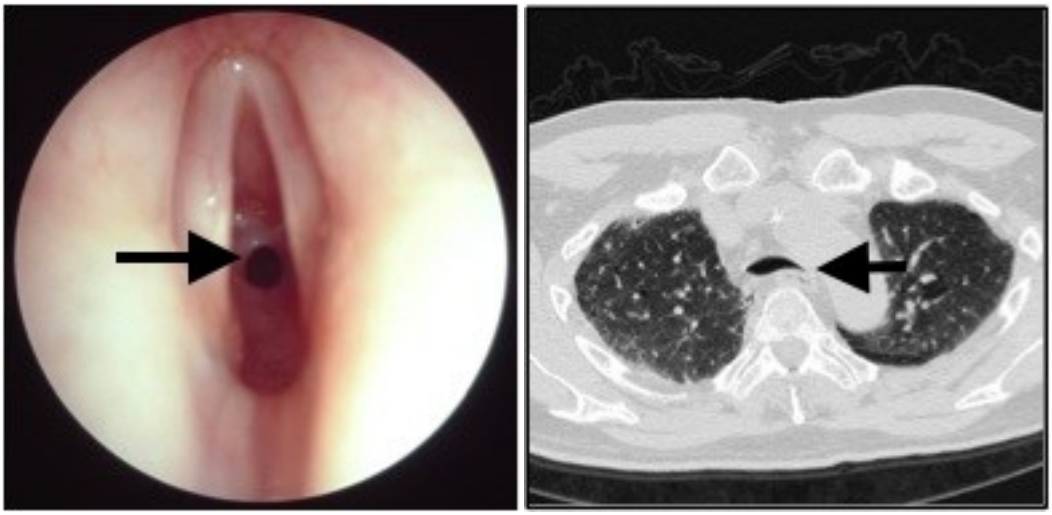

Figure 1.2. Examples of clinical problems that can necessitate reconstructive tracheal surgery. Endoscopic image of severe subglottic stenosis (left) and computed tomography scan image of tracheomalacia (right). Narrowed areas of the upper airway are shown with black arrows.

Other alternative surgical procedures such as cartilage grafting of the upper airway can be used for some tracheal diseases (Tojo et al. 1998). However, for severe diseases, these procedures have led to poor clinical results as they do not fully re-establish the tracheal luminal contour and regenerate normal respiratory epithelium concurrently

(Yu et al. 2011). Furthermore, reconstruction with autologous tissue can be limited by donor site morbidity.

Invasive, open reconstructive surgery may be necessary when treating more extensive tracheal diseases. In some cases, the stenotic or diseased portion of the trachea can be excised and the two remaining ends reapproximated primarily. However, when the defect is too long, end-to-end anastomosis may not be possible and a tracheal replacement is necessary. Short tracheal defects, up to 2 cm in length, may be closed primarily (Grillo, 2002; Belsey, 1950). Longer defects, up to 4 cm in length, may be reapproximated using neck flexion and release maneuvers to minimize tension at the anastomotic site. Generally, the length of the defect should be less than half of the entire length of an adult trachea (≈ 6 cm) or less than one-third in young children for primary anastomosis to be carried out safely (Asakura et al. 1997). However, higher anastomic complication rates are observed as the length of the tracheal defect increases (Mitchell et al. 1999; Mitchell et al. 2001). Furthermore, in patients with less flexible trachea (e.g. older patients with calcified trachea or patients who have received radiation therapy), primary anastomosis may be more challenging and the subsequent tension can lead to more complications. These patients may require procedures such as total laryngectomy and mediastinal tracheostomy, which are associated with high mortality rates. Therefore, reconstruction with a replacement tissue is needed for extensive tracheal diseases.

Non-viable cadaveric human tracheal allografts have been used both experimentally and clinically in humans as tracheal replacements, but in general they have produced disappointing results due to excessive host scar tissue development over time (Grillo and McKhann, 1964; Jacobs et al. 1996; Elliott et al. 1996). One exception was reported in two pediatric cases where the tracheal allograft reconstruction led to

somewhat encouraging short-term results for children with long-segmental congenital tracheal stenosis (Rose et al. 1979; Levashov et al. 1993). However, the growth potential of the tracheal allograft is unknown (and has not been reported) and long-term complications such as re-stenosis have been reported over time (Pacheco et al. 1954).

Viable (non-cadaveric) donor tracheal transplantation is also technically feasible but practically limited because of the need for tissue matching and long-term immunosuppression. Successful clinical tracheal allotransplantation was first published in 1950 (Jackson et al. 1950). However, this report involved only one patient and long-term follow-up was lacking (results at 9 weeks reported). Other cases of viable tracheal allograft transplantations have been reported but they have all required immunosuppressive therapy, in addition to invasive adjunctive procedures such as omental revascularization to cover the graft material (Harrington et al. 1977). Viable tracheal allograft transplantation without immunosuppressive therapy has been shown to result in graft ischemia and ultimately rejection of the transplant (Delaere et al. 2010). Even shorter segment transplants have resulted in graft necrosis and fibrotic stenosis (Belsey, 1950). Therefore, the mechanism of graft failure in these cases is thought to involve immunological mismatch and tissue loss from devascularization, reperfusion injury, and surgical trauma. Finally, as with any organ transplants, donor supply is always a concerning issue when considering the practicality of using viable tracheal transplants.

Recently, the Leuven Tracheal Transplant Group reported a case of partially successful tracheal allotransplantation without the need for long-term immunosuppressive therapy (Glowacki and Mizuno, 2008). Their method involved establishing revascularization by first implanting the allograft in a heterotopic position (the recipient's forearm). Although there was no explicit rejection upon withdrawal of perioperative

immunosuppressive therapy, parts of the allograft underwent avascular necrosis and scarring post-transplantation. Therefore, further studies are required to examine whether this approach has actual therapeutic potential.

CHAPTER 2: BACKGROUND

2.1 Tissue Engineering

Tissue engineering is an interdisciplinary field that combines the principles of life sciences and engineering. The basic approach to tissue engineering involves combining cells, scaffolds, and biologically active molecules, or combinations thereof, to promote repair and regeneration of tissue in hopes of replacing a defective body part or organ. Typically, tissue-specific source cells are expanded in vitro and seeded onto a scaffold material with appropriate signaling molecules. Ideally, the scaffold provides a structure and an environment where the source cells can attach, migrate, proliferate, and perform normal functions such as tissue-specific extracellular matrix (ECM) production. The bioactive signaling molecules (e.g. growth factors) serve to enhance the cellular function and overall tissue growth and maintenance (Badylak, 2007).

Tissue engineering techniques have demonstrated great potential in functional restoration of tissues and organs, and therefore may serve as a promising approach in tracheal reconstruction. A tracheal substitute must have the following two key requirements: 1) be rigid enough to maintain an open lumen (non-collapsible) but also be somewhat flexible longitudinally, and 2) possess an intact luminal/surface lining composed of ciliated respiratory epithelium (Badylak, 2005). The combined respiratory and secretory function of the trachea, along with its segmental blood supply, makes it challenging to regenerate and reconstruct this organ.

2.2 Scaffolds

One of the most important elements in tissue engineering is the scaffold material (Jungebluth et al. 2012). An ideal scaffold should demonstrate the following properties:

1) allow cell attachment and migration similar to native tissue; 2) promote cell viability and cell-specific function; 3) allow for the diffusion of nutrients and waste products; 4) undergo controlled degradation without inducing deleterious effects on the surrounding tissue; 5) maintain adequate size and mechanical integrity; 6) be biocompatible; and 7) be easily fabricated without being too costly (Badylak, 2007). A tissue engineering scaffold should provide a temporary milieu that mimic the native tissue microenvironment in order to promote healing or new tissue formation that will eventually replace the scaffold and become incorporated into the surrounding environment. Most scaffolds therefore contain porous architecture to allow cell colonization and migration, and as well, they provide temporary mechanical support. Ideally, the degradation rate of the scaffold should match the rate of new tissue formation or tissue healing, and the by-products of degradation should not elicit a chronic inflammatory response.

2.2.1 Synthetic Scaffolds

A wide range of synthetic and natural materials have been investigated as a possible scaffold in tracheal tissue engineering. Most synthetic scaffolds have been fabricated from biodegradable polymers because the mechanical properties and degradation characteristics can be easily modified (Fishman et al. 2011). In addition, other material properties such as porosity and microstructure can be controlled with various techniques. There are also no concerns associated with limited donor supply or risks of microorganism transfer.

Over the past two decades, novel synthetic materials generated with innovative processing techniques have provided (in combination with chondrocytes or stem cells) tissue engineered cartilage similar in appearance and characteristics to the human ear (Vacanti et al. 1992) and nasoseptal cartilage (Peulacher et al. 1994). There have been

other potential synthetic materials investigated for tracheal tissue engineering applications, such as peptides and ceramics (Fishman et al. 2011). However, most synthetic scaffolds to date have lacked the natural microarchitectural anatomic characteristics that truly mimic the native tracheal ECM. Other problems have been reported as well. By-products from polyglycolic acid led to a low pH environment and stimulated a toxic inflammatory response when transplanted (Britt and Park, 1998). Synthetic hydrogels have been found to demonstrate slow degradation rates, which can lead to uncontrolled long-term biological responses (Temenoff and Mikos, 2000).

More recently, two types of synthetic tracheal scaffolds have been tested in the clinical setting. First, a scaffold composed of propylene mesh tube covered with collagen sponge was tested in human subjects (Nomoto et al. 2012). The scaffold was seeded with autologous venous blood from recipients and was transplanted into four patients with severe stenosis or malignancy of the trachea. Long-term (3 years) bronchoscopic assessments revealed no evidence of rejection. However, mild dehiscence with air leakage occurred in one patient and the mucociliary function (i.e. normal respiratory epithelialization) of the new epithelium was not assessed (Omori et al. 2008).

The other synthetic tracheal scaffold used in a human subject was made using a polymer, polyhedral oligomeric silsesquioxane (POSS)-poly(carbonateurea) urethane (PCU) (Del Gaudio et al. 2014). Briefly, a long-segment circumferential trachea along with carina and main stem bronchi was fabricated from a nanocomposite polymer POSS covalently bonded to PCU polymer chains. The casted form was made into U-shaped cartilaginous rings and the coagulated form was used for the membranous part of the trachea. This nanocomposite material was then seeded with bone marrow stem cells and was transplanted into a patient with widespread cancer of the trachea. The scaffold was

found to be well integrated with patent anastomoses with no granulation tissue; the lining of the trachea was well vascularized but there was only partial epithelialization. Clinically, the patient was reported to be asymptomatic with no evidence of tumor recurrence at 5 months (Jungebluth et al. 2011). The authors concluded that the POSS-PCU polymer may be a viable scaffold material for tracheal tissue engineering. Yet, it should be mentioned that POSS-PCU has not been tested in many other areas, and for applications in esophageal tissue engineering, the epithelialization and neovascularization were not fully attained (Totonelli et al. 2012).

2.2.2 Natural Scaffolds

Even though advances have been made with synthetic tracheal scaffolds, there continues to be concerns about biocompatibility, unreliable epithelialization, and neovascularization. Therefore, some researchers have focused their attention on naturally derived scaffolds. Many natural materials such as collagen, gelatin, hyaluronic acid, fibrin, agarose, alginate, and chitosan, have been explored as bioactive scaffolds for cartilage engineering (Badylak, 2007; Vacanti et al. 1992). Although promising, there are concerns with immunogenicity and disease transfer when considering xenogeneic or allogeneic scaffolds, and some natural materials have mechanically inferior properties that are subject to premature host enzymatic degradation. More recently, derivatives of the ECM has shown potential as a viable scaffold material in tracheal tissue engineering. ECM is the product of resident cells of tissues and it serves structural, functional, and signaling roles. The main components of ECM are structural molecules such as collagen, elastin, proteoglycans, and glycosaminoglycans (GAGs) (Badylak, 2005; Badylak, 2007). Interestingly, ECM may serve as an ideal natural scaffold material and several studies have successfully utilized this concept in different parts of the body (Gilbert et al. 2006).

Tissue-specific ECM is typically produced by removing cellular/genetic material, a process commonly called *decellularization*. Natural scaffolds composed of tissue-specific ECM derived by decellularization has shown great promise, as it retains the essential structural and functional proteins of the original tissue, and repopulating the ECM with appropriate cells may lead to formation of the desired tissue or organ (Badylak, 2005). Naturally derived ECM can provide not only the physical support to cells but also the appropriate biological signals in promoting repair or formation of the original tissue (Badylak, 2005; Badylak, 2007).

2.2.3 Decellularization

Although many different decellularization techniques have been described to generate tracheal tissue engineering scaffolds, most have used some form of detergent-enzymatic method (DEM). Several studies have shown that decellularization is feasible with DEM as the final products are largely devoid of genetic material, and allows cell repopulation and new ECM production (Sutherland et al. 1996; Macchiarini et al. 2008). These are important characteristics since it confers biocompatibility and integration into host tissue. Consequently, decellularized scaffolds have been used in both pre-clinical animal studies and in humans with some success (Gilbert et al. 2006). There have been several studies that assessed decellularization of non-tracheal tissue to generate a suitable tracheal scaffold material. Walles et al. decellularized segments of jejunum, which were then seeded with chondrocytes, smooth muscle cells, respiratory epithelium, and endothelial progenitor cells (Walles et al. 2004). Chondrocyte proliferation along with extracellular cartilaginous matrix production were noted within 2 weeks of cell seeding, and the structure of the scaffold somewhat resembled native tracheal tissue. At the same time Macchiarini and colleagues created a tissue engineered tracheal patch using

decellularized porcine jejunum seeded with autologous muscle cells and fibroblasts (Macchiarini et al. 2004). After a 3 week incubation period in a bioreactor, the scaffold was used to reconstruct a tracheal defect in a 58-year old man. Postoperative bronchoscopic examinations revealed that the graft took well with no signs of chronic inflammation or granulation tissue formation. However, no long-term outcomes have been reported with non-tracheal decellularized scaffold-cell constructs. As well, concerns about the mechanical stability have not been fully addressed. Therefore, more research has been done on decellularizing tracheal tissue, rather than heterotopic donor tissues.

Jungebluth et al. used DEM to produce porcine tracheal matrices that did not possess any major histocompatibility complex (MHC) antigens, which were shown to maintain structural and functional integrity, similar to that of native tracheal tissue (Jungebluth et al. 2009). A total of 17 cycles (35 days) of repetitive DEMs was required to produce the sufficient immunogenicity profile to avoid rejection in animal models but the higher number of cycles was associated with less optimal mechanical properties. When implanted in human leukocyte antigen (HLA)-unmatched pigs and mice (allotransplantation and xenotransplantation, respectively), the constructs showed no histological signs of graft rejection after 30 days.

Perhaps, the most well known example of tracheal decellularization is the first human airway transplantation case reported in 2008, which received a great deal of press coverage (Macchiarini et al. 2008). Briefly, the authors generated a decellularized airway (mainstem bronchus) scaffold from a cadaveric donor through a lengthy DEM process. The scaffold was then repopulated with autologous epithelial cells and chondrocytes from a 30-year old female with complete collapse of her left main stem bronchus. After a period of ex-vivo incubation in a bioreactor, the cell-scaffold construct was transplanted

into the 30-year old patient and the authors reported successful take of the graft. No immunosuppression was required. However, long-term results are lacking and this method of decellularization was too long to be used consistently in the clinical setting.

Other studies have also shown that various DEM techniques are effective in decellularizing animal and human tracheae (Conconi et al. 2005; Baiguera et al. 2012). Overall, the DEM strategy has produced scaffolds that avoid the issue of allorejection and xenorejection in animal models and in some humans, thereby obviating the need for immunosuppression (Macchiarini et al. 2008; Jungebluth et al. 2009). This success is most likely due to the similar characteristics of decellularized scaffolds in terms of their microanatomic environment. The improved cell adhesion and migration, along with angiogenesis and ECM formation is most likely due to the influence of the remaining resident peptides, growth factors, and cell adhesion molecules on the decellularized matrix, and by the presence of factors that primary and stem cells may recognize in their natural environment (Gilbert et al. 2007).

Overall, decellularizing trachea to develop a suitable scaffold material seems to be the most promising strategy in tracheal tissue engineering to date. However, there are still significant concerns regarding long-term stability, structural/mechanical characteristics, and the intensive and prolonged DEM procedure required to generate decellularized tracheal scaffolds. That is, the repeated cycles of DEM treatments required to remove cellular material in many decellularization protocols have led to reduction in mechanical stability, mainly through the loss of GAGs (Haykal et al. 2012). These changes can lead to scaffold collapse and subsequent airway stenosis (Ma et al. 2013). Therefore, it is crucial to find the right balance between treating the tissue sufficiently to confer non-immunogenicity while trying to maintain the biomechanical integrity.

2.3 Cells

Cells utilized in tissue engineering can come from many different sources, including autologous, allogeneic, xenogeneic, or syngeneic. Ideally, the cells should be highly proliferative, easy to harvest, and non-immunogenic to the host.

Although fully differentiated (primary) autologous cells are the most desirable in regards to biocompatibility and to avoid pathogen transmission, there are drawbacks that need to be considered. In particular, developing a construct with primary cells usually requires taking a biopsy from the patient, which may cause pain and morbidity at the donor site. For harvesting chondrocytes, the supply can be limited and the donor site defect may not fully regenerate and lose their function due to the inherent poor healing capacity of cartilaginous tissues. As well, due to the low yield rates, isolated chondrocytes must undergo expansion, during which they may lose their function and undergo dedifferentiation or become another cell type (Walles et al. 2004; Komura et al. 2008). Due to these challenges, some researchers have focused their attention on stem cells as potential source cells.

Embryonic stem cells (ESCs) have an immense regenerative capacity as they have the ability to develop into all three germ layers and their subsequent tissues. However, the risk of tumor formation, possibility of immunological rejection, and ethical dilemmas, have made its use limited. Mesenchymal stem cells (MSCs) have also shown some potential for cartilage tissue engineering. Specific differentiation can induce MSCs into a variety of connective tissue cell phenotypes, including chondrocytes. MSCs can also be genetically engineered to express specific genes and proteins, and they have the advantage of not forming tumors when implanted in vivo in an undifferentiated state. Adult MSCs have already proven their safety and efficacy in several phase I and II human

clinical trials (Lee et al. 2008). However, MSCs typically requires harvesting from bone marrow and expansion/differentiation in vitro. Consequently, there are concerns regarding donor site morbidity and dedifferentiation (Lee et al. 2008).

The relatively recent discovery of inducible pluripotent stem cells (iPSCs) is also showing promise as their use avoids the ethical issues that come with using ESCs. The iPSCs are initially well differentiated cells but have been reprogrammed into a progenitor or stem cell (Zhou et al. 2009). And although iPSC has shown promise, there are drawbacks related to the genetic and epigenetic alterations required for adult cells to become multipotent or pluripotent. The clinical safety in terms of viral infection (viral vectors), tumor genesis, or immunogenicity, has not been fully established (Takahashi et al. 2006; Zhou et al. 2009). In addition, iPSCs have been shown to have some 'memory' of their former cell phenotype and may not always fully function as their reprogrammed cell type (Kim et al. 2010). However, new advances may reduce some of these concerns since the number of inducible genes required for iPSCs formation is decreasing. Furthermore, it may now be possible to generate iPSCs without any genetic alteration of the adult cell. For instance, Zhou et al., induced pluripotency by performing repeated treatment of adult primary cells with certain recombinant proteins channeled into the cells via poly-arginine anchors (Zhou et al. 2009).

For tracheal tissue engineering, two major types of cells are required: respiratory epithelial cells and chondrocytes. Resident tracheal epithelial cells are found along the basal layer, which can be isolated, cultured, and differentiated in vitro (Gray et al. 1996; Yoon et al. 2000; Sachs et al. 2003). However, harvesting these cells requires an invasive procedure with bronchoscopic guidance or open approach under general anesthesia. Therefore, nasal epithelial cells have been used most commonly but in vivo, they have

not effectively reproduced the pseudo-stratified columnar epithelium with functioning cilia that is found in tracheal lining. This has led to abnormal mucociliary clearance and post-transplant infections (Berg et al. 2013). Consequently, exogenous cells that can be used for epithelial regeneration, such as ESCs, iPSCs, and cells of mesenchymal origin such as MSCs, human amniotic fluid fetal stem cells, and umbilical blood cord-derived stem cells, is being studied more extensively (Chistiakov, 2010). Regardless of the origin of the source cells, optimization of epithelial cell cultures and differentiation protocols is still required in order to produce large quantities of fully functional cells for airway tissue engineering.

Primary chondrocytes have also posed challenges in terms of harvesting and expansion. Autologous sources of chondrocytes include nose, ears, and ribs, which have all been isolated and expanded in vitro in both monolayer and three-dimensional (3D) cultures systems (Walles et al. 2004; Komura et al. 2008; Gong et al. 2011; Hong et al. 2012; Weidenbecher et al. 2008). Despite the formation of a well-vascularized neo-trachea with primary chondrocytes, there are still concerns about the reduced mechanical strength and the fibrous (and not hyaline) nature of the regenerated cartilage tissue (Igai et al. 2007; Igai et al. 2006). Allogeneic chondrocytes have been extensively studied in articular joint cartilage tissue engineering, but it has not been applied to tracheal cartilage regeneration as exogenous non-tracheal (autologous) source cells are now deemed to be the safer alternative and better option for cell amplification. Mainly, these include autologous MSCs and iPSCs (Iamizumi et al. 2013). Currently, autologous bone marrow-derived MSCs are the most commonly utilized cell type in clinical applications of tracheal tissue engineering. They are readily accessible with no potential for rejection and can lead to high cell yield (Giordano et al. 2007). While iPSCs have been made to

undergo differentiation into functional airway cells (Mou et al. 2012; Wong et al. 2012), the necessary use of external growth factors and proteins associated with iPSCs to date is very costly. As mentioned above, newer research suggest that iPSCs may be generated on a more cost-effective basis with physical stress or chemical strain induction, rather than growth factors and gene transduction, but this research is in its infancy (Zhou et al. 2009).

2.4 Bioreactors

Earlier work in tissue engineering usually involved standard monolayer static cell culture conditions for most in vitro studies. The in vivo environment is however quite different as cells are in a 3D dynamic surrounding. To recapitulate this milieu, bioreactors have been used instead of traditional culture conditions. Bioreactors are tissue culture devices that enable the production of 3D constructs and provide optimal physiological environment for cell adhesion, proliferation, and differentiation by provision of flow of nutrient and the provision of mechanical regulatory cues, such as directly applied compression or strain mimicking conditions of growing or functioning organ (Tan et al. 2006; Freed et al. 2006). Their operational conditions can be manipulated, such as pH, temperature, oxygen tension, and nutrient supply. Several bioreactors have been described for tracheal tissue engineering (Asnaghi et al. 2009; Lin et al. 2009; Miller et al. 2010; Vunjak-Novakovic et al. 1999), and in general they have shown favourable results compared to static two-dimensional (2D) culture conditions. For instance, Vunjak-Novakovic et al. showed that hydrodynamic conditions in convective-flow tissue culture bioreactors improved the quality of tissue engineered cartilage in terms of composition, morphology and mechanical properties, compared to standard monolayer culture conditions (Vunjak-Novakovic et al. 1999). In fact, most recent tracheal tissue engineering studies have all used bioreactors and a commercial version of a tracheal

bioreactor (Harvard Bioscience, Boston, MS) currently exists. Other major advantages of using bioreactors in tracheal tissue engineering are the highly efficient cell seeding and uniform cell distribution throughout the scaffold material, and the provision of co-culturing chondrocytes and respiratory epithelial cells (Fishman et al. 2011). A widely cited example of a tracheal tissue engineering bioreactor is shown in Figure 2.1.

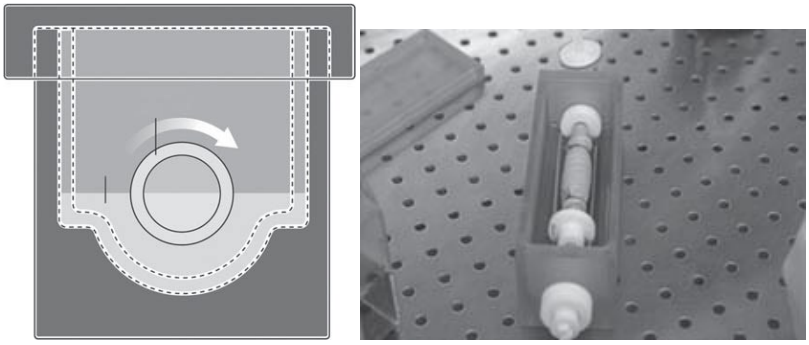

Figure 2.1. Bioreactor for tracheal tissue engineering. The top part of the bioreactor is exposed to air, while the bottom part is immersed in a culture medium. The construct composed of cells and scaffold is slowly rotated along the air-medium interface. This allows viability of both chondrocytes and epithelial cells. Figure adapted from Macchiarini et al. 2008.

The rotation of the cell-scaffold construct in the bioreactor is thought to provide the hydrodynamic shear stress necessary to promote appropriate differentiation and function of the seeded cells (Macchiarini et al. 2008). The exposure to air recapitulates the environment of the mature epithelial cells, while the culture medium aids both chondrocyte and epithelial cell differentiation, function, and viability. This tracheal construct was transplanted into a human subject and the endoscopic examination demonstrated good healing with minimal inflammation at 2 months postoperatively (Asnaghi et al. 2009). However, the epithelial layer was found to be discontinuous on microscopic analysis and the mucociliary clearance mechanism was not fully

reestablished. Therefore, further work to improve the epithelial coverage of the tracheal lumen is required and can be an important consideration for future refinements of bioreactors for upper airway tissue regeneration.

To avoid some of the drawbacks associated with bioreactors, which include high costs, long-lasting cell seeding period, possible risk of cell differentiation instability, and contamination, some researchers are now turning their attention to in situ or in vivo tissue engineering in which the patient can serve as their own natural bioreactor (Kajbafzadeh et al. 2015). Natural bioreactors have shown some positive results in both animal and human subjects. A very recent pre-clinical study reported on decellularized rat trachea, which was implanted between the paravertebral muscles of nude mice to act as a natural bioreactor for total graft recellularization (Kajbafzadeh et al. 2015). After ensuring that the decellularization process was effective, the scaffolds were implanted for 1-12 months before they were harvested and characterized for recellularization by staining for various cell markers. At 12 months, the histological examination demonstrated well organized cell repopulation in both cartilage and membranous tissues. The authors concluded that natural bioreactors can recellularize DEM treated tracheal scaffolds, which may facilitate homologous transplantation in the future.

2.5 Summary of the Current State of Tracheal Tissue Engineering

Many tracheal replacement strategies have been reported, including cell-free artificial prostheses (Okumura et al. 1994; Omori et al. 2005; Tatekawa et al. 2010), autografts (Fabre et al. 2013), decellularized allografts seeded with the recipient's own cells (Jungebluth et al. 2012), and autologous de novo tissue engineered constructs (Vacanti et al. 1994; Kunisaki et al. 2006). In spite of the various approaches, limitations persist, which prohibit tracheal tissue engineering to be routinely used in the clinical

setting. Acellular tracheal prostheses can often result in granulation tissue formation, implant migration/extrusion, progressive fibrosis, and stenosis of the airway lumen (Grillo, 2002). Autografts and allografts are often limited by availability, poor mechanical properties, and their propensity to undergo remodeling upon implantation, which can lead to fibrosis, collapse, and airway stenosis (Grillo, 2002; Fabre et al. 2013). As well, there is a risk of disease transmission and immunogenicity/rejection with allogeneic grafts, and therefore diligent removal of antigens must be conducted when decellularizing non-autologous tissue. Tissue engineering constructs comprised of autologous cells circumvent immunogenicity and possibility of rejection, but the structural and biomechanical properties of the scaffold must be cautiously devised to promote cell adhesion, migration, and neo-tissue formation.

To date, tissue engineered tracheae have been successfully implanted in a small number of patients on compassionate grounds. However, long-term remodeling and outcome remain largely unknown. Overall, decellularizing trachea to develop a suitable scaffold material seems to be the most promising strategy in tracheal tissue engineering. However, there are still significant concerns regarding long-term stability and structural/mechanical characteristics of the decellularized product. As well, tracheal decellularization protocols reported to date are labour-intensive and they require too many steps. In fact, published protocols usually takes weeks to months to complete. Such process is inappropriate and unworkable for prospective manufacturing in emergency clinical situations when a graft material may be required within a certain time. Clearly, more work is needed to reduce the time and cycles required for effective and practical decellularization of tracheal tissue.

2.6 Research Objectives

The main goal of this study was to develop a naturally derived tissue engineering scaffold by decellularizing rabbit tracheal tissue. Ideally, the scaffold will lack cells and genetic material that can elicit immunogenic reaction, while maintaining the structural and mechanical properties of the native ECM that is required for recellularization and function.

The New Zealand white rabbit was chosen as the animal model since the size and dimensions of the rabbit trachea is similar to a neonatal human trachea. As well, many previous tracheal tissue engineering studies involved New Zealand white rabbits.

Decellularization protocol previously developed in our laboratory was used to treat rabbit tracheal tissue. This protocol was optimized for human skin. Therefore, modifications to the protocol were made to potentially enhance the decellularization process for rabbit tracheal tissue. The resulting decellularized tissue then underwent various characterization studies to determine the effectiveness of the decellularization process. The specific objectives are as follows:

1. To develop a naturally derived tissue engineering ECM scaffold by decellularizing rabbit tracheal tissue that is devoid of cells and genetic material.
2. To develop a naturally derived tissue engineering ECM scaffold by decellularizing rabbit tracheal tissue that retains GAGs and mechanical properties.
3. To develop a naturally derived tissue engineering ECM scaffold by decellularizing rabbit tracheal tissue that is biocompatible.
4. To develop a naturally derived tissue engineering ECM scaffold by decellularizing rabbit tracheal tissue that has the potential to be repopulated with cells and implanted in in vivo models.

2.7 Research Hypotheses

The main hypothesis of this study is that an efficient decellularization process can be optimized to produce a scaffold material suitable for tissue engineering applications. Specifically, we hypothesize the following:

1. Decellularization treatment of rabbit tracheal tissue will significantly reduce the DNA content.
2. Decellularization treatment of rabbit tracheal tissue will not significantly change the GAG content.
3. Decellularization treatment of rabbit tracheal tissue will demonstrate removal of cells on histological and immunohistochemical analyses.
4. Decellularization treatment of rabbit tracheal tissue will not alter the histoarchitecture of the ECM on histological analysis.
5. Decellularization treatment of rabbit tracheal tissue will not significantly reduce the mechanical properties on tensile testing.
6. Decellularization treatment of rabbit tracheal tissue will not significantly alter the ultrastructure of the ECM on scanning electron microscopy.
7. Decellularized rabbit tracheal tissue will demonstrate biocompatibility on contact cytotoxicity assay.

CHAPTER 3: METHODS

3.1 Tissue Retrieval

Fresh trachea from adult male New Zealand white rabbits weighing 3.0-3.5 kg (Charles River Laboratories, St. Constant, Québec) were harvested at the Carleton Animal Care Facility under sterile condition. The animals were sacrificed using pentobarbital sodium (2 ml/4.5 kg) injections (Comparative Medicine Animal Resource Centre at McGill University, Montréal, Québec). The rabbits were placed in supine position with the neck extended. A midline sagittal incision was made from mid-hyoid region superiorly to the thorax inferiorly. Blunt dissection was carried out to expose the laryngotracheal complex. All overlying soft-tissues and the posteriorly positioned esophagus were carefully removed to generate an isolated, intact laryngotracheal complex (Figure 3.1); the superiorly positioned larynx was removed, leaving only the trachea. Each trachea was then divided along the transverse plane to produce two to three ring segmental units; half of the specimens served as fresh (native or control) tissue and the other half underwent decellularization.

The study protocol pertaining to the use of animal tissue was approved by the Dalhousie University Committee on Laboratory Animals (Protocol Number: I15-09).

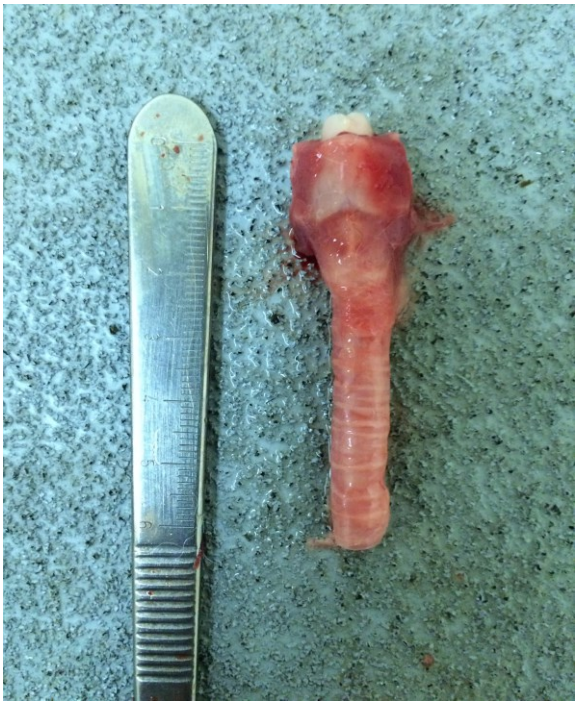

Figure 3.1. A laryngotracheal tissue harvested from a New Zealand white rabbit. The superior part includes the larynx (thyroid and cricoid cartilages, epiglottis, cricothyroid membrane, true and false vocal folds, and posterior glottis), which was removed to generate isolated tracheal tissue.

3.2 Decellularization of Rabbit Trachea

The initial decellularization technique followed a patented procedure developed in our laboratory [PCT/IB2011/001538], which was optimized for human skin. This process involved an automated software controlled set-up containing solenoids and peristaltic pumps, which allowed for specific solutions to be dispensed into a dish containing the tissue to be decellularized at specified times (Figure 3.2). Another pump was utilized to remove the solutions after the tissue was treated for appropriate amount of time. Each step (see below) of the decellularization process could be modified through the computer program (e.g. increased exposure time to Solution A). The specimen dish was placed on a shaker table, which provided continuous agitation to allow the solutions to constantly mix with the tissue. The dish and the shaker table were housed in a temperature-controlled

closed chamber (Figure 3.2).

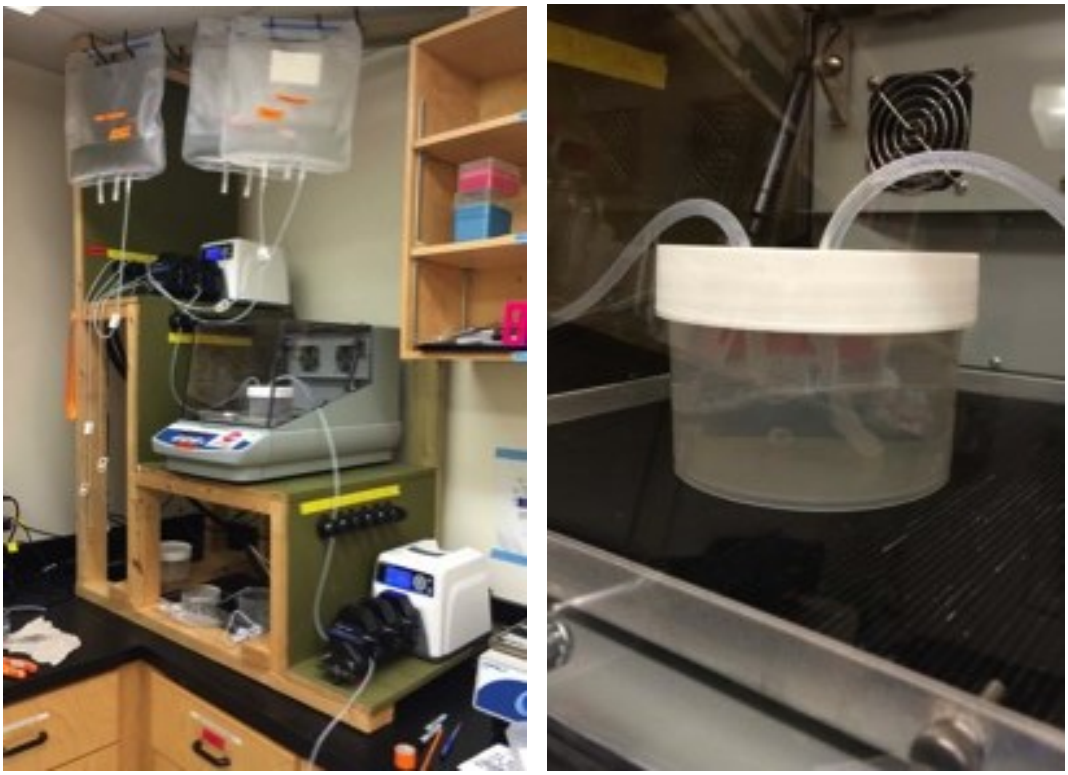

Figure 3.2. Decellularization set-up during a practice run. Left panel shows solution bags hanging with dispensing tube going through pumps into the specimen dish. There is also a tube to remove the solution. Right panel shows tracheal tissue in the specimen dish, which is on a shaker table housed in a temperature-controlled chamber.

Generally, the decellularization process used in this study involved cycles of hypo- and hyper-osmotic solutions, chemicals, enzymes, detergents, and solvent solutions, which were interspersed with washing steps to remove residues from previous steps (Table 3.1). All chemicals and reagents were obtained from Sigma-Aldrich Canada, Oakville, Ontario, unless otherwise specified.

Table 3.1. Summary of the decellularization process in sequential order of each solution with its respective contents, notes, and purpose of inclusion.

Solution A	
Contents Trizma base Ethylenediaminotetraacetic acid (EDTA) Phenylmethylsulfonyl fluoride (PMSF) Penicillin and streptomycin (Pen/Strep)	**Proposed Action** Hypotonic solution → water absorption and cell lysis PMSF (serine protease inhibitor) and EDTA (metalloprotease inhibitor) → prevent tissue degradation of proteases Basic pH → prevent the action of non-specific proteases Pen/Strep → antimicrobial
Notes pH 8 Room temperature 9 hours	

Solution B	
Contents Trizma base EDTA Potassium chloride (KCl) Triton X-100 Pen/Strep PMSF	**Proposed Action** Triton X-100 (non-ionic surfactant) → removes cell membranes and cytoskeletal components Hypertonic solution → solubilize and extract proteins
Notes pH 8 Room temperature 12 hours	

Hanks' Physiological Buffer	
Contents Sodium chloride (NaCl) KCl Sodium phosphate (Na_2HPO_4) Potassium phosphate (KH_2PO_4) Sodium bicarbonate ($NaHCO_3$)	**Proposed Action** Hanks' buffer and DNAse/RNAse → degrade DNA and RNA, to facilitate their subsequent removal Neutral pH → enable these enzymes to work

4-(2-hydroxyethyl)-1-piperazineethanesulfonic acid (HEPES) Calcium chloride ($CaCl_2$) dihydrate Magnesium sulfate ($MgSO_4$) heptahydrate Magnesium chloride ($MgCl_2$) hexahydrate DNAse and RNAse	
Notes pH 7.35 37°C DNAse and RNAse is added midway through this step 5.5 hours	

Solution C	
Contents 70% Ethanol Trizma base Tributyl phosphate (TnBP) Pen/Strep	**Proposed Action** TnBP (surfactant like solvent) → removes remaining cellular components (cytoskeletal proteins, cell membrane debris, DNA, RNA)
Notes pH 9 Room temperature 12 hours	

pH 9 Solution	
Contents Trizma base Pen/Strep	**Proposed Action** Buffered solution → removes residual or bound surfactant from the tissue
Notes pH 9 Room temperature 22 hours	

1% Peracetic Acid

Contents 100% Ethanol Peracetic acid	**Proposed Action** Peracetic acid → reduce the bioburden and deactivate viral proteins
Notes Room temperature 4 hours	

Phosphate Buffered Saline (PBS)	
Contents NaCl KCl Na_2HPO_4 KH_2PO_4 Pen/Strep	**Proposed Action** PBS → a final wash to remove residual peracetic acid and to return tissue to normal physiological conditions
Notes pH 7.4 Room temperature 19 hours	

The tissue samples were immersed in 500 ml of decellularization treatment solutions on a constant basis, except during times when a new solution was introduced. The time in between solutions (e.g. Solution A → Solution B) was brief since the following solution was immediately introduced when the preceding solution was removed via the pumps.

The specific make-up of each solution was as follows:

- Solution A: 2.41 g of Trizma base, 2.92 g of EDTA, 1.5 ml of Pen/Strep, and 105 µl PMSF in 2 L of distilled water
- Solution B: 12.12 g of Trizma base, 223.66 g of KCl, 2.92 g of EDTA, 20 ml of Triton X-100, 1.5 ml Pen/Strep, and 105 µl PMSF in 2 L of distilled water

- Solution C: 12.12 g of Trizma base, 20 ml of TnBP, and 1.5 ml of Pen/Strep in 2 L of 70% ethanol
- Hanks' Solution: 16 g of NaCl, 0.8 g of KCl, 0.074 g of Na_2HPO_4, 0.12 g of KH_2PO_4, 0.70 g of $NaHCO_3$, 5.20 g of HEPES, 2.44 g of CaCl dihydrate, 0.10 g of $MgSO_4$ heptahydrate, and 0.10 g of $MgCl_2$ hexahydrate in 2L of distilled water
- pH 9 solution: 12.12 g of Trizma base and 1.5 ml of Pen/Strep in 2 L of distilled water
- DNAse: 0.175 g of NaCl, 10 ml of glycerol in 10 ml of distilled water; 200,000 units of DNAse in 15 ml NaCl/glycerol solution; 665 µl added to tissue sample
- RNAse: 0.03 g of Trizma base, 0.22 g of NaCl in 25 ml of distilled water; 250 mg of RNAse protein in 20 ml of Trizma/NaCl solution; 665 µl added to tissue sample

After treatment, the samples were retrieved and subjected to various characterization studies to assess the effectiveness of the decellularization process. They included macroscopic examination, histological and immunohistochemical analyses, biochemical tests, scanning electron microscopy (SEM), mechanical testing, and biocompatibility assay (see below for details).

3.3 Modification of the Decellularization Process

It is to be noted that the abovementioned decellularization protocol has been optimized for human skin. Therefore, modification of the protocol was carried out in an attempt to improve the decellularization process for rabbit tracheal tissue (depending on

initial results).

There were several steps in the decellularization process that could have been altered to potentially change the characteristics of the resulting ECM scaffold. Mainly, they include adjusting the conditions (e.g. temperature, agitation, pH) or modifying the treatment solutions/reagents (e.g., adding different chemicals or reagents, increasing/decreasing concentrations of reagents, increasing/decreasing duration of exposure). Ideally, all or most of these variables would have been individually and separately assessed; however, considering the results of our previous work decellularizing cartilage tissue [porcine auricular cartilage (manuscript in preparation); human nasoseptal cartilage (Graham et al. 2016)], only the most relevant variables were considered for modification. Specifically, the length of exposure to Solutions A, B, and C was adjusted as they were deemed to have the most influence on the decellularization process (Table 3.2). Solution A is an overall hypotonic solution designed to cause cell lysis via water absorption; therefore, longer exposure time may lead to more cell lysis. Solution B is an overall hypertonic solution intended to solubilize proteins and remove cellular components, after cell lysis, via the non-ionic surfactant; therefore, longer exposure time may result in more cellular/genetic debris being removed from the tissue. The major role of Solution C is to remove remaining cellular components; therefore, increased exposure may lead to less residual cellular/genetic components.

Table 3.2. Summary of modification of the decellularization protocols.

	Protocol DC2a	**Protocol DC2b**	**Protocol DC2c**	**Protocol DC2d**	**Protocol DC2e**
Solution A	9 hours	18 hours	9 hours	9 hours	18 hours
Solution B	12 hours	12 hours	24 hours	12 hours	24 hours
Solution C	12 hours	12 hours	12 hours	24 hours	24 hours

All other solutions remained constant.

Protocol DC2a has the same exposure times to Solutions A, B, and C as the original protocol optimized for human skin. Protocol DC2b has exposure time that is twofold higher for Solution A; Protocol DC2c has exposure time that is twofold higher for Solution B; and Protocol DC2d has exposure time that is twofold higher for Solution C. Protocol DC2e has exposure times that is twofold higher for Solutions A, B, and C.

In addition to adjusting the exposure times to Solutions A, B and C, a change in physical method of tissue handling was introduced to assess its effect on decellularization. Specifically, the tracheal samples were subjected to three cycles of dry freeze-thaw maneuvers before initiating the original decellularization process. This modification was chosen because previous studies have reported increased cell lysis with freeze-thaw techniques (Stapleton et al. 2008). The fresh samples were placed in a -80°C freezer for 3 hours and then the tissue was allowed to thaw at room temperature for 4 hours (Stapleton et al. 2008); this was repeated three times. Afterwards, the tracheal tissue underwent DC1 decellularization treatment.

3.4 Biochemical Analysis

Biochemical analysis was performed to determine the effectiveness of the

decellularization process. Decellularized and the corresponding fresh tissues were freeze dried, weighed in duplicate, and then digested in 200 mg/ml of working papain digest solution at 64°C for 48 hours to solubilize the cartilage tissue. The working papain digest solution was prepared by dissolving 10 mg papain in 10 ml of papain digest solution, which was made from dissolving 0.272 g ammonium acetate, 0.038 g disodium EDTA dihydrate, and 0.031 g DL-dithiothreitol in 90 ml of distilled water (all from Sigma-Aldrich).

The DNA content was measured using the Quant-iT PicoGreen® dsDNA Assay Kit (Life Technologies, Grand Island, NY) and normalized to the initial dry weight of the tissue. High range (for fresh tissue) and low range (for decellularized tissue) sets of DNA standard solutions were made to generate standard DNA curves (Tables 3.3 and 3.4). The DNA standard solutions were made by mixing 500 mg of DNA sodium salt from calf thymus (Sigma-Aldrich) and 1 ml of 1X TNE buffer solution (1.21 g Trizma base, 3.7 g EDTA di-sodium salt, and 116.9 g of NaCl in 1 L of distilled water at pH 7.4; filtered using a Nalgene™ 75 mm filter unit).

The sample solutions were composed of the following: 1) 50 µl of the working papain digest solution containing solubilized fresh (control) tissue in 950 µl of 1X TNE buffer solution, and 2) 100 µl of the working papain digestion solution containing solubilized decellularized tissue in 900 µl of 1X TNE buffer solution.

In darkness, 100 µl Quant-iT PicoGreen® dsDNA reagent was added to 19.9 ml of 1X TNE buffer solution; 1 ml of this solution was then added to all standards and specimen samples. After mixing on the shaker table for 5 minutes at 450 rpm, 200 µl aliquots of standards and samples were placed in a black 96 well microplate in duplicates.

The microplate was then placed in a Tecan microplate reader (Tecan US, Inc., Morrisville, NC) and absorbance was read at the appropriate wavelengths [excitation 485 nm and emission 535 nm]. A standard curve was generated using the DNA standard solution absorbance measurements; the absorbance measurements of the sample solutions were then used to determine the DNA content of both fresh and decellularized specimens.

Table 3.3. Volume preparation of standards for high range DNA standard curve with final DNA concentration.

2 μg/ml DNA Standard (μl)	1X TNE (μl)	[DNA] (ng/ml)
0	1000	0
10	990	10
100	900	100
500	500	500
1000	0	1000

Table 3.4. Volume preparation of standards for low range DNA standard curve with final DNA concentration.

50 ng/ml DNA Standard (μl)	1X TNE (μl)	[DNA] (ng/ml)
0	1000	0
10	990	0.25
100	900	2.5
500	500	12.5
1000	0	25

The GAG content was quantified using the same papain digested solution with the Blyscan™ Sulfated GAG assay kit (Biocolor Life Science Assays, Carrickfergus, UK) and normalized to the dry weight of the samples. Standard calibrator GAG solutions were prepared as shown in Table 3.5. Fresh and decellularized sample solutions were prepared in duplicates by combining 60 μl of the working papain digestion buffer containing the tissue specimens and 40 μl of papain digestion buffer only. To all standards and sample solutions, 1 ml of Blyscan™ GAG assay dye reagent was added; all tubes were placed in

a microcentrifuge rack to be mixed on a shaker table for 30 minutes at 450 rpm. Next, the standards and samples were centrifuged for 10 minutes at 10,000 rpm. Supernatant was carefully discarded and the pellet was resuspended in 1 ml of Blyscan^{TM} GAG assay dye dissociation reagent. Similar to above (DNA content measure), 200 µl aliquots of standards and samples were placed in a clear 96 well microplate in duplicates; the microplate was then placed in the Tecan microplate reader. The GAG absorbance was read at the wavelength of 650 nm, and a standard curve was used determine the GAG content of both fresh and decellularized samples.

Table 3.5. Volume preparation of standards for GAG measurement.

GAG Standard (µl)*	Papain Digestion Buffer (µl)
0	100
10	90
20	80
30	70
50	50

*GAG standard 100 µg/ml from the Blyscan^{TM} Sulfated GAG assay kit

3.5 Histology and Immunohistochemistry

To further evaluate the effectiveness of the decellularization process, histological and immunohistochemical analyses were performed. Both fresh and decellularized specimens were fixed in 10% neutral buffered formalin solution at room temperature for 48 hours. The specimens were then dehydrated in graded ethanol, embedded in paraffin and sectioned at 5 µm. Sectioned tissues were stained with the following: 1) hematoxylin and eosin (H&E) to qualitatively assess for cell nuclei and the general appearance of the ECM, and 2) Masson's trichrome to qualitatively assess for collagen distribution in the ECM and the tissue histoarchitecture including the basement membrane and submucosa.

All images were captured digitally and qualitatively assessed (Nikon Eclipse TE2000-S, Nikon Canada Inc., Mississauga, ON).

Immunohistochemical analysis was carried out using an indirect streptavidin-horseradish peroxide (HRP) immunoperoxidase method at room temperature. Specifically, monocloncal antibodies to HLA ABC (1:50 dilution) and β-actin (1:10,000 dilution) (both from Invitrogen, Hamilton, Ontario) were used to establish the presence of nucleated cell membrane fragments and cytoskeletal elements, respectively.

The paraffin embedded sectioned slides were deparaffinized using xylene and graded ethanol. Samples were rinsed in PBS and treated with Proteinase K (Sigma-Aldrich) for 10 minutes. The slides were placed in 2% hydrogen peroxide solution for 10 minutes, which was followed by additional PBS washes. Dako® Protein Block (1-2 drops for 10 minutes; Markham, Ontario) solution was placed on each slide before applying the primary antibodies (anti-HLA ABC and anti-β actin), which was left to incubate overnight. The primary antibodies were omitted for negative control specimens; fresh human skin tissue served as positive controls.

Sections were incubated with biotinylated immunoglobulin (secondary antibody for amplification) for 30 minutes and streptavidin-HRP complex for another 30 minutes (both from Dako® LSAB Kit) with PBS washing step in between. Bound antibody was then visualized using DAB (3,3'-diaminobenzidine HRP; Sigma-Aldrich); counterstaining was performed with filtered Mayer's hematoxylin. Finally, specimen slides were placed in Scott's water and dehydrated in graded ethanol and xylene. Images were captured digitally and qualitatively assessed (Nikon Eclipse TE2000-S, Nikon Canada Inc., Mississauga, ON).

3.6 Scanning Electron Microscopy

Scanning electron microscopy (SEM) was performed to qualitatively evaluate the surface ultrastructural characteristics of fresh and decellularized rabbit tracheal tissues. Tissue specimens were fixed in 2.5% (w/v) glutaraldehyde in distilled water for 2 hours; secondary fixation was performed with 1% (w/v) osmium tetroxide in distilled water for 2 hours. The specimens were then dehydrated in graded ethanol and critical point dried with Leica EM CPD300 apparatus (Leica Microsystems, Vienna, Austria). Finally, the specimens were coated with gold/palladium alloy using Leica EM ACE200 sputter coating apparatus to a thickness of 10 nm (Figure 3.3) and observed in a scanning electron microscope (Hitachi S-4700 SEM, Toronto, ON).

Figure 3.3. Sample preparation for scanning electron microscopy. Tracheal specimens were coated with gold/palladium alloy.

3.7 Mechanical Testing

Uniaxial tensile mechanical testing was performed using the MTS Servo-Hydraulic custom built biaxial testing machine using two opposing actuators (Figure 3.4, Norwood, MA). Fresh tissue and their corresponding samples were subjected to low strain rate uniaxial loading to failure. For each run, one open tracheal ring segment (Figure 3.5) was used; each end of the specimens was mounted onto a purpose-built holder (Figure 3.6). The dimensions of the open tracheal ring specimens were measured prior to being subjected to tensile testing. The specimen holders were supported by a movable bracket that allowed alignment of the two holder grips, which permitted the sample to be straight and flat without obvious twists (Korossis et al. 2002). The gauge length (exposed mid-portion of the specimen actually being subjected to tensile forces) of the specimens was kept relatively consistent (≈5 mm) before load was imposed at the start of the test. Tissue samples were maintained at room temperature and preconditioned through 10 cycles of tensile forces to 10% strain and then pulled until failure, which was noted by the first loss of load during extension and the appearance of obvious tears in the tissue. Several drops of PBS were placed on the tissue sample throughout testing to prevent drying out of the specimen. The stress-strain responses of the specimens (force-displacement curve) were used to calculate the modulus and ultimate tensile stress.

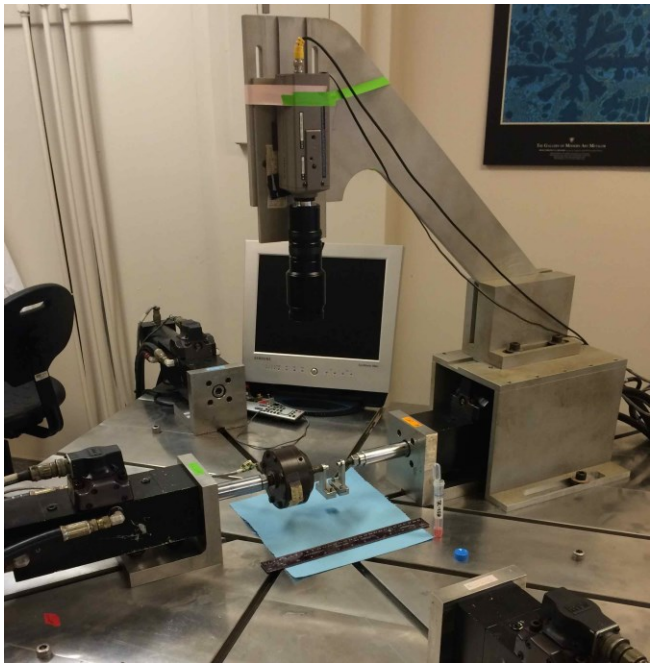

Figure 3.4. The MTS Servo-Hydraulic biaxial tensile testing machine.

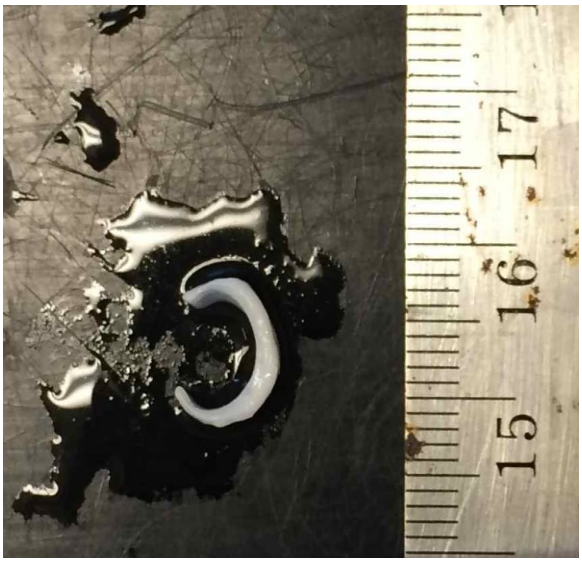

Figure 3.5. Sample preparation for uniaxial tensile testing. Tracheal ring segments were cut open to produce a flat rectangular specimen.

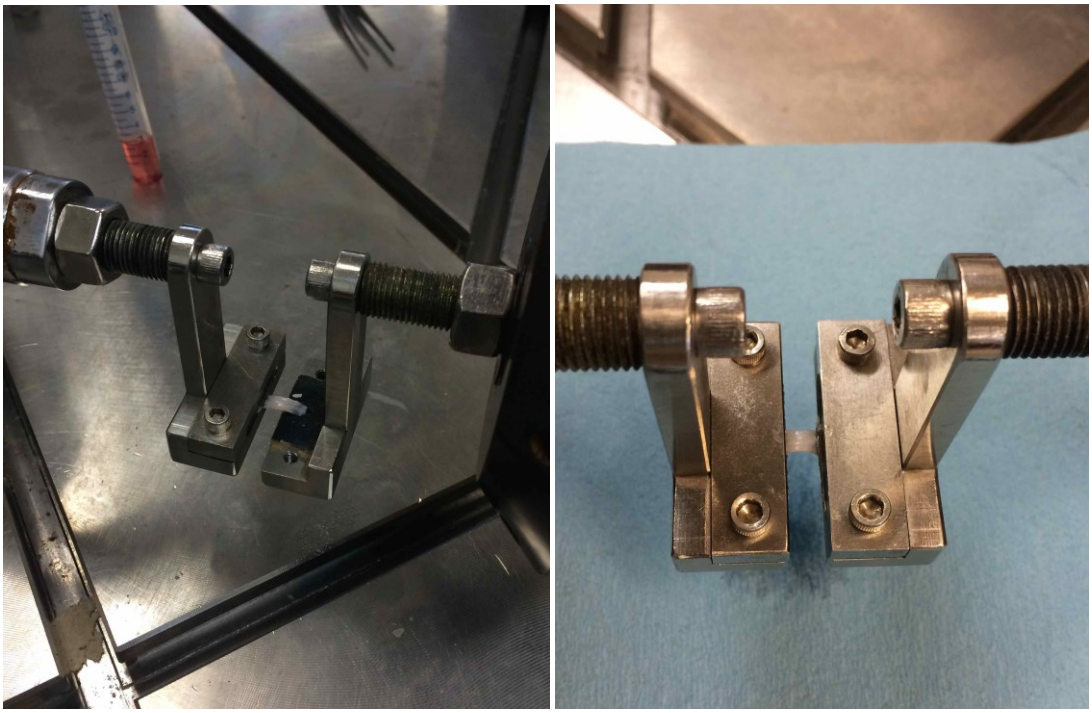

Figure 3.6. Sample preparation for uniaxial tensile testing. Each end of the trachea was clamped and secured into the sample holder.

3.8 Biocompatibility Testing

To determine the biocompatibility of the decellularized tissue, contact cytotoxicity assay was conducted as previously described (Kheir et al. 2011).

Human Embryonic Kidney (HEK) 293 cells were obtained, in kind, from the Department of Biology at Dalhousie University. The HEK 293 cells originated from human embryonic kidney tissue and have widely been used in cell biology research (Stepanenko and Dmitrenko, 2015). A 1 ml stock tube of HEK 293 cells was retrieved from liquid nitrogen storage and thawed at room temperature. They were added to 12 ml of media composed of Dulbecco's Modified Eagle Medium (DMEM), 10% Fetal Bovine Serum (FBS), and 1% Pen/Strep (all from Sigma-Aldrich; hereafter referred to as standard culture medium) and placed in a humidified 37°C, 5% CO_2 incubator for 48-72

hours. When the cells reached a density of ≈80% confluency in the T75 flasks, they were split using 1-2 ml of 0.25% Trypsin-EDTA (Sigma-Aldrich). The trypsinized cells were centrifuged at 1000 rpm for 5 minutes; cell pellet was resuspended in fresh media and placed back in the incubator. Cells at passage three or four were used for the contact cytotoxicity assay experiments.

Fresh and decellularized specimens were cut into ≈5 x 5 mm pieces with a sterile scalpel blade to generate samples with flat edges. The samples were then attached to the center of 100 x 20 mm Petri dishes using double-sided tape (3M, London, ON). Cyanoacrylate glue (Krazy Glue, Westerville, OH) and double-sided tape alone, in duplicates, were used as positive and negative controls, respectively.

The HEK 293 cells were seeded into the Petri dishes at the required density to allow complete confluency of the wells in standard culture medium. The cell-tissue constructs were incubated at 37°C in 5% (v/v) CO_2 in air for 2-3 days. The Petri dishes were then examined by light microscopy (Nikon Eclipse TE2000-S, Nikon Canada Inc., Mississauga, ON) to assess for any changes in cell morphology and to assess whether cells grew around the cartilage specimens.

3.9 Statistical Analysis

All data were analyzed using SPSS Statistics for Windows Version 17.0 (SPSS Inc, an IBM Company, Chicago, IL).

Quantitative data is expressed as mean ± standard deviation. Statistical analysis was performed with unpaired 2-tailed t-test to compare the mean results between fresh and decellularized samples (all fresh and decellularized specimens that were compared originated from the same animal). One-way analysis of variance (ANOVA) and a post-

hoc Tukey test was used to compare the different runs within a decellularization protocol. A P value less than 0.05 was considered statistically significant.

A two-sided power analysis was performed based on the initial DNA and GAG results to determine the sample size. Using an effect size of 0.5 for DNA and 0.10 for GAG, with an α level of 0.05, and a power of 0.8, the sample size was calculated to be six. Therefore, each decellularization treatment had at least six samples per group per run.

CHAPTER 4: RESULTS

4.1 Decellularization

Overall, a total of 10 decellularization treatment runs were performed. Every decellularization treatment run had eight tracheal specimens from two rabbits (four from each rabbit; different specimen dishes used for each rabbit to keep them separate). The remainder of the tracheal samples from the same animals did not undergo decellularization and served as fresh (control) tissue. Specifically, the following decellularization runs were carried out:

- Original decellularization protocol (optimized for human skin)
    - Same protocol repeated three times (hereinafter referred to as DC1)
    - *A total of three runs*
- Modified decellularization protocols (Table 3.2)
    - Five different protocols with altered solution exposure times (hereinafter referred to as DC2a-e)
    - *A total of five runs*
- Freeze-thaw pre-treatments and original decellularization protocol
    - Freeze-thaw pre-treatments and DC1 protocol repeated twice (hereinafter referred to as DC3)
    - *A total of two runs*

All decellularized specimens, along with their corresponding fresh tissues, underwent the following characterization studies.

4.2 Macroscopic Analysis

Macroscopic examination following DC1 and DC2a-e decellularization protocols showed that the rabbit trachea was whitened and had a glistening appearance (Figure 4.1). The overall structure of the trachea was maintained throughout the entire decellularization process with no breakdown, and manual compression with surgical instruments during tissue handling demonstrated no noticeable weakening of the cartilage. Similar findings were observed in specimens that underwent the freeze-thaw pre-treatments before decellularization (DC3). All specimens maintained the ring structure during and after the decellularizaton process.

Figure 4.1. Macroscopic appearance of representative specimens of fresh (left) and decellularized (right) rabbit trachea. All decellularization protocols (DC1, DC2a-e, and DC3) generated similarly appearing specimens. See Figure 3.1 for approximate dimensions.

4.3 Biochemical Analysis

4.3.1 DNA Content

The DNA content was significantly reduced in all samples after decellularization using the original protocol, DC1 (Figure 4.2). Overall, the DNA content was reduced by

an average of 97.14% (Table 4.1). There was no significant difference between different specimens in terms of DNA removal (P = 0.9895).

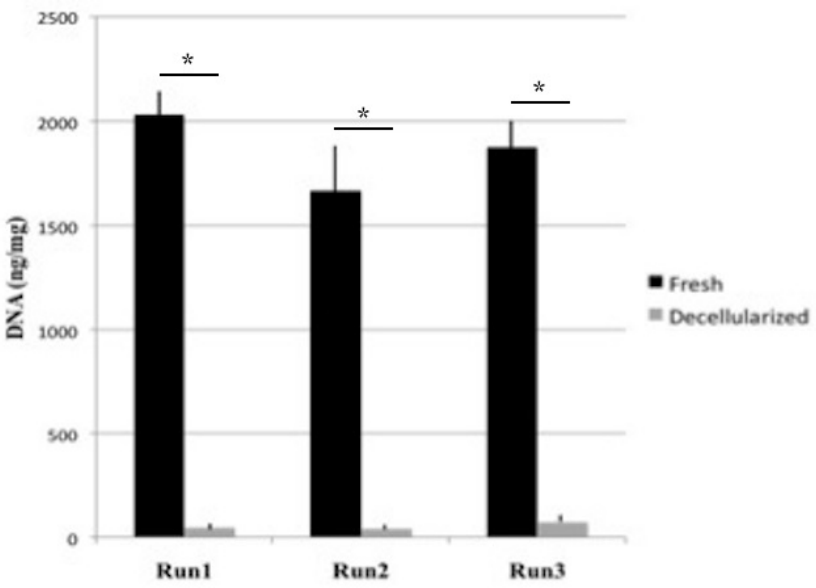

Figure 4.2. The mean DNA content results for each run in ng/mg of dry tissue sample using the DC1 protocol. Post-decellularization, DNA contents were significantly reduced in all samples (noted by *). Error bars represent standard deviation (n = 8 per run).

Similar findings were noted for samples that underwent the modified decellularization protocols DC2a-e (Figure 4.3). There were no significant differences between the different decellularization protocols in terms of DNA removal (P = 0.9993).

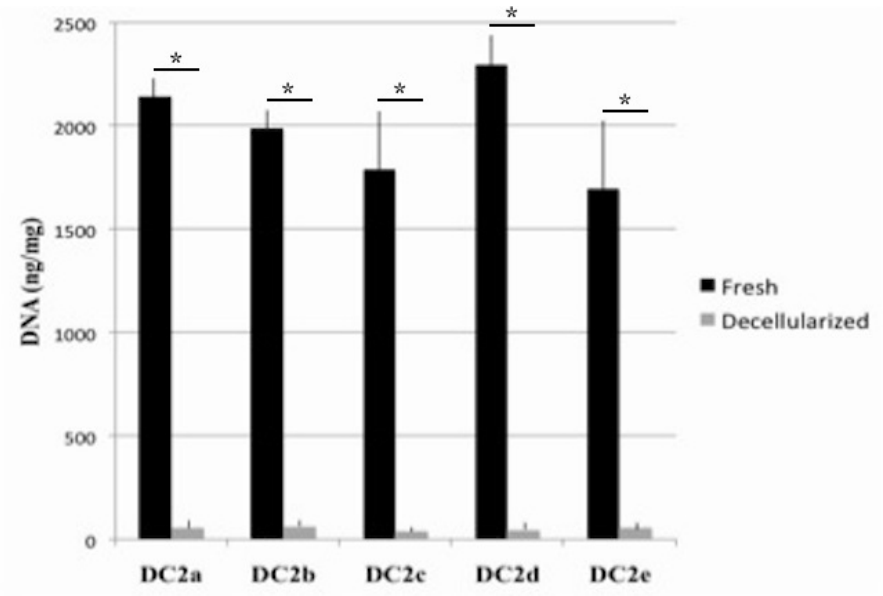

Figure 4.3. The mean DNA content results for each run in ng/mg of dry tissue sample using the DC2a-e protocols. Post-decellularization, DNA contents were significantly reduced in all samples (noted by *). Error bars represent standard deviation (n = 8 per protocol).

The DNA content was also significantly reduced in all samples post-decellularization using the DC3 protocol with freeze-thaw pre-treatment (Figure 4.4). Overall, the DNA content was reduced by an average of 98.44% (Table 4.1). There was no significant difference between different specimens in terms of DNA removal (P = 0.9978).

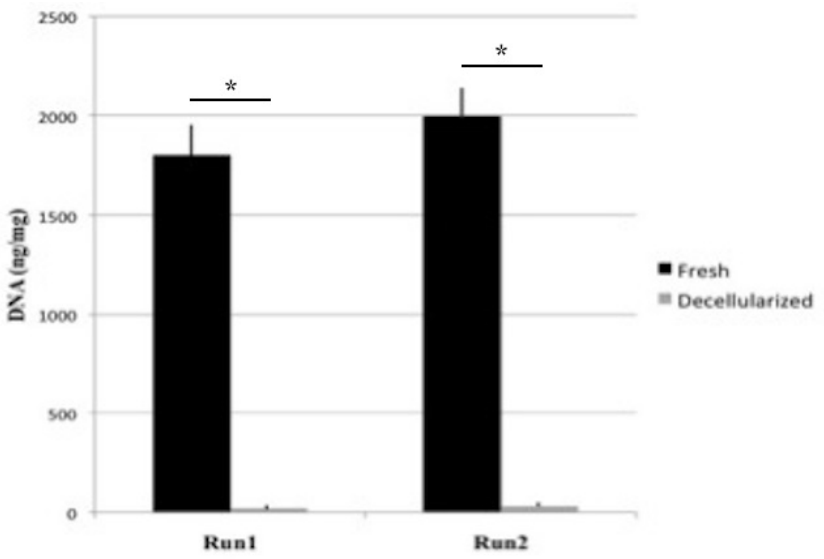

Figure 4.4. The mean DNA content results for each run in ng/mg of dry tissue sample using the DC3 protocol. Post-decellularization, DNA contents were significantly reduced in all samples (noted by *). Error bars represent standard deviation (n = 8 per run).

Table 4.1. Summary of combined mean DNA results (ng/mg of dry tissue).

	Fresh	**Decellularized**	**P value***
DC1 (n = 12)	1857.6 ± 98.7	53.2 ± 17.4	< 0.0001**
DC3 (n = 8)	1902.9 ± 39.7	29.7 ± 0.8	0.0002**

*Two-tailed P value; **significant difference; DC2a-e results were not combined due to the variability in the protocols and small sample sizes. All samples were tested in duplicates to attain adequate sample size for statistical analyses.

4.3.2 GAG Content

The GAG content was not significantly affected by the original decellularization protocol, DC1 (Figure 4.5 and Table 4.2). Also, there were no significant differences between different specimens and runs with respect to GAG content in both fresh and decellularized tissue (P = 0.2500).

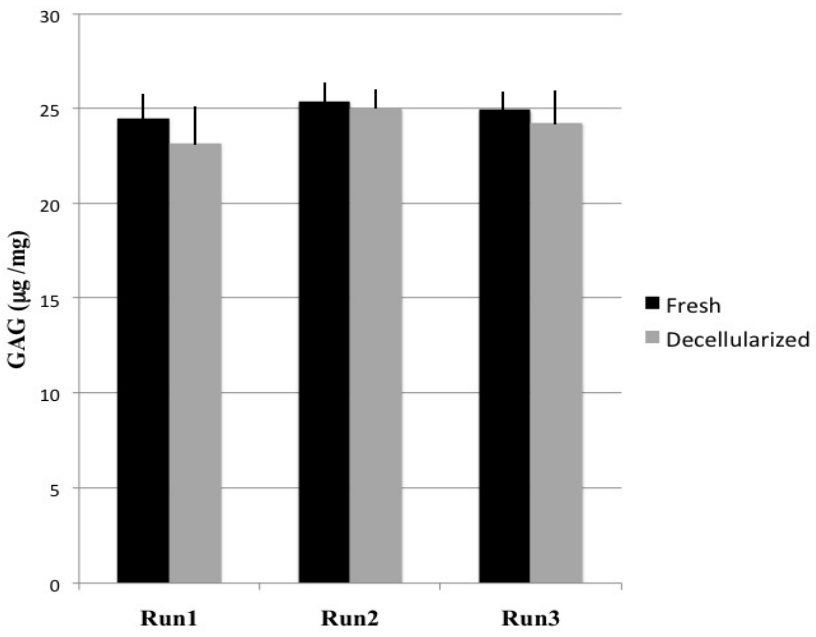

Figure 4.5. The mean GAG content results for each run in µg/mg of dry tissue sample using the DC1 protocol. Post-decellularization, the GAG contents were not significantly reduced. Error bars represent standard deviation (n = 8 per run).

Similar findings were noted for samples that underwent the modified decellularization protocols DC2a-e (Figure 4.6). None of the protocols were associated with significant reduction in GAG content post-decellularization. As well, there were no significant differences between the different decellularization protocols in terms of GAG content ($P = 0.3265$).

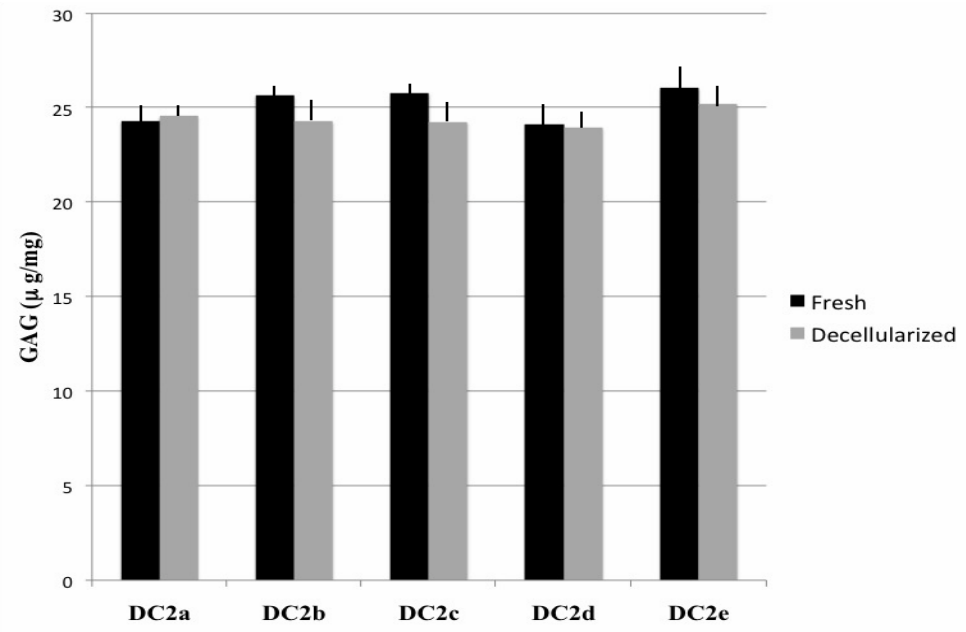

Figure 4.6. The mean GAG content results for each run in µg/mg of dry tissue sample using the DC2a-e protocols. Post-decellularization, the GAG contents were not significantly reduced. Error bars represent standard deviation (n = 8 per protocol).

The GAG content was significantly reduced in all samples after decellularization using the DC3 protocol with freeze-thaw pre-treatments (Figure 4.7 and Table 4.2). There were no significant differences between different specimens and runs in terms of GAG content in both the fresh and decellularized tissue (P = 0.9917).

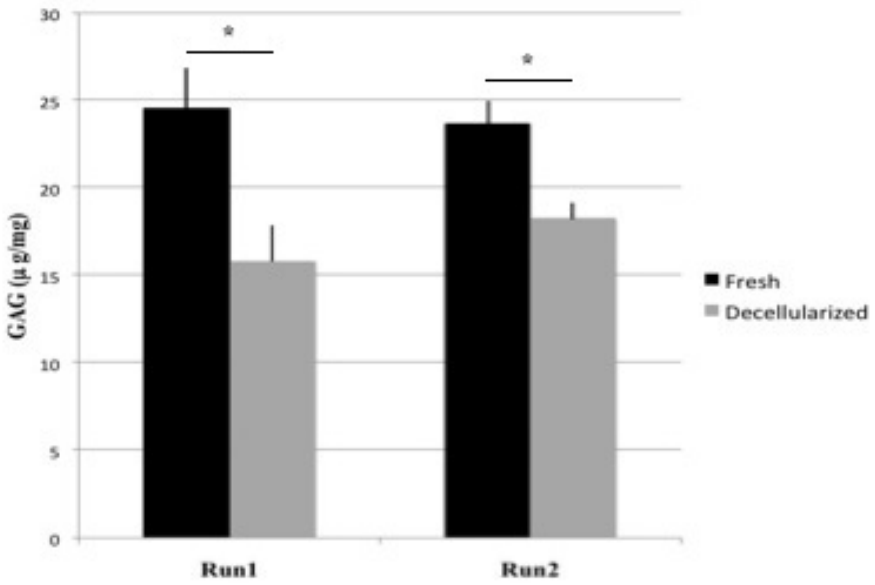

Figure 4.7. The mean GAG content results for each run in µg/mg of dry tissue sample using the DC3 protocol. Post-decellularization, the GAG contents were significantly reduced in all samples (noted by *). Error bars represent standard deviation (n = 8 per run).

Table 4.2. Summary of combined mean GAG results (µg/mg of dry tissue).

	Fresh	**Decellularized**	**P value***
DC1 (n = 12)	24.96 ± 1.89	24.17 ± 2.01	0.6459
DC3 (n = 8)	24.14 ± 1.65	17.06 ± 1.02	0.035**

*Two-tailed P value; **significant difference; DC2a-e results were not combined due to the variability in the protocols. All samples were tested in duplicates to attain adequate sample size for statistical analyses.

4.4 Histological Analysis

4.4.1 H&E Staining

Staining with H&E revealed that most visible cell nuclei within the lacunae of the peripheral regions of the ECM and perichondrium were removed in the decellularized tissue treated with the DC1 protocol (Figure 4.8).

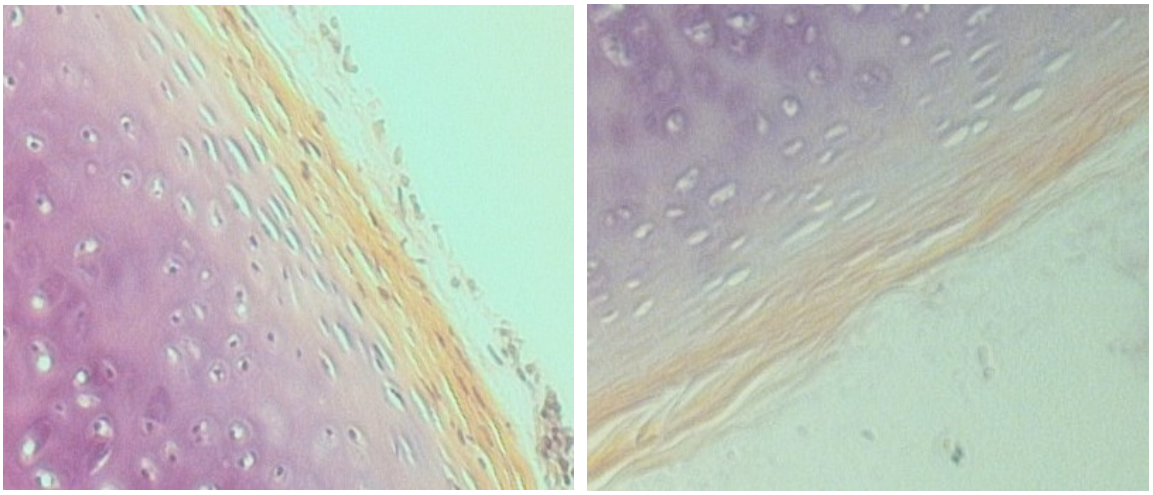

Figure 4.8. H&E stained fresh (left) and decellularized (right) tracheal cartilage tissue treated with DC1 protocol. Cell nuclei are clearly visible inside the cartilage lacunae and perichondrium of the fresh tissue, whereas the decellularized tissue lacked definitive nuclei staining.

However, within the deep regions of the ECM of the tracheal cartilage tissue treated with the DC1 protocol, some cell nuclei persisted to exist (Figure 4.9). On higher magnification, the persistence of some nuclei staining away from the periphery was also appreciated (Figure 4.10). Yet, even within the deep regions of the ECM, there were many empty lacunae spaces in the decellularized tissue.

Figure 4.9. H&E stained decellularized (DC1) rabbit tracheal tissue at 100X magnification. Some cell nuclei are clearly visible inside the lacunae within the deep regions of the cartilage ECM (black arrows). The peripheral areas, including the perichondrium and inner lining, lacked nuclei staining. Bar, 100 µm.

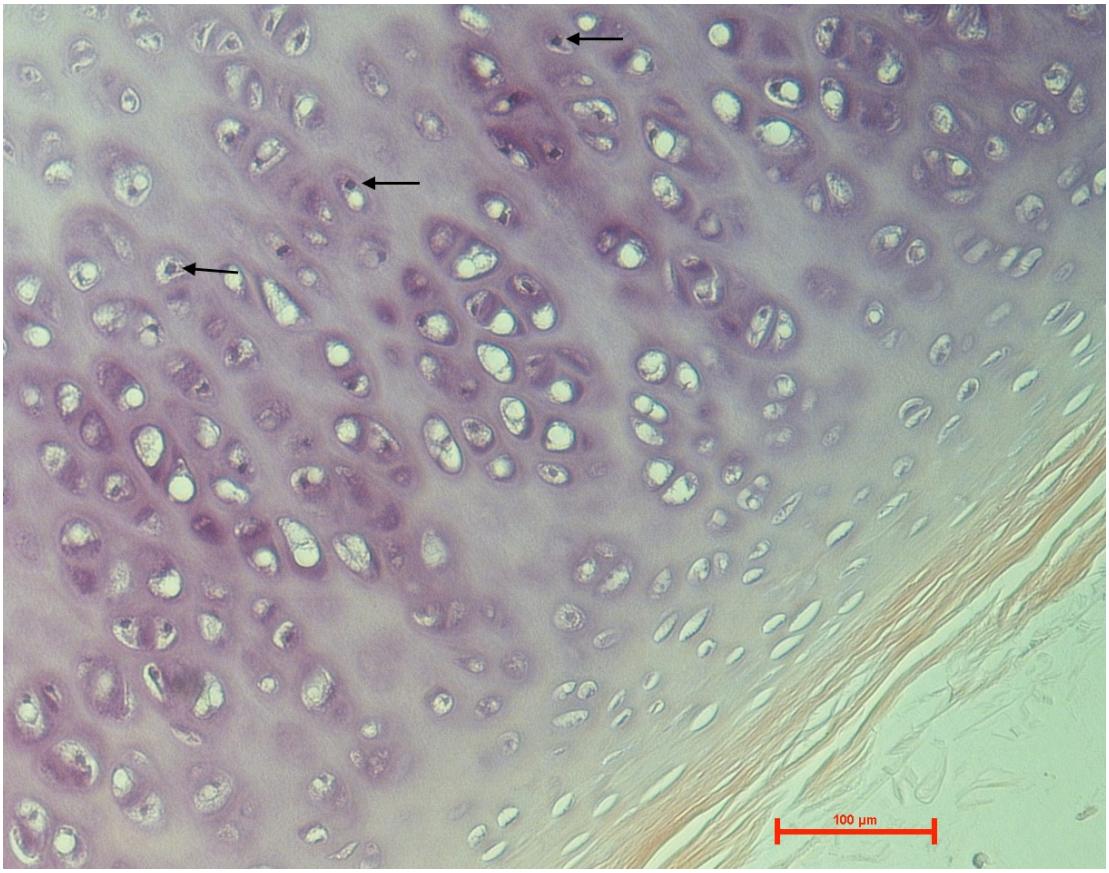

Figure 4.10. H&E stained decellularized (DC1) rabbit tracheal tissue at 200X magnification. Some cell nuclei are clearly visible inside the lacunae within the deeper regions of the cartilage tissue (black arrows). There were also empty lacunae spaces in the same area. The peripheral regions, including the perichondrium, lacked cell nuclei staining. Bar, 100 µm.

Further H&E staining was performed on all decellularized (and corresponding fresh) tissues treated with DC2a-e protocols. Under qualitative, visual examination, there appeared to be no difference between any of the five protocols in terms of nuclei staining (Figures 4.11 and 4.12). Similar to DC1 treated samples, no cell nuclei staining was observed in the perichondrium, inner lining, and the periphery of the tissue, but within the deep areas of the ECM, some nuclei staining persisted.

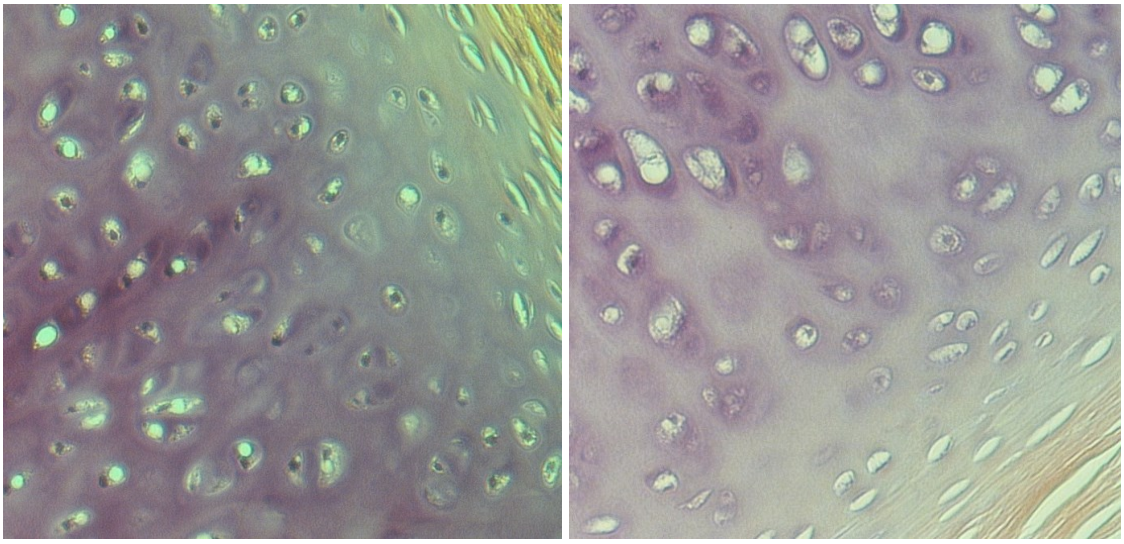

Figure 4.11. H&E stained fresh (left) and decellularized (right) tracheal cartilage tissues treated with the DC2c decellularization protocol. Cell nuclei are visible inside most cartilage lacunae and the perichondrium of the fresh tissue, whereas the decellularized tissue lacked nuclei staining in the perichondrium and outer edges of the tracheal tissue.

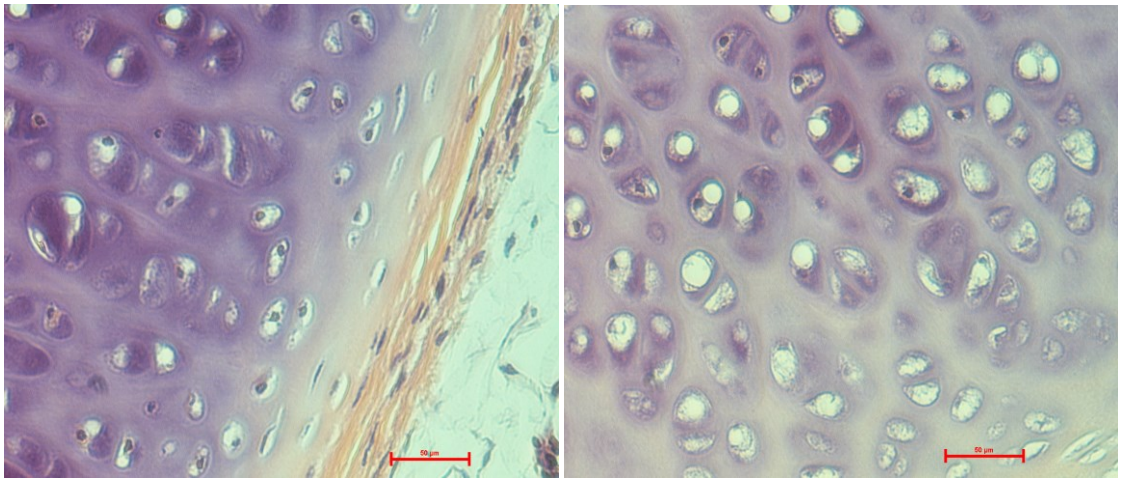

Figure 4.12. H&E stained fresh (left) and decellularized (right) tracheal cartilage tissues treated with the DC2e decellularization protocol. Cell nuclei are visible inside most cartilage lacunae and the perichondrium of the fresh tissue, whereas the decellularized tissue lacked nuclei staining in the perichondrium and outer edges of the tracheal tissue. Some cell nuclei staining was visualized within the deep regions of the ECM. Bar, 50 μm.

Tracheal specimens treated with freeze-thaw pre-treatments (DC3 protocol) were also subjected to H&E staining. As expected there was obvious nuclei staining observed throughout the entire depth of all fresh tissue samples (Figure 4.13).

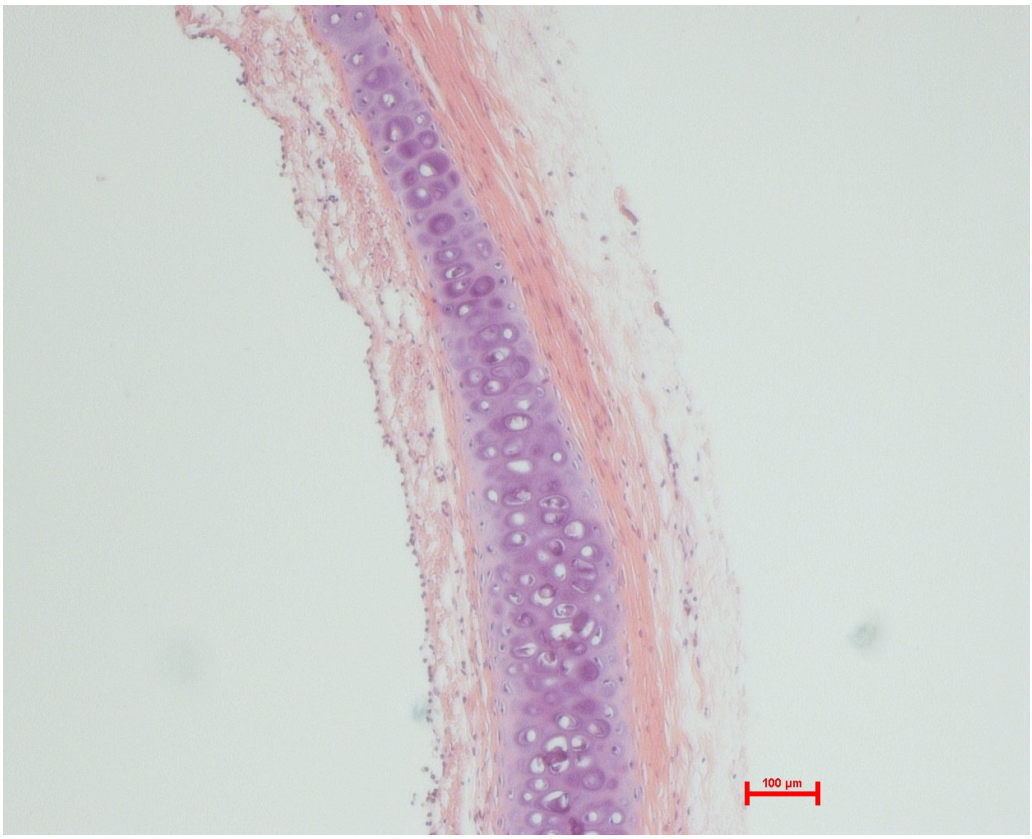

Figure 4.13. H&E stained fresh rabbit tracheal tissue at 100X magnification. Cell nuclei are clearly visible throughout the tracheal tissue. Bar, 100 µm.

In contrast, no nuclei staining was observed in decellularized specimens throughout the entire tissue (Figure 4.14). Even within the deep regions of the cartilage ECM, cell nuclei staining was not consistently noted.

Figure 4.14. H&E stained decellularized (DC3) rabbit tracheal tissue at 100X magnification. Unlike the corresponding fresh tissue (Figure 4.13), cell nuclei staining is not seen throughout the decellularized tissue. Bar, 100 µm.

There were some infrequent areas of staining observed in the lacunae throughout the cartilage ECM, but on higher magnification this staining was found to be weak and indeterminate (Figure 4.15).

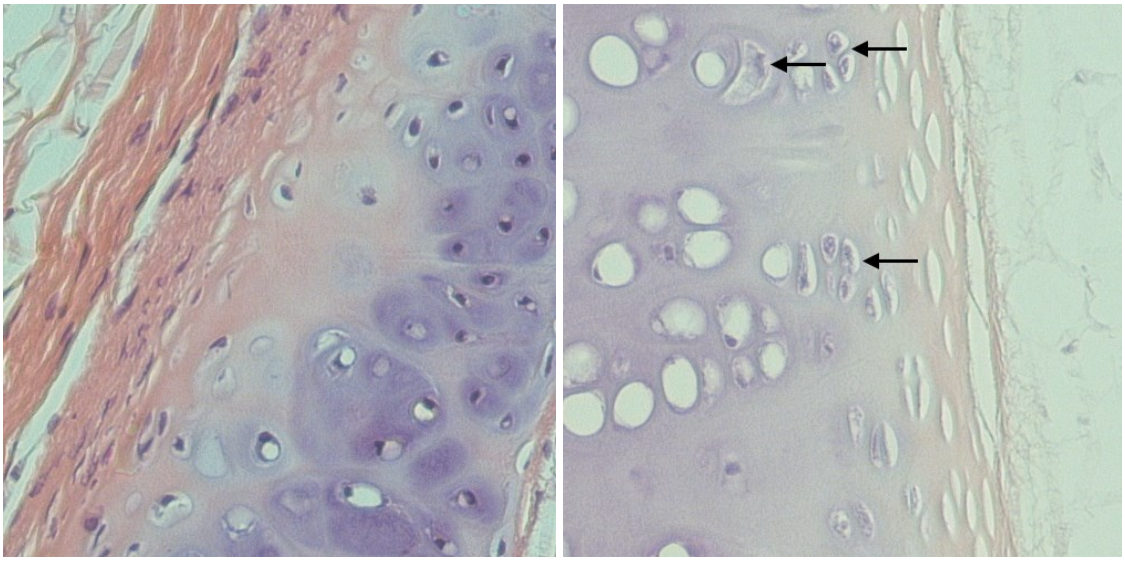

Figure 4.15. H&E stained fresh (left) and decellularized (right) tracheal tissues treated with the DC3 protocol. Cell nuclei are visible as discrete and focal blue stains inside cartilage lacunae and within perichondrium of the fresh tissue. Similar staining is not present in the decellularized tissue. Staining is observed in some lacunae of the decellularized tissue but this is noted to be less intense and discrete (black arrows).

4.4.2 Masson's Trichrome Staining

Staining with Masson's trichrome showed that the major histoarchitecture of the ECM remained largely unchanged following decellularization with all protocols (Figures 4.16-4.18). Specifically, the organization of the cartilage, basement membrane, and submucosa were retained after decellularization without obvious evidence for loss of lacunar structure or subepithelial damage. Masson's trichrome staining also revealed that the distribution of collagen was concentrated on the periphery of the ECM in both fresh and decellularized tissues. The only noteworthy difference between the fresh and decellularized specimens was that less nuclei staining was observed in decellularized tissue for all protocols.

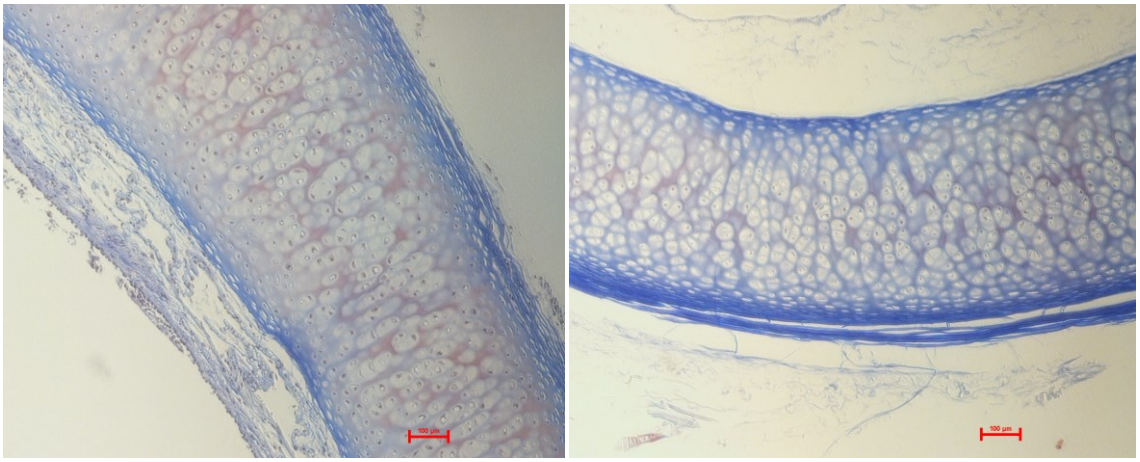

Figure 4.16. Masson's trichrome stained fresh (left) and decellularized (right) tracheal tissues treated with the DC1 protocol at 100X magnification. The general histoarchitecture of the tissue remained similar after decellularization. Collagen was mainly found at the periphery of both ECMs (stained in blue). Bar, 100 μm.

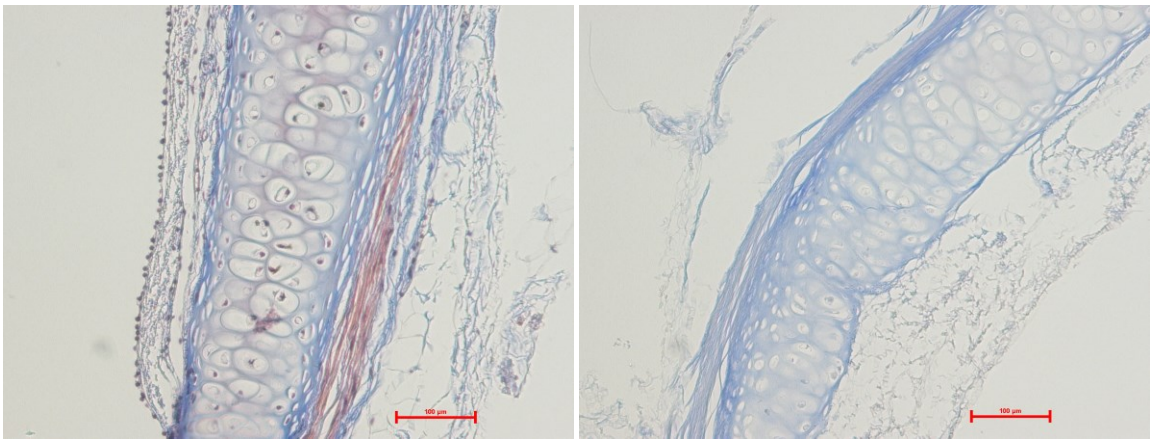

Figure 4.17. Masson's trichrome stained fresh (left) and decellularized (right) tracheal tissues treated with the DC2c protocol at 200X magnification. The general histoarchitecture of the tissue remained largely unchanged after decellularization. Collagen was mainly found at the periphery of both ECMs (stained in blue). Bar, 100 μm.

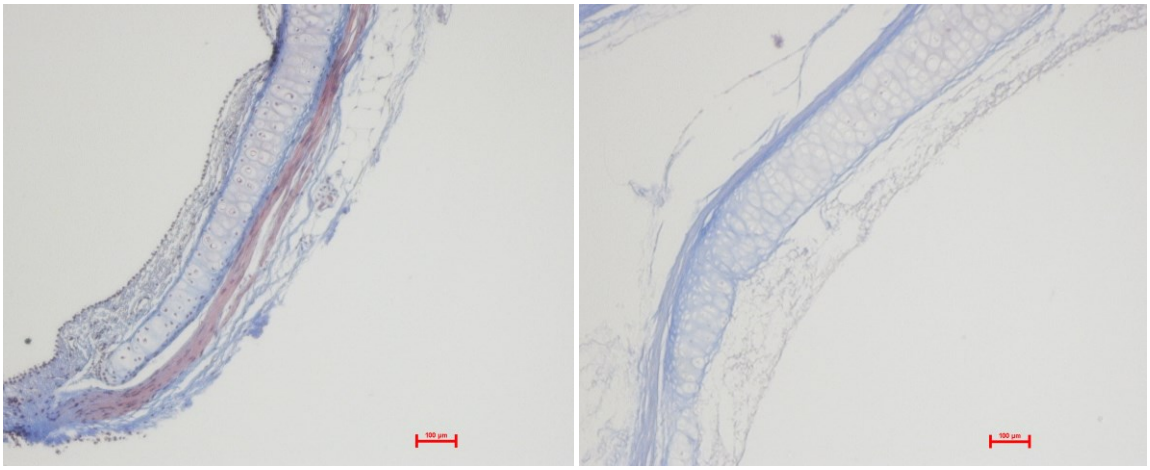

Figure 4.18. Masson's trichrome stained fresh (left) and decellularized (right) tracheal tissues treated with the DC3 protocol at 100X magnification. The general histoarchitecture of the tissue remained similar after decellularization. Collagen was mainly found at the periphery of both ECMs (stained in blue). Bar, 100 μm.

4.5 Immunohistochemistry

Both positive (human skin) and negative (omission of primary antibody) controls for immunohistochemical analyses demonstrated results as expected. Specifically, HRP associated brown staining was observed in positive controls while no brown staining was seen in negative control specimens (data not shown).

4.5.1 HLA-ABC Expression

Immunohistochemical analysis with fresh tissue sections demonstrated HLA-ABC positivity (brown staining) in the overlying perichondrium, underlying respiratory epithelium, and within the substance of the ECM (Figures 4.19-4.21). However, only occasional traces of HLA-ABC staining were observed in the decellularized tracheal tissue treated with DC1, DC2a-e, and DC3 protocols (Figures 4.19-4.21).

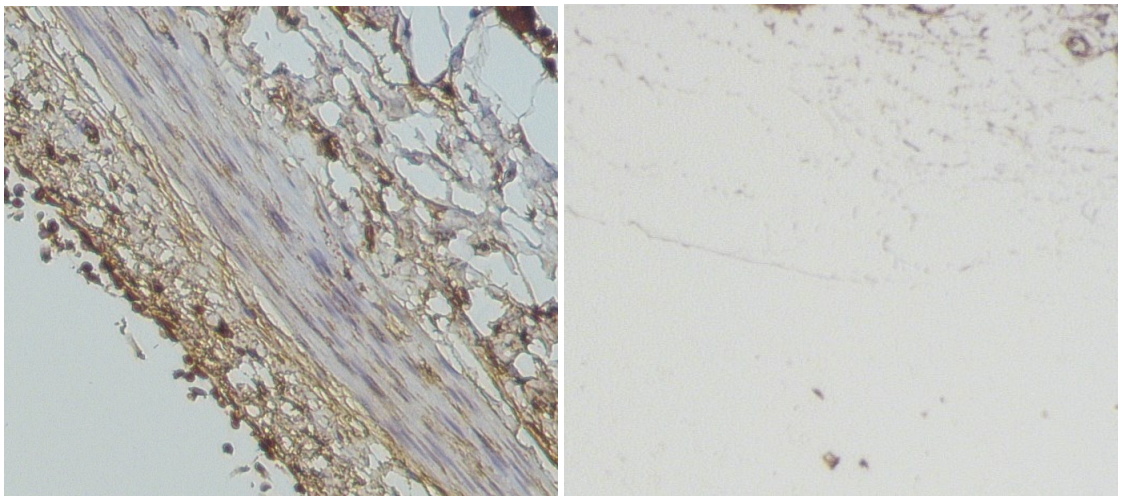

Figure 4.19. Immunohistochemical staining for HLA-ABC of fresh (left) and decellularized (right) tracheal tissues treated with the DC1 protocol. Fresh tissue showed positive staining of HLA-ABC throughout (brown staining), while only traces of brown staining was found in decellularized tissue.

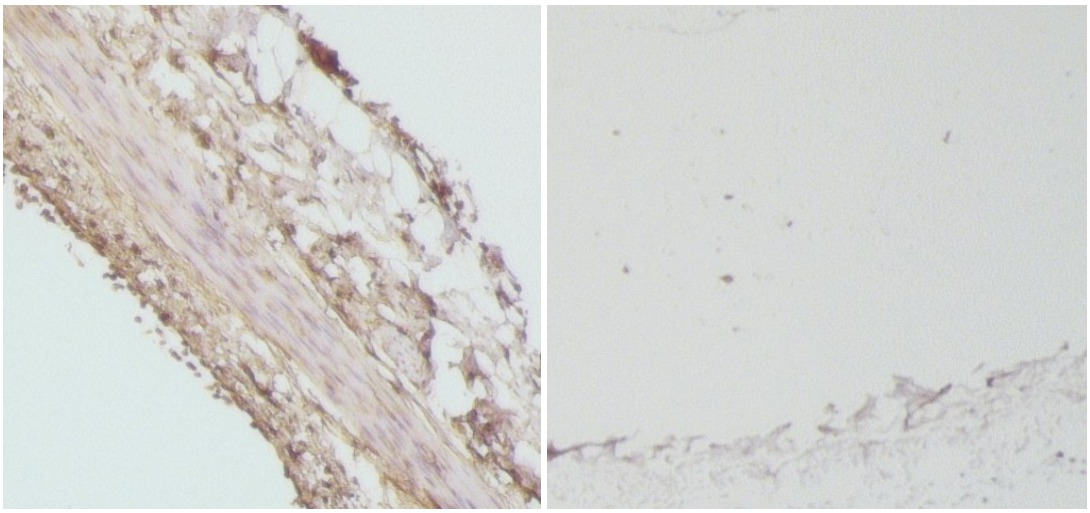

Figure 4.20. Immunohistochemical staining for HLA-ABC of fresh (left) and decellularized (right) tracheal tissues treated with the DC2d protocol. Fresh tissue showed positive staining of HLA-ABC throughout (brown staining), while only traces of brown staining was found in decellularized tissue.

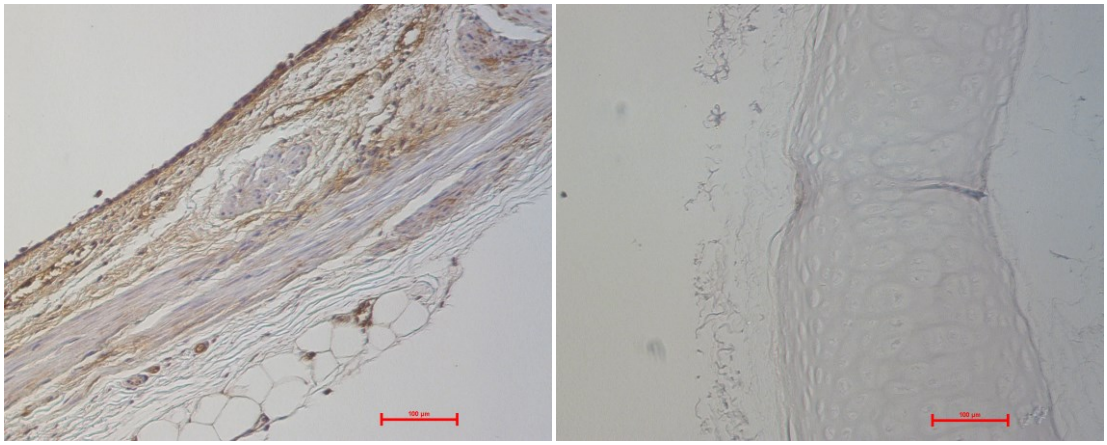

Figure 4.21. Immunohistochemical staining for HLA-ABC of fresh (left) and decellularized (right) tracheal tissues treated with the DC3 protocol at 100X magnification. Fresh tissue showed positive staining of HLA-ABC throughout (brown staining), while no similar staining was observed in the decellularized tissue. Bar, 100 μm.

4.5.2 β-Actin Expression

Immunohistochemical analysis of fresh tissue sections with anti-β-Actin primary antibody demonstrated positive staining throughout the entire tracheal tissue, including the perichondrium, ECM, and epithelium (Figures 4.22-4.24). Staining of decellularized tissues treated with DC1 and DC2a-e protocols showed either infrequent traces of β-Actin positivity or no staining at all (Figures 4.22 and 4.23). No β-Actin staining was observed in DC3 treated specimens (Figure 4.24).

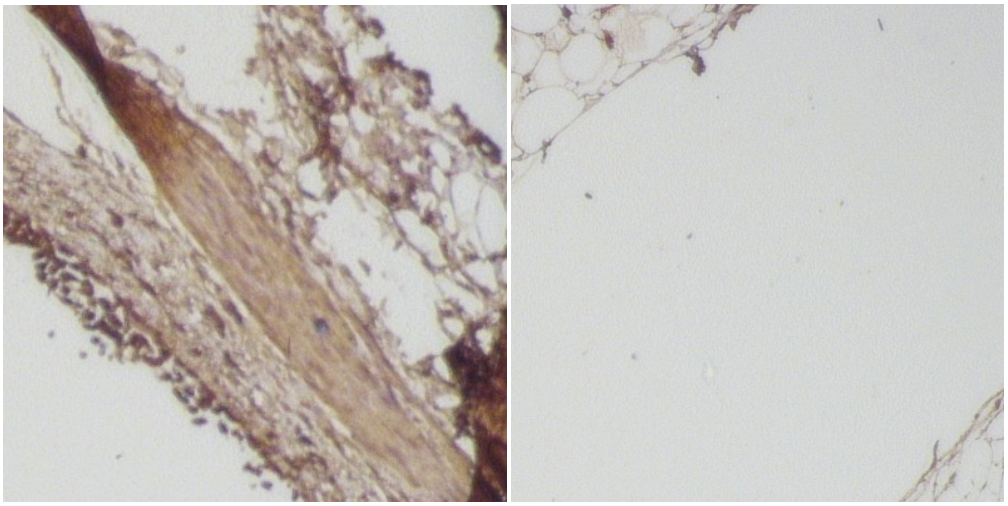

Figure 4.22. Immunohistochemical staining for β-Actin of fresh (left) and decellularized (right) tracheal tissues treated with the DC1 protocol. Fresh tissue showed positive staining of β-Actin throughout (brown staining), while only traces of brown staining was found in decellularized tissue.

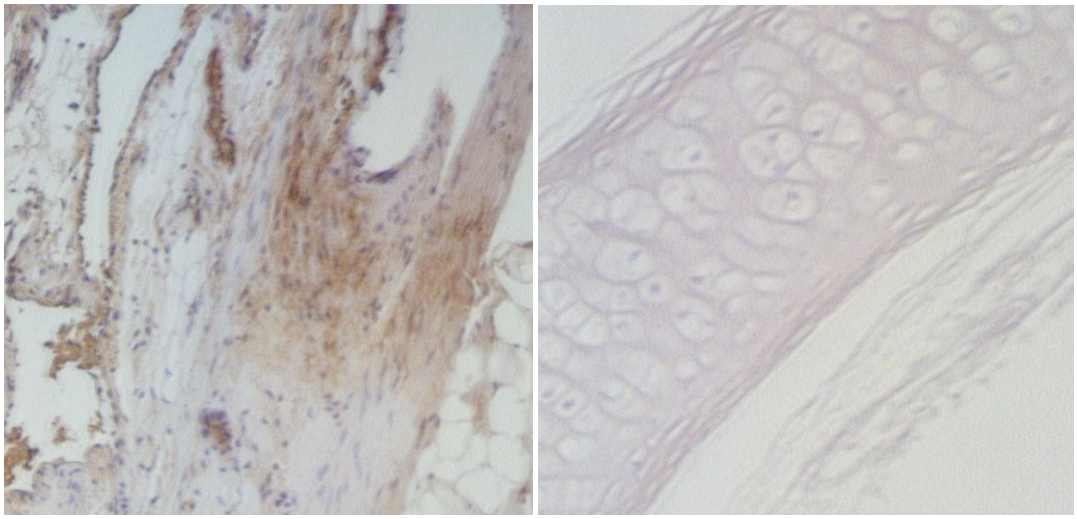

Figure 4.23. Immunohistochemical staining for β-Actin of fresh (left) and decellularized (right) tracheal tissues treated with the DC2b protocol. Fresh tissue showed positive staining of β-Actin throughout (brown staining), while no staining was found in decellularized tissue.

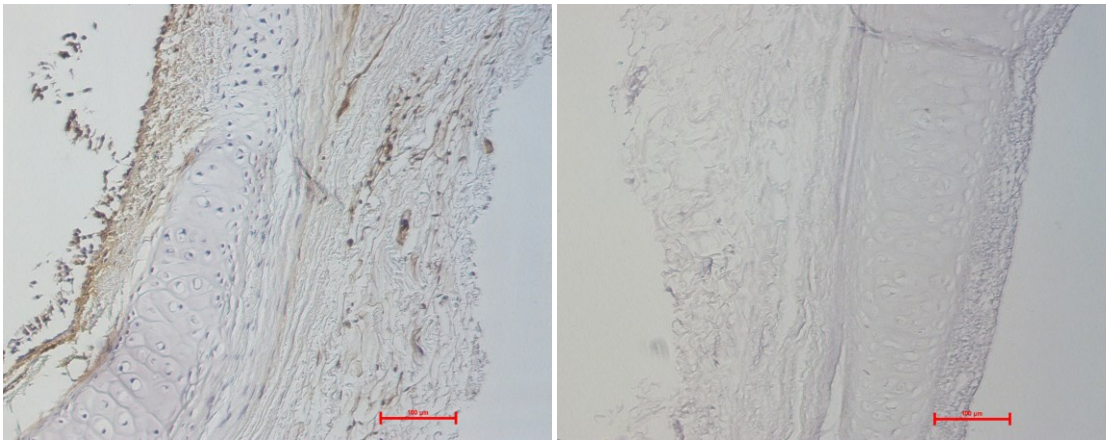

Figure 4.24. Immunohistochemical staining for β-Actin of fresh (left) and decellularized (right) tracheal tissues treated with the DC3 protocol at 100X magnification. Fresh tissue showed positive staining of β-Actin throughout (brown staining), while no staining was found in decellularized tissue. Bar, 100 μm.

4.6 Mechanical Testing

The native tubular structure of the trachea was maintained throughout the decellularization process with all protocols (DC1, DC2a-e, and DC3). As well, manual compression with surgical instruments suggested no obvious weakening of the trachea post-decellularization with all protocols. These findings were supported by the tensile testing results for the DC1 and DC2a-e treated specimens (Table 4.3). More specifically, the modulus and ultimate tensile stress did not significantly change after decellularization with DC1 and DC2a-e protocols. However, there was a significant reduction in both modulus and ultimate tensile stress in tracheal specimens treated with DC3 protocol (Table 4.3).

Table 4.3. Tensile testing results of fresh and decellularized rabbit tracheal tissue.

	Fresh	Decellularized	P value*
DC1 (n = 6)			
Modulus (MPa)	13.63 ± 1.78	17.30 ± 3.52	0.1823
Ultimate Tensile Stress (MPa)	2.50 ± 0.62	3.03 ± 0.42	0.2855
DC2 (n = 5)			
Modulus (MPa)	14.20 ± 2.38	12.90 ± 3.21	0.4877
Ultimate Tensile Stress (MPa)	3.27 ± 0.45	2.63 ± 0.61	0.0957
DC3 (n = 6)			
Modulus (MPa)	26.98 ± 4.22	18.98 ± 3.39	0.0244**
Ultimate Tensile Stress (MPa)	4.50 ± 1.29	2.65 ± 0.19	0.0297**

MPa: megapascal; *unpaired *t* test; **significant difference.

4.7 Scanning Electron Microscopy

The SEM analysis of fresh tracheal cartilage demonstrated a fine, interwoven network of collagen fibers with some visible cells (Figure 4.25). Decellularized specimens treated with protocols DC1 and DC2a-e showed a similar ultrastructural 3D arrangement of collagen fibers (Figure 4.25). Also, both fresh and decellularized ECM retained multiple similarly sized pores (i.e. spaces between the collagen fibers bundles) on their surfaces (Figure 4.26).

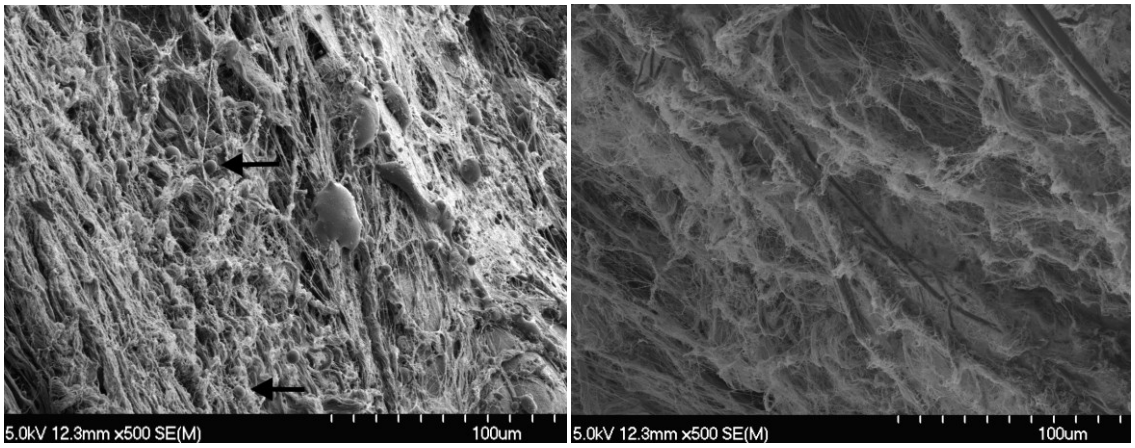

Figure 4.25. SEM images of fresh (left) and DC1 treated decellularized (right) tracheal matrix. The ultrastructure of both tissue surfaces demonstrated interwoven network of collagen fibers. Fresh tissue also had interspersed circular structures consistent with cells (black arrows).

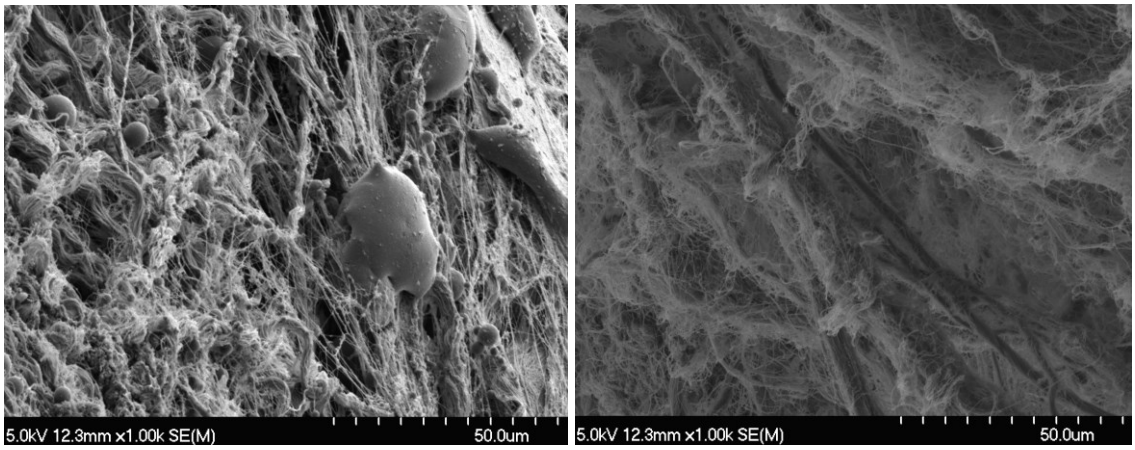

Figure 4.26. SEM images of fresh (left) and DC1 treated decellularized (right) tracheal matrix at higher magnification. The ultrastructure of both tissue surfaces demonstrated interwoven network of collagen fibers. The spaces between the collagen fibers appeared similar in both fresh and decellularized tissues.

The SEM analysis of DC3 protocol treated decellularized trachea also demonstrated a fine, interwoven set of connections of collagen fibers with no visible cells (Figure 4.27). However, the arrangement of collagen fiber bundles were dissimilar between the fresh and DC3 treated tissue; that is, the collagen fiber bundles showed varying directionalities, and loop-like structures were observed throughout the surfaces of DC3 treated specimens (Figure 4.28). The change in collagen fiber bundle arrangements may indicate disruption of ECM surface ultrastructure secondary to repeated ice crystal formation and thaw.

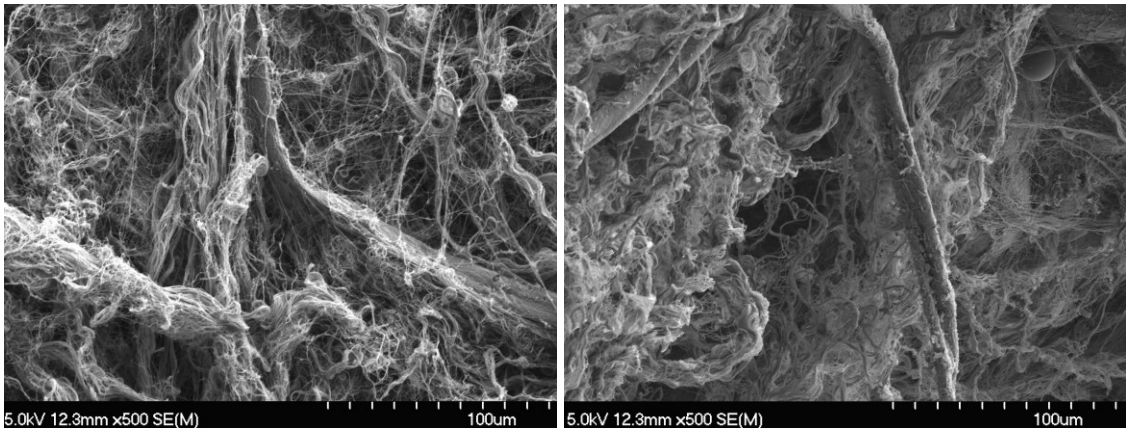

Figure 4.27. SEM images of DC3 protocol treated decellularized tracheal matrix (left and right). The ultrastructure of ECM surface demonstrated interwoven network of collagen fibers similar to DC1 and DC2a-e treated specimens; however, the arrangement of fiber bundles were different.

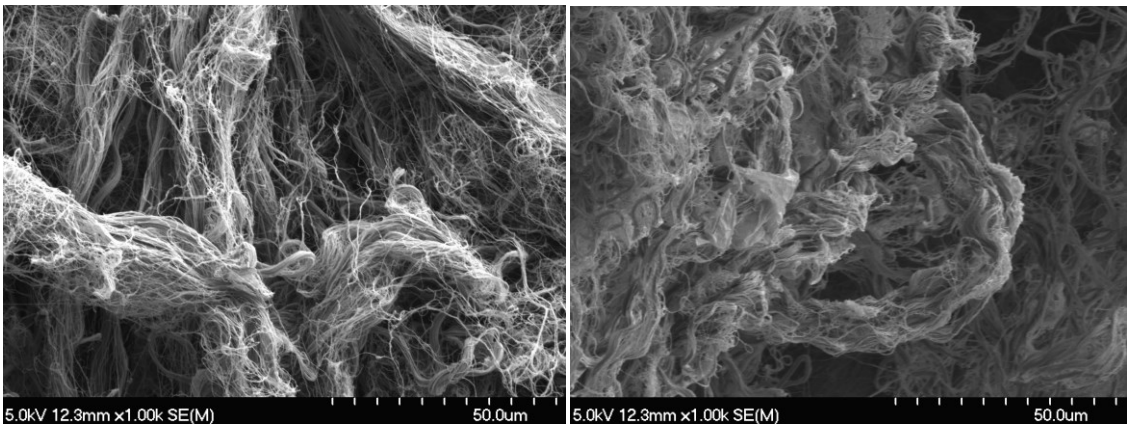

Figure 4.28. SEM images of DC3 protocol treated decellularized tracheal matrix (left and right). The ultrastructure of ECM surface demonstrated interwoven network of collagen fibers similar to DC1 and DC2a-e treated specimens; however, the collagen fiber bundles had multiple directions and loop-like structures. This change may indicate disruption of ECM surface ultrastructure secondary to repeated ice crystal formation and thaw.

4.8 Biocompatibility Testing

Microscopic analysis of the contact cytotoxicity plates showed that the HEK 293 cells grew up to and in contact with the decellularized tissues treated with all protocols (Figures 4.29 and 4.30). The same finding was also noted for fresh tissue. No areas of cell

lysis or morphological change were observed in any of the plates with decellularized specimens.

Double-sided tape alone (negative control) demonstrated no signs of cytotoxicity. Conversely, signs of cytotoxicity was seen with cyanoacrylate glue (positive control) as no cells grew up to and in contact with the glue.

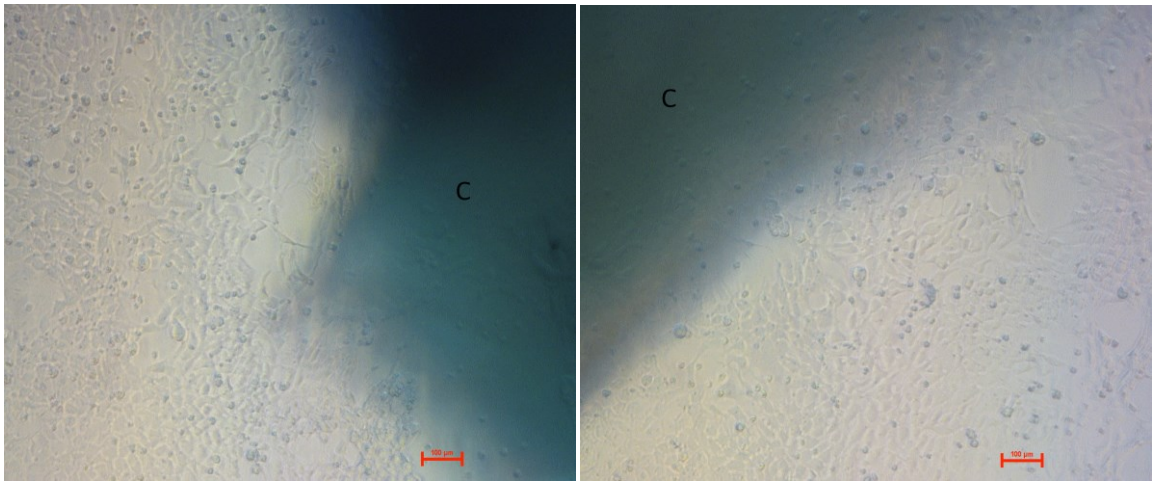

Figure 4.29. Microscopic view of contact cytotoxicity assay plates at 100X magnification. The HEK 293 cells grew in contact with decellularized cartilage tissues (labeled as C) that underwent DC1 (left) and DC3 (right) treatments. Bar, 100 μm.

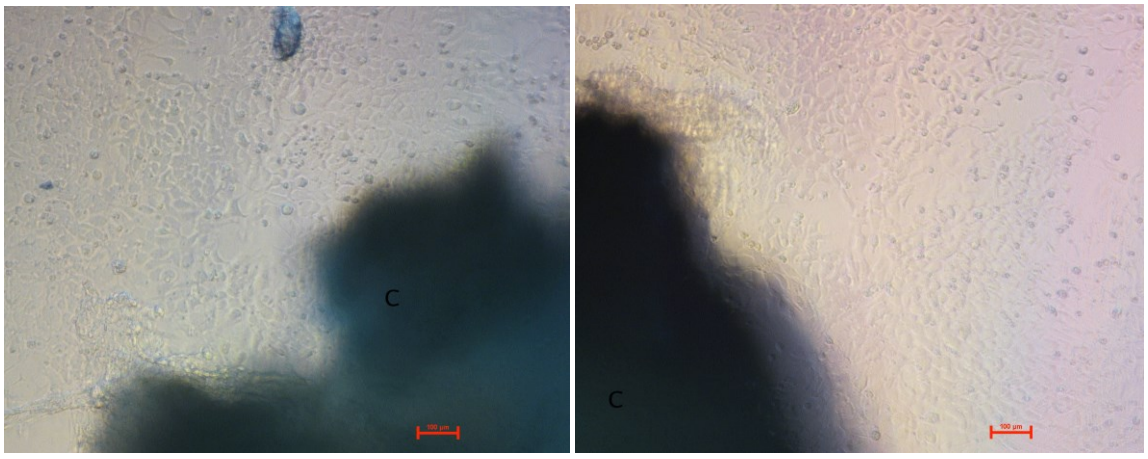

Figure 4.30. Microscopic view of contact cytotoxicity assay plates at 100X magnification. The HEK 293 cells grew in contact with decellularized cartilage tissues (labeled as C) that underwent DC2b (left) and DC2e (right) treatments. Bar, 100 μm.

CHAPTER 5: DISCUSSION

5.1 Summary of Results

5.1.1 Introduction

This study aimed to develop a decellularized rabbit tracheal matrix that can be used as a tissue engineering scaffold material. The challenge was to decellularize the dense matrix of the tracheal cartilage while leaving a structurally intact, biocompatible ECM scaffold.

Decellularization was achieved through a protocol developed in our laboratory optimized for human skin (DC1 protocol). Briefly, the decellularization protocol involved hypotonic solution to cause cell lysis, hypertonic solution to extract and solubilize proteins, protease inhibitors to inhibit endogenous proteinases, surfactants to penetrate the ECM to remove cellular debris, DNAse and RNAse to digest nucleic acids, peracetic acid to reduce the bioburden, and finally extensive washing in PBS to remove debris and cytotoxic reagents used in the decellularization protocol.

Modifications were also made to the original protocol to determine whether the effectiveness of decellularization can be enhanced for rabbit tracheal tissue. First, based on our previous work with cartilage tissue (Woods et al. 2005; Graham et al. 2016), the exposure times to key decellularization solutions were altered. Second, based on the early results using the original decellularization protocol, a simple freeze-thaw cycle method was introduced to potentially open up the tracheal matrix (Stapleton et al. 2008).

Overall, the results revealed that the decellularization protocols were mostly effective in removing cellular material while retaining the biomechanical properties of the ECM. However, there were differences among some of the decellularization protocols.

Although the freeze-thaw pre-treatments (DC3 protocol) resulted in better extraction of cells within the deep regions of the ECM, it also led to reduced biomechanical properties. Future studies with cell repopulation, bioreactor use, and in vivo experiments are required to conclude whether the decellularized ECM generated in the current study will be a viable scaffold material in tracheal tissue engineering.

5.1.2 Removal of Cells

In general, the decellularization process optimized for human skin (DC1) was found to be effective in removing cells from rabbit tracheal tissue. Specifically, the DNA content was significantly reduced in all decellularized samples by an average of 97.1%. Similar results were obtained with modified decellularization protocols DC2a-e; all treatment runs resulted in a significant reduction of DNA levels post-decellularization. However, there was still some residual DNA present in the treated tissues on Quant-iT PicoGreen® dsDNA Assay. Presumably, this DNA content originated from the retained chondrocytes within the deep regions of the cartilage ECM, as most cells in the perichondrium, respiratory epithelium, and outer regions of the ECM were absent post-decellularization on H&E staining. However, with the freeze-thaw pre-treatments (DC3 protocol), there was very near-complete removal of cells from tracheal tissues, as H&E staining demonstrated the absence of visible cells even within the deep regions of the cartilage ECM.

Previously published decellularization protocols have also led to significant decreases in DNA content (Stapleton et al. 2008; Jungebluth et al. 2009; Zang et al. 2012; Lange et al. 2015; He and Callanan, 2013). At the same time, none of the protocols to date have produced scaffolds that *completely* lacked cells and/or cellular debris (Crowley et al. 2015). That is, all decellularization protocols resulted in ECM products with some

residual cellular or genetic materials. Taken together, these findings may indicate that it is not possible to remove 100% of all cellular material from the ECM without significantly damaging or physically breaking up the tissue. The related concern is that cellular and genetic material can contribute to cytocompatibility problems in vitro and adverse host responses in vivo, such as acute rejection or chronic inflammation (Nagata et al. 2010; Brown et al. 2009). However, it is unknown what amount of genetic material can cause problems with recellularization with allogeneic cells and/or implantation as an allo- or xeno-graft. That is, the level of genetic material that should be considered 'acceptable' in decellularized scaffolds remains unknown. Some groups have defined acceptable decellularization as <50 ng/mg ECM by dry weight, <200 base pair DNA fragment, or lack of visible nuclear material on histological staining, such as H&E (Gilbert et al. 2006; Crapo et al. 2011; Reing et al. 2010). The results from the current study demonstrated effective decellularization as the post-treatment DNA levels were mainly <50 ng/mg ECM by dry weight of sample tissue (Table 4.1). Yet, there is no widely accepted standard amongst researchers, and the Federal Drug Administration in the United States and Health Canada do not have explicit guidelines pertaining to this matter.

Currently, it is unclear whether minimal amounts of cells or poorly soluble cellular elements within an ECM will cause unwanted reactions when used as a tissue engineering scaffold. There is some evidence that residual cellular material in decellularized dermal matrices can cause increased inflammation and stimulation of inflammatory macrophages instead of regenerative macrophages (Orenstein et al. 2010; Chauviere et al. 2014). The cellular elements may indeed result in a limited host response (Macchiarini et al. 2008; Gilbert et al. 2006), which would be demonstrated in future in vivo studies. It is possible that the minute amounts genetic material may not present a

significant problem in vivo. Therefore, further studies should aim to determine what level of remnant DNA can be considered acceptable for tissue engineering purposes.

5.1.3 Maintenance of Glycosaminoglycans

Cartilage tissue typically has an ECM primarily composed of proteoglycans, collagen, and elastic fibers (Muir, 1995). Differences in composition of these ECM proteins will determine the type of cartilage tissue (hyaline, elastic, or fibrocartilage) and its biomechanical properties. Hyaline cartilage, found in anatomic areas such as the larynx, trachea, ribs, nose, and articular joints, is the most common type of cartilage in humans (Poole, 1997), and their major role is to provide structural support, while allowing some flexibility at the same time. Elastic cartilage contains the most elastin and elastic fibers, which makes it very flexible and pliable. Fibrocartilage is situated in areas dominated by tensile and compressive forces, such as intervertebral disks (Junqueira et al. 1979).

Proteoglycans make up a substantial portion of the ground substance of the ECM. They consist of a protein core and many side-chains made up GAGs. The charged carboxyl and sulfate groups on the GAG side-chains confer the major structural characteristics of the ECM, which is provided by osmotic swelling (via water absorption) and resulting compressive stiffness (Ghosh and Taylor, 1987). As expected, GAG is an important component of tracheal ECM since it is responsible for attracting water to give its biomechanical properties (Teng et al. 2012). GAG molecules are also involved binding growth factors within the ECM to aid in cell recruitment and directing cell-specific function (Allison and Grande-Allen, 2006). Unfortunately, many previous decellularization studies have resulted in significant reduction of GAGs while collagen and other ECM constituents remained (Fishman et al. 2011). Therefore, even though

collagen is the major tensile stress bearing protein in the ECM (and the body), we focused on measuring GAGs post-decellularization. Clearly, retaining GAGs within the ECM was an important goal for the current study, as this result is expected to be a favourable property for future tissue engineering applications.

Previously reported tracheal decellularization techniques have commonly resulted in scaffolds with reduced mechanical properties, mainly through the loss of GAGs (Stapleton et al. 2008; Haykal et al. 2012; Jungebluth et al. 2009). Other studies with different cartilage tissues have also shown similar findings with significant reductions in mechanical strength post-decellularization (Schwarz et al. 2012; Jungebluth et al. 2009). All together, these changes may contribute to cell repopulation problems, chondrocyte loss, and post-implant airway stenosis (Ma et al. 2013). In contrast, the GAG content was not significantly altered with our decellularization protocols DC1 and DC2a-e. However, the added freeze-thaw pre-treatments did result in significant reductions in GAGs post-decellularization (DC3 protocol). Uniaxial tensile testing showed that there were significant decreases in both modulus and ultimate tensile stress. Therefore, the DC1 and DC2a-e decellularization protocols may be considered to have achieved the most optimal balance between treating the tissue sufficiently to confer non-immunogenicity (i.e. significant reduction of DNA) while maintaining the ECM structure (i.e. no significant change in GAG content and tensile properties). However, as mentioned above, it is unclear if the residual cells more prevalent in the DC1 and DC2a-e treated specimens will lead to problems with negative host responses post-implantation. As well, although the reduction in GAG content was statistically significant in DC3 treated ECMs, this change was not noticeable on macroscopic analysis. That is, the tubular structure was maintained and tissue handling was similar to fresh tissue and to DC1 and DC2a-e treated tissues.

Therefore, future studies with cell repopulation and in vivo experiments are required to determine which parameter (reduction in DNA versus maintenance of GAGs) should be considered the most imperative in terms of tissue regeneration.

5.1.4 Histological Analysis

H&E staining was used as another assessment to determine whether cells were present in the decellularized ECM (via cell nuclei staining). Overall, similar histological results were obtained with DC1 and DC2a-e decellularization protocols. After treatment, no cell nuclei staining were visible within the perichondrium, respiratory epithelium, and the outer regions of the cartilage ECM. Concurrently, a small number of nuclei staining was observed in the lacunae within the deep areas of the cartilage ECM. However, DNA quantification assay showed that DNA content was significantly reduced to trace amounts compared with fresh trachea.

Under qualitative, visual examination, there appeared to be no substantial difference between any of the five modified decellularization protocols DC2a-e in terms of nuclei staining. This indicates that increasing the exposure times to Solutions A, B, and C, did not result in noticeable changes with respect to cell removal. Also, no significant differences were noted on other characterization studies between the modified decellularization protocols. Therefore, future studies should be carried out with the shortest decellularization protocol to increase the efficiency of the entire process. Moreover, in order to determine which specific steps can be further shortened without affecting the efficacy, characterization studies should be carried out after each step. Such a process analysis will give insight into the detailed mechanism of decellularization, provide evidence for the assumed purposes of each solution, and will assist in developing an optimized protocol.

Specimens treated with the DC3 protocol showed no residual cell nuclei staining even within the deep areas of the cartilage ECM. There were some scattered areas of staining in the lacunae in some parts of the decellularized cartilage ECM, but on higher magnification, this staining was observed to be weak and indeterminate. That is, the staining visualized in the lacunae of fresh tissue, which was more intense and discrete, was not visualized in the DC3 treated ECMs. This likely indicates that the rare staining in the decellularized tissue was due to poorly soluble cytoskeletal components and remnant cellular debris rather than intact cell nuclei (Stapleton et al. 2008). There is potential that the remaining cellular debris within the ECM scaffold may cause unwanted host reaction when implanted in non-autologous recipients. However, there is some evidence that the host response may be more limited compared to ECM scaffolds that contain completely intact cells and genomic DNA within the substance of the ECM (Macchiarini et al. 2008; Gilbert et al. 2008). Again, further in vivo studies are needed to assess whether cellular debris react in the same manner as intact cell in terms of host response.

Masson's trichrome staining results showed that the major histoarchitecture of the tracheal tissue, including the basement membrane and submucosa, was maintained following decellularization. This was found consistently after all decellularization protocols (DC1, DC2a-e, and DC3). Furthermore, the general distribution and organization of collagen was similar between fresh and decellularized ECM treated with all protocols. More specifically, collagen was found to be concentrated around the outer regions of the cartilage ECM in both fresh and decellularized tissues. Future studies that quantitatively assess for collagen (e.g. hydroxyproline assay) or immunolabeling for collagen and other important ECM proteins should be done to confirm the results of Masson's trichrome and H&E staining.

5.1.5 Immunohistochemistry

To further assess for cell and cellular debris removal from the ECM, immunohistochemical analysis was performed. Overall, the results showed that cell and cellular components were largely removed, which verified the H&E findings. Specifically, immunostaining with anti-HLA-ABC and anti-β-Actin primary antibodies of DC1 and DC2a-e decellularized tissue sections demonstrated only minute traces of HLA-ABC and β-Actin positivity, respectively. There was strong staining for HLA-ABC and β-Actin in the fresh tissue and comparatively weaker staining in the decellularized tissue treated with the DC3 protocol.

The rare areas of positive staining may be attributed to the poorly soluble cytoskeletal component (β-Actin) or cellular debris (HLA-ABC). This indicates that cell lysis had occurred, which exposed the cell membrane fragments with their antigenic cell surface markers, as well as some of the intracellular components. Immunolabeling in other studies also demonstrated minor traces of positive staining suggesting that poorly soluble cytoskeletal components, such as β-Actin, or cellular debris, such as fragments of cell membrane with their cell surface markers, were not fully removed following decellularization (Badylak et al. 2011). Similar to DNA, it is unclear whether trace amounts of foreign antigens can result in antibody-mediated inflammation that has the potential to result in tissue injury and calcification post-implantation.

5.1.6 Mechanical Testing

To further support the functional importance of retaining GAGs and to determine the post-decellularization biomechanical properties of the resulting ECM, uniaxial tensile testing was performed. The decellularization protocols DC1 and DC2a-e did not

significantly affect the modulus and ultimate tensile strength of the resulting ECM scaffold. These outcomes are additional evidence that the structural integrity was satisfactorily maintained in comparison to the native tissue. However, the DC3 decellularization protocol resulted in significant reduction of both the modulus and ultimate tensile strength. Therefore, the mechanical testing results were in keeping with the GAG content outcome, which was found to be significantly reduced after the freeze-thaw pre-treatments. This may affect scaffold performance when implanted into a host since there is a higher risk of complication at the anastomotic site, such as excessive granulation tissue formation, stenosis, dehiscence, and collapse (Fishman et al. 2014). Hence, even though the DC3 protocol was associated with further reduction in cells on histological analysis, the mechanical properties were significantly changed, which in turn can lead to negative host responses. Despite the weakening of the tracheal cartilage, however, the decellularized trachea was able to maintain its patent lumen, and during tissue handling no noteworthy difference was observed compared to fresh tissue (and tissues treated with DC1 and DC2a-e decellularization protocols). Thus, cell repopulation and in vivo studies are required to determine whether the reduction in tensile properties will cause actual problems.

It must be noted that the mechanical properties measured in this study will be influenced by friction at the tissue/instrument interface, which needs to be considered when comparing the results to other studies (Nimeskern et al. 2014). As well, the tensile testing was not carried out under physiologic conditions. However, the main purpose of the tensile testing was to determine whether the decellularization protocols in the current study significantly altered the mechanical properties of the tracheal tissue and not to measure the biomechanics of rabbit trachea per se.

5.1.7 Scanning Electron Microscopy

SEM was performed to qualitatively evaluate the surface ultrastructural characteristics of the fresh and decellularized ECM. The surface properties of any tissue engineering scaffold (e.g. topography, pore size, porosity) is crucial because reseeded cells will not attach if the surface is not conducive to perform this very important function. With SEM, the interwoven collagen network of decellularized tissue treated with DC1 and DC2a-e protocols appeared to be similar to what was observed in the fresh tissue. This was in contrast to several previously reported studies of tracheal decellularization, which resulted in some changes in the surface ultrastructural characteristics (Zang et al. 2012; Crowley et al. 2015; Lange et al. 2015). For example, a study with human and porcine tracheal decellularization showed collagen fibers being bound more loosely post-treatment (Lange et al. 2015). Therefore, the DC1 and DC2a-e decellularization protocols used in the current study may have advantages over other protocols, as the ability to maintain the surface ultrastructural characteristics was demonstrated.

The freeze-thaw pre-treatments used in this study (DC3 protocol), however, seem to have disrupted some of the surface ultrastructural appearance of the tracheal ECM. More specifically, the arrangements of the collagen fiber bundles were not as uniform in the decellularized tissue compared to fresh trachea (i.e. the ECM may have slightly "opened up" due to ice crystal formation and thaw). Yet, the collagen fibers showed no gross evidence of damage. As well, the SEM analysis did not reveal any major changes in the pore-like structures on the tracheal surface (i.e. spaces between collagen fiber bundles). Therefore, it is unclear whether the disruption in the surface topography of the

DC3 treated decellularized trachea will negatively affect its ability for cell adhesion and engraftment.

5.2 Tissue Engineering Scaffolds

5.2.1 Extracellular Matrix

All tissues and organs possess naturally occurring ECM that is secreted and maintained by resident cells. The complex structure and organization of the ECM is specific to each tissue or organ (Brown et al. 2006; Gilbert et al. 2008); however, many components (e.g. collagen, GAGs) are highly conserved across species, thereby allowing non-autologous implantation. That is, although some components of the ECM may be considered immunogenic (e.g. cells), most ECM structural molecules are highly conserved between eukaryotic species and are not known to be histoincompatible (Egelman, 2011). Normally, the structural and functional proteins of the ECM are in a state of dynamic equilibrium within the surrounding microenvironment (Bissell and Aggeler, 1987). In addition to providing structural support, ECM components also aid cells to communicate with each other and to its surroundings (Kleinman et al. 2003; Rosso et al. 2004). The ECM is also biocompatible, and able to undergo degradation and remodeling within the appropriate host system. Finally, ECM can provide a supportive milieu for angiogenesis and allow for the diffusion of nutrients from blood vessels to cells within the ECM (Gilbert et al. 2007). Therefore, ECM can be considered the ideal scaffold material in tissue engineering (Gilbert et al. 2007).

Naturally occurring ECM possesses many bioinductive properties that allow for constructive remodeling of tissue after in vivo implantation (Badylak et al. 2011). This favourable remodeling or healing of tissue is due to many intrinsic characteristics of the ECM including its biomechanical properties, and cellular and external environmental

cues provided by the ECM components (Badylak et al. 2011). For instance, host cell attachment may occur through naturally occurring collagen, fibronectin, and laminin ligands within the ECM. Growth factors, such as basic fibroblast growth factor (bFGF) (Hodde et al. 2005), transforming growth factor-β (TGF-β) (Hodde et al. 2002), and vascular endothelial growth factor (VEGF) (Hodde et al. 2001) are also required for normal cell function (e.g. cell infiltration, mitogenesis, angiogenesis) within an ECM. Importantly, previous studies have shown that these intrinsic molecules and growth factors within an ECM can survive some forms of tissue processing and sterilization (Hodde et al. 2002). When such an ECM undergoes degradation post-implantation, the important bioinductive molecules and growth factors may be released, which can have a positive impact on tissue healing and remodeling (Hodde et al. 2001; Hodde et al. 2002). The degradation process itself, which is mostly guided by repopulated and surrounding cells, could potentially be a mechanism for controlled release of the vital ECM constituent molecules required for normal tissue healing or regeneration (Hodde et al. 2002). This process, in turn, will further recruit and maintain primary cells or bone marrow-derived undifferentiated progenitor cells that are involved in long-term tissue remodeling (Badylak et al. 2001). Other related events may include generation of antimicrobial peptides that can help protect the healing site from pathogens (Medberry et al. 2012), and angiogenesis and endothelial cell recruitment modulated by other signaling peptides that originate from intrinsic factors within the ECM (Li et al. 2004). These naturally occurring ECM molecules and growth factors crucial for tissue remodeling are difficult to reproduce on a synthetic scaffold. Thus, decellularized ECM may have advantages over synthetic scaffolds.

5.2.2 Synthetic Scaffolds

Although a great deal of attention has been focused on naturally derived scaffolds or decellularized ECMs, important advances in synthetic scaffolds have also been made in tracheal tissue engineering. One of the major advantages of synthetic scaffolds is the relatively straightforward and customizable nature of fabricating the desired shape, dimensions, and physical and biomechanical properties (e.g. porosity). More recently, some researchers have attempted to generate synthetic scaffolds to mimic natural ECM. For instance, 'smart' polymers with embedded signaling molecules to promote cell-scaffold interaction similar to naturally derived ECM have been reported (Fishman et al. 2011). As well, alternative polymers, such as electrospun polyethylene terephthalate and polyurethane scaffolds, have been designed to closely resembles the microarchitecture seen in native tracheal ECM (Badylak, 2007; Gilbert et al. 2006). Novel nanocomposite synthetic materials have also been studied as a possible scaffold for tracheal tissue engineering (Del Gaudio et al. 2014). However, some of the more recent techniques used to generate synthetic scaffolds may require the use of potentially cytotoxic agents. For example, organic solvents used in electrospinning, if retained, could be cytotoxic in vitro or in vivo (Ott et al. 2015). Also, adverse events have been observed even with well-established synthetic biomaterials. For instance, rabbit deaths due to polyglycolic acid (PGA)-derived cell-scaffold constructs that appeared to cause a significant inflammatory response due to prolonged degradation in animal model experiments has been reported (Sittinger et al. 1996). Conversely, it is well known that naturally derived scaffolds tend to exhibit more rapid degradative properties (Grayson et al. 2004), whereas persistent synthetic scaffold material may promote unwanted chronic inflammatory response. Future studies pertaining to synthetic scaffolds should therefore ensure that there are no

residual cytotoxic agents and there isn't a prolonged degradation period. Also, studies that directly compare synthetic scaffolds to other synthetic scaffolds, and also to naturally derived scaffolds should help researchers and clinicians determine the best option for clinical trials.

5.2.3 Novel Scaffolds

Researchers have also attempted to generate naturally derived scaffolds in a customizable manner by using prefabricated molds and allowing cell/scaffold construct to gel and cast to its shape. Shin et al. recently reported seeding MSCs on a porcine cartilage powder (PCP) scaffold to repair a tracheal defect in a rabbit model (Shin et al. 2015). The PCP was made with minced and decellularized porcine articular cartilage and molded into a 5 x 12 mm (height x diameter) scaffold. MSCs from rabbit bone marrow were seeded onto the PCP scaffold and after 7 weeks of culturing, the constructs were implanted in six rabbits with induced tracheal defects. Endoscopic examination at 10 weeks post-surgery showed that there was respiratory epithelial regeneration with no signs of collapse or stenosis. Histological evaluation demonstrated successful neocartilage formation with minimal inflammation or granulation tissue formation, and ciliary beating frequency was not significantly different than the normal adjacent mucosa. The authors concluded that MSCs cultured with a PCP scaffold in a prefabricated mold generated an implantable tracheal graft material in rabbits without any signs of graft rejection (Shin et al. 2015). Although promising, no mechanical testing or long-term outcomes were reported. As well, the tracheal defect was small (i.e. not a full circumferential defect) and therefore the long-term performance of the cell/scaffold construct in a larger segmental defect remains unclear.

Another very recent study used a fibrous synthetic scaffold, which demonstrated promising outcomes even without the use of cells (Ott et al. 2015). Specifically, a tunable, fibrous scaffold with encapsulated chondrogenic growth factor (TGF-β3) or seeded allogeneic rabbit bone marrow mesenchymal stromal cells (BMSCs) were studied in an induced tracheal defect rabbit model. After 6 or 12 weeks, the in vivo functionality of the scaffold with and without TGF-β3 or BMSCs was assessed. Overall, the results demonstrated that a relatively straightforward, acellular scaffold alone was a viable option to allow healing of tracheal defects in rabbits (Ott et al. 2015). The authors concluded that the native trachea-like performance of the scaffold-only group suggests that an acellular approach may be a possibility for tracheal defect repair. The implication is that a simple, material-based construct alone could be adequate in tracheal tissue engineering. However, similar to the above study, the tracheal defect was quite small and long-term results were lacking.

5.2.4 Tracheal Scaffolds Summary

Although progress has been made in terms of synthetic and novel scaffolds in tracheal tissue engineering, decellularization remains the most promising approach. Naturally derived ECM can provide not only the physical support to cells but also the optimal biological cues and signals in promoting tissue repair or regeneration (Badylak, 2005; Badylak, 2007). However, the intricate nature of the microanatomic organization and composition of signaling and structural molecules and growth factors of the ECM has not yet been fully elucidated. Hence, it is not possible to replicate naturally derived ECM in a laboratory setting at this time (Crapo et al. 2011). In order to overcome the incomplete knowledge of naturally derived ECM structure, protein release quantification

and bioactivity testing should be performed to accurately assess the microanatomical characteristics. Promisingly, previous studies of some synthetic scaffolds have shown that ECM associated molecules and growth factors can be incorporated into a synthetic construct and they can maintain the intended bioactivity after release from the scaffolds. Furthermore, various adjunct tissue engineering techniques, such as salt complexation, coaxial electrospinning, hydrophilic additives, and pH-maintaining basic salt additives, can be utilized to improve the stability and function of ECM associated proteins in synthetic scaffolds (Ji et al. 2011; Li et al. 2015). Overall, ECM generation by decellularization of natural tissues still seems to have advantages compared to other techniques at this time.

5.3 Previous Decellularization Treatments

5.3.1 Detergents and Enzymes

Many different decellularization protocols have been published for various types of tissues. The specific agents involved and length of the decellularization process differ greatly. However, there are some common themes found in nearly all published decellularization protocols. Most protocols have used some form of detergent-enzymatic treatment, which was initially developed to isolate basement membranes by using sodium deoxycholate supplemented with distilled water and DNAse (Meezan et al. 1975). Detergents are used to cause ECM disruption and cell lysis; they also to help with removal of cellular debris. Enzymes usually digest unwanted substances (e.g. nucleases breaking down DNA and RNA) to aid their removal from the ECM. A later step to sterilize the scaffold is also included in most decellularization protocols (see below).

Decellularization of very thin tissues, such as skin, has demonstrated relative success, which have led to commercial products being available for clinical use (e.g.

GRAFTJACKET® and AlloDerm®). Thicker tissue, like cartilage, however, is more challenging to decellularize effectively. Traditionally, attempts to decellularize cartilage tissue through its dense ECM required stronger decellularizing agents, such as ionic detergents (Stapleton et al. 2008; Elder et al. 2009). In general, ionic detergents in biomedical research are surfactants used to disrupt cell membranes to help release intracellular components in a soluble form. That is, they are effective in breaking down and solubilizing cell membranes where the immunogenic MHC antigen markers reside (Seddon et al. 2004). Ionic detergents are very efficient in removing cellular debris but they also tend to disrupt the native tissue structure, which may weaken the integrity of ECM (Gilbert, 2006; Conconi et al. 2005; Jungebluth et al. 2009). One of the most frequently used ionic detergents in decellularization is sodium dodecyl sulfate (SDS). SDS is an anionic surfactant found in some cleaning products that has shown to be an effective decellularization agent in terms of cell removal. However, SDS has also been found to be a very disruptive substance (Gilbert, 2006). Specifically, previous decellularization studies with porcine heart valves (Bodnar et al. 1986) and bovine pericardium (Courtman et al. 1994) demonstrated that SDS treatment resulted in significant fragmentation and edema of collagen fibers in the ECM. SDS has also been shown to remove GAGs and significantly weaken biomechanical properties (Gilbert, 2006). The precise mechanism of SDS related ECM damage is unknown but most likely involves the proteases released from cells rather than SDS itself (Booth et al. 2002). Also, research suggests that SDS can slightly alter the triple helical structure of collagen, which may in turn lead to changes in how cells respond to the ECM (Gratzer et al. 2006).

While it is desirable that the decellularization process will not alter the structure and composition of the ECM, some disruption is unavoidable as the agents involved in

cellular removal must access the entire ECM. As well, the removal of cellular components through the ECM requires some opening up of the ECM structure to allow movement of the cells and cellular debris out. The decellularization protocols used in the current study did not contain SDS; however, similar detergent/surfactant agents (Triton X-100 and TnBP) were employed to remove cellular debris. In order to avoid potential damage to the ECM due to detergent use during the decellularization process, we incorporated protease inhibitors (EDTA, PMSF) into the protocol. Some other studies using SDS and other detergents have also used protease inhibitors in conjunction to reduce the potential negative effect on the ECM structure (Lee et al. 2014). Our results also verify that adding protease inhibitors is a viable strategy when using detergents during decellularization. Moreover, the detergents/surfactants used in this study were non-ionic in nature and therefore, higher concentrations were utilized without any negative consequences. This approach may have contributed to the successful removal of cells and immunogenic material, while not causing major disruption to the ECM structure.

5.3.2 Sterilization

As mentioned above, most decellularization protocols contain a sterilization or decontamination step to remove endotoxins and intact viral and bacterial genetic components that may be present. Sterilization can be done with straightforward treatments, such as incubation with acids and solvents, or with more involved methods, such as gamma-radiation, ethylene oxide treatment, and electron beam irradiation. Newer sterilization methods, such as treatment with supercritical carbon dioxide, have also been reported (Qiu et al. 2009). Some techniques can be considered too weak and lack the necessary penetration required for adequate sterilization, but more aggressive methods

may damage important ECM components and negatively affect the biomechanical properties (Gorschewsky et al. 2005; Sun and Leung, 2008). Therefore, a balance must be achieved between sufficient sterilization and maintenance of adequate ECM structure. Also, consideration must be given to the practical aspects (e.g. wider-scale standardization and quality assurance) before a sterilization technique can be broadly accepted in the manufacturing of tissue engineering scaffolds.

Peracetic acid is an organic compound with antimicrobial properties that has been used in many previous decellularization protocols. It has been proven to be an effective disinfecting agent and is commonly used to sterilize hospital equipments (Rutala and Weber, 1999). However, peracetic acid is recognized to be a potential cytotoxic agent (Ryu et al. 2013). Peracetic acid was used to treat the tracheal cartilage tissue in the current study. It was the last agent to be applied during the decellularization process before the final washing step in PBS. The final wash with PBS was extensive (19 hours) to ensure that peracetic acid and other chemical and biological reagents used earlier were not retained within the decellularized ECM. To confirm the removal of peracetic acid and other potential cytotoxic agents, biocompatibility assay was performed. Specifically, contact cytotoxicity assays were carried out to determine the effect of any potential remaining decellularization agents within the scaffold on the growth of HEK 293 cells in vitro, as previously described (Kheir et al. 2011). The results showed that there was no cytotoxicity associated with decellularized tracheal tissue treated with all protocols. This was an important finding as ECM scaffolds with high concentrations of residual chemicals are likely to be toxic to cells (Gilbert, 2006) and may result in adverse host responses in vivo (Nagata et al. 2010; Brown et al. 2009). Thus, it is probable that the current ECM scaffolds will demonstrate cell compatibility with future recellularization

experiments.

5.3.3 Adjunct Treatments

In addition to the standard decellularization agents described above, adjunct treatments have been used to enhance the decellularization process. In general, these methods are typically used to increase exposure and penetration of the decellularization agents to all parts of the tissue that is being treated. Some of the more straightforward adjunct techniques used in the past involves applying physical treatments (e.g. making actual holes in the tissue with micro-punctures) to make the tissue being treated more porous (Lovati et al. 2016; Asghari et al. 2016). The current study also employed a relatively simple adjunct strategy of freeze-thaw pre-treatments (DC3 protocol) with the expectation that the decellularization agents will achieve deeper penetration into the tracheal cartilage tissue. The main reason for applying the freeze-thaw pre-treatments was that within the deep regions of the ECM of the tracheal cartilage, some cell nuclei persisted to exist after DC1 and DC2a-e protocols, and the freeze-thaw process has been reported to increase cell lysis by opening up the ECM and allowing decellularization solution to better penetrate the tissue (Stapleton et al. 2008). Specifically, early results showed that the cell nuclei staining density on H&E analysis appeared to intensify with increasing distance from the periphery of the cartilage tissue. However, the tissues that underwent the freeze-thaw pre-treatments had no such cell nuclei staining pattern, even within the deep regions of the cartilage ECM. The proposed mechanism of freeze-thaw treatment involves freezing and thawing of the cells, which should promote cell lysis. In turn, the lysed cells with its exposed cellular debris and fragments will be more readily removed from the ECM with decellularization agents, such as surfactants and solvent solutions (e.g. Triton X-100, TnBP). Although effective in enhancing the overall

decellularization process, the main concern regarding the freeze-thaw treatments is that there could be weakening of the ECM through physical damage and reduction of vital constituent molecules such as GAGs (Giannitelli et al. 2015). That is, the ECM itself will also undergo freezing and thawing, which can disrupt structural arrangements. This finding was noted in the current study as the GAG content and the tensile parameters measured were significantly reduced post-DC3 treatment. These changes may negatively alter the recellularization process. Despite some degree of weakening, however, the tracheal tissue was able to maintain its lumen patency and handling of the tissue was deemed to be similar qualitatively to DC1 and DC2a-e treated and fresh tissue. Furthermore, cell extraction was seen throughout the entire cartilage tissue and the overall histoarchitecture was well preserved, indicating no substantial change in the macrostructure of the ECM. Clearly, further studies are warranted to determine the whether the freeze-thaw pre-treated ECM scaffold can resist physiological forces and pressures required in in vivo experiments.

More recent studies of adjunct treatments in development of tissue engineering scaffolds include fabrication of direct micro-perforations using a femtosecond laser (Wang et al. 2015), particle transport through hydrogels (Vladescu et al. 2012), and placement of synthetic hollow fibers to the center of scaffolds (Bettahalli et al. 2011). Another very recently published study used vacuum assisted decellularization to treat porcine tracheal tissue (Lange et al. 2015). The negative pressure of the vacuum applied was thought to draw the decellularization agents deeper into the tracheal tissue (see below for details). As mentioned above, most of the adjunct treatments are intended to improve the delivery or diffusion of decellularization agents to the deep central regions of the scaffold to perform optimal cellular extraction to confer non-immunogenicity. Another

advantage of increased permeability may involve enhanced cell repopulation and in-growth of surrounding tissue, cells, and signaling biomolecules in an in vivo setting to optimize tissue healing and regeneration (Wang et al. 2015).

As tissue micro-architecture plays a critical role in how effective the decellularization process is, further refinements and comparison between different adjunct techniques are required before wide acceptance can occur. Future experiments should therefore include studies to explore the diffusion issues related to exposure of decellularization agents to optimize cellular and genetic material extraction, while maintaining the overall ECM structure.

5.3.4 Cartilage Regeneration

As indicated above, a well-designed tissue engineering scaffold is suppose to disintegrate as repopulated cells gain their normal phenotype and produce their own ECM. The neo-tissue then assumes function and becomes incorporated into the in vivo surrounding environment. Although the issue of neo-cartilage formation is beyond the scope of this study, it is important to consider because the eventual objective is to generate new tissue that can be used as replacement trachea. However, the specific mechanism of how new cartilage is generated in tracheal tissue engineering is not well known. Research does suggest that both chondrocytes (either primary chondrocytes or precursor cells, such as bone marrow derived MSCs) and respiratory epithelial cells, in addition to an adequate bioscaffold, are required for normal cartilage regeneration (Fishman et al. 2011). Yet, the details involved in this process have not been fully elucidated. For instance, the role of perichondrium and adjacent periosteum in joint cartilage healing is well known as they can provide (in time) cells for new cartilage formation (Duynstee et al. 2002; O'Driscoll and Fitzsimmons, 2001). However, there are

no studies to show a similar healing process is involved in tracheal hyaline cartilage regeneration. In the current study, the inner most layer of perichondrium (cambium) was left attached to the tracheal cartilage and was subjected to the decellularization processes. As shown in the histological and immunohistochemical images, perichondrial cells were removed by all decellularization treatments but at the same time the ECM of the inner layer of perichondrium appeared intact and undisturbed. Again, the role of this perichondrial ECM in cell repopulation and new tissue formation is unknown at this time and requires further studies.

5.4 Animal Models

A number of different animal models have been used in previous tracheal tissue engineering studies. Mainly, they include mice (Wu et al. 2007), rats (Zang et al. 2012), pigs (Lange et al. 2015), and rabbits (Jacobs et al. 2016). Although there is no agreed upon animal model for tracheal research, New Zealand white rabbits appear to be the most commonly employed animal (ten Hallers et al. 2004). The current study also used New Zealand white rabbits due to its anatomical similarity to human trachea, and because the size of the rabbit trachea is similar to a pediatric (neonatal) trachea. However, due to the fragile nature of the rabbit trachea, some studies have reported difficulties with reconstructive surgery and inconsistent results with tracheal implantation (Ott et al. 2010). Furthermore, a recent study showed that the rabbit trachea has reduced capacity to resist tensile or compressive forces compared to human trachea (Jones et al. 2014). Hence, a better animal model for tracheal tissue engineering may be a larger animal such as sheep or dog.

An additional potential concern regarding the use of rabbit tracheal tissue is that most human tracheal diseases that may require replacement tissue involve adults. Adult

human trachea is thicker and more dense than pediatric and rabbit trachea and therefore, the effectiveness of the current decellularization protocols on adult trachea is unknown.

Another related consideration regarding animal models is gender selection. While choosing the optimal species is important, inclusion of both male and female animals should also be deemed necessary in future studies. Although it is unclear if there are significant differences between female and male rabbit trachea, the significance of accounting for gender differences has been recognized by the National Institutes of Health in United States, who stated that having both male and female animals will add strength to preclinical studies (Clayton et al. 2014). The male rabbit used in this and other tracheal tissue engineering studies was an adequate model for small animal work, but future in vivo studies should be gender inclusive and have a more mechanically robust trachea.

In the future, human trachea may serve as the ideal tissue to be decellularized to generate allografts for human transplantation (Macchiarini et al. 2008). Yet, a practical limitation is the need for cadaveric donors for allotransplants, which can be overcome by using xenogeneic sources. As well, a more refined and proficient decellularization protocol needs to be developed so that a wide scale production of decellularized tracheal ECM scaffold can occur. Obtaining human pediatric trachea for decellularization may also be difficult and not always practical.

Currently, most commercially available ECM scaffold biomaterials approved for surgical implantation are of xenogeneic origin (Crapo, 2011). For example, bovine (e.g. insulin) or porcine (e.g. heart valves) sourced biomaterials have been in clinical use for numerous years without evidence of significant adverse events. However, the tissue processing method must ensure that immunogenic cellular antigens that can cause

hyperacute rejection responses [e.g. porcine epitope 1-3 alpha galactosyl (α-gal)] are fully removed (Kheir et al. 2011). At the same time the major components of the ECM (e.g. GAGs, collagen), which are greatly conserved among species and well tolerated after xenotransplantation, should remain similar to the native structure. Therefore, the overall host response to any ECM biomaterial will vary according to the processing techniques used to prepare the implantable scaffold.

Although decellularized human tracheal ECM may be considered the most desirable scaffold choice since it can be considered the least immunogenic and structurally similar, xenogeneic grafts have been studied extensively and offer less constrained source of donor tissues. Also, many decellularization protocols have shown successful removal of immunogenic surface epitopes (Badylak and Gilbert, 2008). As such, animal model research is still important and should continue before using human tracheal tissue for decellularization on a wider scale.

5.5 Recent Advances in Decellularization and Tracheal Tissue Engineering

To date, tissue engineered tracheae have been successfully implanted in a small number of patients on compassionate grounds. However, the long-term remodeling and functional outcome remain largely unknown. In order for tissue engineering to a become widely accepted treatment modality in the clinical setting, the time and labour taken to produce the tracheal construct, along with the resultant financial costs, must be reduced. The first step in realizing this goal is to find methods to develop a scaffold material that is suitable (i.e. no significant immunogenicity and adequate biomechanical characteristics) to be used in tracheal tissue engineering. Fortunately, new research has attempted to resolve some of these issues.

5.5.1 Whole Organ Decellularization

Several recent decellularization studies have focused on generating whole organ ECM scaffolds that can be recellularized to create entire organs to be transplanted into xenogeneic and allogeneic recipients (Arenas-Herrera et al. 2013; He and Callanan, 2013). Although the specific protocols vary in many aspects (e.g. different decellularization agents used in different animal models), numerous studies have still utilized the underlying concept of DEM in decellularizing whole organs. This indicates the universal applicability of the DEM principle of decellularization to all types of tissues. For whole organ decellularization, researchers have used a relatively new method known as 'perfusion decellularization', which makes use of the native vasculature to perform the cell and genetic material extraction. More specifically, the decellularization and sterilization agents are introduced through the existing vascular system, either via antegrade or retrograde manner, which may allow sufficient exposure of the agents to all vital parts of the organ. In turn, cell and genetic material removal can be very effective as the necessary decellularization agents are able to reach all areas of the tissue, which allows for the production of complex ECM bioscaffolds of an organ in its entirety with preservation of the intrinsic vascular network (Crapo et al. 2011; Faulk et al. 2014). This complete 3D structure provides site-specific micro-environment, which control function at a local level within the organ. Such a scaffold combines the natural advantages and properties of the ECM, along with the organizational and architectural complexity of the whole organ. In addition, the inherent vascular network required for delivery of nutrients and oxygen for optimal tissue metabolism is maintained. These scaffolds then can be repopulated with cells, again via the intrinsic vascular system, to regenerate functioning organ constructs that can be placed in bioreactors. To date, whole organ decellularization

has been reported in animal model studies of the heart (Ott et al. 2008), lungs (Ott et al. 2010; Song et al. 2011), liver (Uygun et al. 2010), and kidney (Ross et al. 2009). Yet, similar to decellularization of other tissue types, the optimal perfusion decellularization process of whole organs has not yet been achieved. Moreover, some tissues such as cartilage are considered avascular (i.e. blood supply is segmental and/or is via diffusion from the surrounding perichondrium) and therefore perfusion decellularization technique may be limited to certain types of tissues.

5.5.2 Novel Methods in Tracheal Tissue Engineering

Modifications of traditional decellularization protocols, which build on the previous successes of DEMs, are starting to emerge to reduce the time and cycles of treatments required. Lange et al., very recently published promising results with vacuum assisted decellularization technique (briefly mentioned above in section 5.3.3), which was used to treat porcine tracheal tissues (Lange et al. 2015). The vacuum was thought to accelerate the delivery of decellularization agents and therefore improve the efficiency of the entire decellularization process. That is, the negative pressure of the vacuum applied during the decellularization process would draw solutions deeper and more rapidly into the tracheal tissue. With this modification, the authors reported less time (9 days) to prepare the scaffold, which showed significant reduction in DNA levels compared to specimens where decellularization was carried out under normal atmospheric pressures (vacuum group 36.83 ± 18.45 ng/mg vs. control group 137.8 ± 48.82 ng/mg, $P < 0.05$) (Lange et al. 2015). And although there were no significant differences in any of the biomechanical parameters tested (ultimate tensile stress, rupture force, elongation at break), the vacuum-assisted approach resulted in significantly lower GAG levels (retained about 40% of GAGs). As well, 9 days may still be considered ‘too long’ in terms of

manufacturing and commercialization, especially for cases where emergent reconstructive surgery is required (e.g. tracheal loss due to acute trauma). Further refinements are therefore required before vacuum-assisted decellularization technique can be accepted for wide clinical use in humans.

Another new strategy in tracheal tissue engineering has been called the modular tracheal tissue replacement strategy, where a traditional scaffold is not used. A recent example of this method was reported by Dikina and colleagues, who employed a custom designed culture wells and a ring-to-tube assembly system, which obviated the need for a scaffold (Dikina et al. 2015). Briefly, human MSCs, along with TGF-β1-delivering gelatin microspheres (to enhance chondrogenesis) were seeded in a donut-shaped culture wells made of agarose to form scaffold-free 3D tissue rings. After 2 days of culture, the ring-shaped materials were removed from the culture wells and stacked on silicone tubes to form 3- and 6-ring fused tubes. These tube constructs were thicker than rat trachea, and biomechanical tests showed similar properties (maximum load at failure, ultimate tensile stress on uniaxial testing) as the rat trachea. Histology and immunohistochemistry analyses revealed new cartilage formation, but no functional analysis (e.g. mucociliary clearance) was performed. The authors stated that the modular, bottom up approach is a promising platform to engineer complex tissues, and the purported advantage may be realized through the increased intercellular communication and signaling in a "scaffold-free" system that may enhance ECM production and remodeling as well as provide better integration upon implantation (Dikina et al. 2015).

Most tissue engineered tracheal cell-scaffold constructs require prolonged time to mature in bioreactors with controllable settings in laboratories. More recently however,

there have been reports of using the recipient's own body as a bioreactor for decellularized tracheal scaffolds. This "in vivo tissue engineering" was performed by seeding decellularized allogeneic tracheal scaffolds intraoperatively with autologous respiratory epithelial cells and bone marrow derived MSCs (Bader and Macchiarini, 2010). The constructs were implanted in a case series of nine pediatric and adult patients with benign and malignant diseases of the trachea all on compassionate basis. All bioengineered tracheal grafts were found to be vascularized and lined with respiratory mucosa and no graft-associated mortality was observed at 12 to 42 months post-transplant. However, partial collapse of the reconstructed airway was noted in three patients (Elliott et al. 2012; Laurence, 2010). The partial collapse was most likely due to the degradation of the ECM architecture and a reduction in the biomechanical properties that may have occurred after long-term in vivo storage (Baiguera et al. 2012). Therefore, similar to other studies, weakening of the cell-scaffold construct could not be avoided with this approach.

5.6 Limitations of Tracheal Decellularization

5.6.1 Limitations of Previous Studies

Past studies of tracheal decellularization have reported varying degrees of success. Overall, there are two major limitations noted when analyzing the previous results. First, several studies with differing decellularization protocols have demonstrated similar efficacy in terms of reducing the cellular and genetic materials (reviewed in Wurtz et al. 2015). Indeed, most protocols are highly proficient in their ability to extract and remove cells. However, repeated cycles of detergent, chemical, and enzyme treatments are necessary to achieve this goal, which can take weeks to months. Hence, the labour-intensive nature of the decellularization protocols published to date can be considered a

key obstacle, as they require too many steps for any of these techniques to be widely used in the clinical setting. That is, for a protocol to gain broad acceptance, practical manufacturing considerations (e.g. length, complexity, cost of the process) must be kept in mind. In addition, such a prolonged process is inappropriate and unworkable for prospective development in emergent and urgent situations when a graft material is required within a very short amount of time period. One of the least labour-intensive tracheal tissue decellularization protocol published to date involves five cycles of detergent-enzymatic treatments (Zang et al. 2012). Briefly, Brown Norway rat tracheae were treated with aggressive detergent-enzymatic treatments, which led to the 'complete' removal of antigenicity. Initial treatments were efficient in removing cells from non-cartilaginous tissues (e.g. perichondrium, membranous trachea), but repeated detergent treatments were needed to remove cellular debris within the tracheal cartilage. After five cycles, minimal amount of chondrocytes and MHC antigens remained within the decellularized matrix. Histoarchitecture of the ECM and basement membrane was retained after decellularization, and the ECM showed good biocompatibility with chondrocytes and epithelial cells on SEM assessment. However, there was a significant reduction in GAG content and decreased stiffness found on mechanical testing. As well, it is unclear whether there was any remnant genetic material in the ECM. Finally, although this was one of least labour-intensive tracheal decellularization protocols published to date, it still needed 2 to 3 weeks to complete. Clearly, more work is needed in reducing the time and cycles required for effective and practical decellularization of tracheal tissue.

To our knowledge, the decellularization protocols used in this study are the shortest protocols reported to date. Specifically, the DC1, DC2a, and DC3 protocols required only 3.5 days to complete since they all had identical solution exposure times.

Therefore, the decellularization protocols in this study can be considered a viable option for tissue engineering application. Since there were increased exposure times to Solutions A, B, and C in decellularization protocols DC2b-e, they were 9 to 33 hours longer than the DC1, DC2a, and DC3 protocols. However, the increased exposure times did not result in any significant improvements in decellularization in terms of biochemical and histological analyses. Thus, the shorter decellularization protocols were deemed to be sufficient enough for effective decellularization and will be used for future studies with cell repopulation and in vivo experiments.

The second major limitation of previous decellularization protocols is also related to the repeated DEMs required for decellularizing allograft or xenograft tracheae. During the decellularization process, the ECM is disrupted to allow exposure of decellularization agents throughout the entire substance of the tissue to promote complete removal of cellular and genetic material (Gilbert et al. 2006). This process has been associated with reduction in mechanical stability, mainly through the loss of GAGs (Haykal et al. 2012). As mentioned above, GAGs are one of the key components of tracheal cartilage ECM and provides much of the mechanical strength to resist compressive forces via its water resorption and storage capacity (Roberts, 1998). Unfortunately, many protocols have led to significant loss of GAGs post-decellularization (Stapleton et al. 2008; Elder et al. 2009; Zang et al. 2012). For example, using multiple cycles of DEM in porcine allografts and mice xenografts, Jungebluth et al. demonstrated that maximum force and rupture force were lower in decellularized trachea compared to native trachea (Jungebluth et al. 2009). Tissue deformity percentage was also higher in the decellularized trachea. Another study with repeated treatments using ionic detergent in rat trachea showed significant loss of GAGs (Zang et al. 2012). This loss of GAGs resulted in reduced compressive strength

(i.e. decreased stiffness and tensile strength), which also likely indicates collagen disruption in the cartilage and the intercartilaginous soft-tissues (Stapleton et al. 2008). Interestingly, the loss of GAGs has also been shown to reduce diffusion of decellularization solutions because there is decreased water retention within the ECM when GAGs are not present (Stapleton et al. 2008). Taken together, significant loss of GAGs may result in decellularization ineffectiveness and weakened structural integrity of the ECM. Subsequently, these changes can contribute to chondrocyte loss and subsequent postoperative airway stenosis (Ma et al. 2013). Therefore, it is crucial to find the right balance between decellularizing the tissue sufficiently to confer non-immunogenicity while trying to maintain the GAG content and biomechanical integrity.

5.6.2 Limitations of Current Study

Characterization of the decellularized ECM could have included other tests than what was included in this study. For example staining with Safranin O could have been performed to qualitatively assess for distribution of GAGs before and after decellularization (Zang et al. 2012). Other stains and antibodies in immunohistochemical studies may have identified different parts of the ECM as well for better characterization of the decellularized scaffold. Also, additional antibody staining against membrane-associated proteins or other immunogenic cellular components that are known to be anchored to ECMs should provide more information about the extent of decellularization. However, the characterization studies conducted in this study were consistent with a common panel of tests that have been used by other groups to demonstrate the important structural properties of ECM scaffolds (Badylak, 2005; Badylak, 2007). That is, the characterization studies are complementary and designed to assess the effectiveness of the decellularization process and properties that are necessary for subsequent recellularization

to occur successfully. More recently, some researchers have started reporting results from functional tests of ECM bioactivity since recellularization heavily depends the functional aspect of the scaffold (De Kock et al. 2011). Although ECM bioactivity was not directly measured in the current study, some of the characterization studies can be considered indirect measures. Moreover, functional tests of ECM bioactivity are still in its infancy as they are limited to single growth factor assays at this time (Soto-Gutierrez et al. 2011). Certainly, further studies with cell repopulation are required to demonstrate that the decellularized ECM generated in this study to be a viable tissue engineering scaffold material. Also, the cell-scaffold construct will have to demonstrate prolonged survival without negative adverse events in in vivo studies before the current decellularization techniques can be applied in the clinical setting (see below).

5.7 Future Directions

A decellularized ECM scaffold needs to be repopulated with appropriate cells for specific tissue regeneration to occur and for this tissue to exert normal function in vivo (Gilbert et al. 2006). For tracheal implant to be used in patients, two main requirements must be fulfilled. First, biomechanical integrity has to be preserved to maintain patency of the upper airway, and second, respiratory epithelial covering must be re-established on the luminal surface (Belsey, 1950). This means that both chondrocytes and epithelial cells are required for graft survival and function (Go et al. 2009; Remlinger et al. 2010). Due to the difficulties in using mature chondrocytes (e.g. donor site morbidity, low yield and need for in vitro expansion), bone marrow derived MSCs have been studied by many groups instead of primary chondrocytes (Fishman et al. 2014). MSCs have been found to be very reliable since they can be expanded in vitro and differentiated into chondrocytes with relative ease to aid in cartilage tissue engineering (Kojima et al. 2004). Therefore,

future studies with the decellularized tracheal scaffolds generated in this study will involve MSCs for chondrocyte recellularization.

Re-establishing epithelialization within the lumen of the tracheal ECM scaffold is also essential in tracheal tissue engineering to avoid granulation tissue formation, bacterial invasion, and stenosis of airway leading to upper airway obstruction and respiratory compromise (Grillo, 2002). However, recellularization with respiratory epithelial cells has not been as straightforward as chondrocyte repopulation. For effective recellularization to occur, the scaffold material must promote cell adherence, proliferation, and function (Badylak, 2007). A successfully decellularized scaffold should be very suitable to achieve these roles because the cells should recognize the ECM as their native "home" with factors that favour normal cell function. Thus, the decellularized ECM scaffolds in this study may have positive effect on respiratory cells in terms of adherence, compatibility, and function.

After the decellularized scaffold has been repopulated with MSCs and respiratory epithelial cells, the tracheal construct will then be placed in a dual chambered bioreactor with air and culture media interface and a rotating cylinder as previously described (Fishman et al. 2014). This unique bioreactor system has been able to support both MSC differentiated chondrocytes and respiratory epithelial cells to proliferate within and on the decellularized tracheal scaffold (Macchiarini et al. 2008). The exact condition and length required in the bioreactor for optimal tracheal construct generation will be determined in future studies.

Prior to clinical use, the cell-scaffold tracheal construct will also undergo in vivo experiments using an animal model. Various characterization studies will be performed to assess the viability and function of the tracheal construct. Specifically, bronchoscopy and

micro-computed tomography will allow whether intraluminal granulation tissue and stenosis formation is occurring in the trachea. Histology and immunohistochemistry will yield important information regarding the histoarchitecture and vascularization of the trachea and the status of the respiratory epithelium. Of note, previous studies have shown that the regenerated epithelial layer can appear to be functioning normally (i.e. clearing mucus) and macroscopically healthy, while at the microscopic level be discontinuous (Fishman et al. 2014). As a result, future research will focus on improving epithelial lining of the trachea pre-implantation through considering different designs and employing refinements of bioreactor conditions. For instance, the application of flow stimuli similar to what a trachea would normally encounter may support the development of an appropriately aligned, orientated, and functioning cilia of the respiratory epithelial cells before the construct is implanted, thereby initiating optimal mucus clearance post-implantation. In order to assess the functional aspect of epithelial covering, ciliary beating frequency will be measured and compared to normal adjacent mucosa as previously described (Shin et al. 2015).

In addition to generating a viable and implantable cell-scaffold construct, practical aspects must be addressed before widespread clinical use can be realized. That is, the implant material must not be too costly, easy to handle, and surgically implantable without too much difficulty in the operating room. Therefore, multidisciplinary research with scientists and clinicians should continue in tracheal tissue engineering.

CHAPTER 6: CONCLUSIONS

The fundamental objective of tracheal reconstruction is to produce an upper airway that is non-collapsible with a stable epithelial lining. As tracheal replacement material is not readily available, the possibility of generating trachea through tissue engineering approach is very attractive. This potential has already been partly realized through the use of decellularized tracheal scaffolds. Yet, several limitations still exist that requires solutions prior to tissue engineering techniques becoming widely used in the clinical setting. Specifically, the complexity and length of decellularization protocols should be optimized. The detergent enzymatic treatment processes used in this study largely preserved the structural integrity and tensile properties of the ECM, while the antigenicity was effectively reduced. As well, the entire decellularization process was very efficient in terms of time required. In turn, the decellularized ECM may serve as a viable tissue engineering scaffold material for tracheal graft generation. Future studies will investigate methods to recellularize the decellularized ECM using appropriate cell types and bioreactor conditioning. Studies will also be performed to assess the long-term viability, functionality, and remodeling of tracheal grafts in in vivo experiments.

REFERENCES

Allison DD, Grande-Allen KJ. Review. Hyaluronan: a powerful tissue engineering tool. Tissue Eng 2006;12:2131-40.

Arenas-Herrera JE, Ko IK, Atala A, Yoo JJ. Decellularization for whole organ bioengineering. Biomed Mater 2013;8:014106.

Asakura K, Shido F, Harabuchi Y, Shirasaki H, Wakashima J, Kataura A. Sternocleidomastoid muscle-clavicle myoosseous flap for single-stage reconstruction of postoperative tracheal defects in patients with invasive thyroid tumor. Three case reports. ORL J Otorhinolaryngol Relat Spec 1997;59:238-42.

Asnaghi MA, Jungebluth P, Raimondi MT, Dickson SC, Rees LE, Go T, et al. A double-chamber rotating bioreactor for the development of tissue-engineered hollow organs: from concept to clinical trial. Biomaterials 2009;30:5260-9.

Asghari F, Samiei M, Adibkia K, Akbarzadeh A, Davaran S. Biodegradable and biocompatible polymers for tissue engineering application: a review. Artif Cells Nanomed Biotechnol 2016; Epub ahead of print.

Bader A, Macchiarini P. Moving towards in situ tracheal regeneration: the bionic tissue engineered transplantation approach. J Cell Mol Med 2010;14:1877-99.

Badylak SF. Regenerative medicine and developmental biology: the role of the extracellular matrix. Anat Rec B New Anat 2005;287:36-41.

Badylak SF. The extracellular matrix as a biological scaffold material. Biomaterials 2007;28:3587-93.

Badylak SF, Brown BN, Gilbert TW, Daly KA, Huber A, Turner NJ. Biologic scaffolds for constructive tissue remodeling. Biomaterials 2011;32:316-9.

Badylak SF, Gilbert TW. Immune response to biologic scaffold materials. Semin Immunol 2008;20:109-16.

Badylak SF, Park K, Peppas N, McCabe G, Yoder M. Marrow-derived cells populate scaffolds composed of xenogeneic extracellular matrix. Exp Hematol 2001;29:1310-8.

Baiguera S, Del Gaudio C, Jaus MO, Polizzi L, Gonfiotti A, Comin CE, et al. Long-term changes to in vitro preserved bioengineered human trachea and their implications for decellularized tissues. Biomaterials 2012;33:3662-72.

Basbaum CB, Finkbeiner WE. Airway secretion: a cell-specific analysis. Horm Metab Res 1988;20:661-7.

Belsey R. Resection and reconstruction of the intrathoracic trachea. Br J Surg 1950;28:200-5.

Berg M, Enjnell H, Kovács A, Nayakawde N, Patil PB, Joshi M, et al. Replacement of a tracheal stenosis with a tissue-engineered human trachea using autologous stem cells: a case report. Tissue Eng Part A 2013;20:389-97.

Bettahalli NM, Vicente J, Moroni L, et al. Integration of hollow fiber membranes improves nutrient supply in three-dimensional tissue constructs. Acta Biomater 2011;7:3312-24.

Bissell MJ, Aggeler J. Dynamic reciprocity: how do extracellular matrix and hormones direct gene expression? Prog Clin Biol Res 1987;249:251-62.

Bodnar E, Olsen EG, Floria R, Dobrin J. Damage of porcine aortic valve tissue caused by surfactant sodiumdodecylsulfate. Thorac Cardiovasc Surg 1986;34:82-5.

Booth C, Korossis SA, Wilcox HE, Watterson KG, Kearney JN, Fisher J, et al. Tissue engineering of cardiac valve prostheses I: development and histological characterization of an acellular porcine scaffold. J Heart Valve Dis 2002;11:457-62.

Brigger MT, Boseley ME. Management of tracheal stenosis. Curr Opin Otolaryngol Head Neck Surg 2012;20:491-6.

Britt JC, Park SS. Autogenous tissue-engineered cartilage: evaluation as an implant material. Arch Otolaryngol Head Neck Surg 1998;124:671-7.

Brown B, Lindberg K, Reing J, Stolz DB, Badylak SF. The basement membrane component of biologic scaffold derived from extracellular matrix. Tissue Eng 2006;12:519-26.

Brown BN, Valentin JE, Stewart-Akers AM, McCabe GP, Badylak SF. Macrophage phenotype and remodeling outcomes in response to biologic scaffolds with and without a cellular component. Biomaterials 2009;30:1482-91.

Chauviere MV, Schutter RJ, Steigelman MB, Clark BZ, Grayson JK, Sahar DE. Comparison of AlloDerm and AlloMax tissue incorporation in rats. Ann Plast Surg 2014;73:282-5.

Chistiakov DA. Endogenous and exogenous stem cells: a role in lung repair and use in airway tissue engineering and transplantation. J Biomed Sci 2010;17:92.

Clayton JA, Collins FS. Policy: NIH to balance sex in cell and animal studies. Nature 2014;509:282-3.

Conconi MT, De Coppi P, Di Liddo R, Vigolog S, Zanon GF, Parnigotto PP, Nussdorfer GG. Tracheal matrices, obtained by a detergent-enzymatic method, support in vitro the adhesion of chondrocytes and tracheal epithelial cells. Transpl Int 2005;18:727-34.

Cotton RT. The problem of pediatric laryngotracheal stenosis: a clinical and experimental study on the efficacy of autogenous cartilaginous grafts placed between the vertically divided halves of the posterior lamina of the cricoid cartilage. Laryngoscope 1991;101:1-34.

Courtman DW, Pereira CA, Kashef V, McComb D, Lee JM, Wilson GJ. Development of a pericardial acellular biomaterial: biochemical and mechanical effects of cell extraction. J Biomed Mater Res 1994;28:655-66.

Crapo PM, Gilbert TW, Badylak SF. An overview of tissue and whole organ decellularization processes. Biomaterials 2011;32:3233-43.

Crowley C, Birchall M, Seifalian AM. Trachea transplantation: from laboratory to patient. J Tissue Eng Regen Med 2015;9:357-67.

Delaere P, Vranckx J, Verleden G, De Leyn P, Van Raemdonck D, Leuven Tracheal Transplant Group. Tracheal allotransplantation after withdrawl of immunosuppressive therapy. N Engl J Med 2010;362:138-45.

Del Gaudio C, Baiguera S, Ajalloueian F, Bianco A, Macchiarini P. Are synthetic scaffolds suitable for the development of clinical tissue engineered tubular organs? J Biomed Mater Res A 2014;102:2427-47.

De Kock J, Ceelen L, De Spiegelaere W, Casteleyn C, Claes, P, Vanhaecke T, Rogiers V. Simple and quick method for whole-liver decellularization: a novel in vitro three-dimensional bio-engineering tool? Arch Toxicol 2011;85:607-12.

Dikina AD, Strobel HA, Lai BP, Rolle MW, Alsberg E. Engineered cartilaginous tubes for tracheal tissue replacement via self-assembly and fusion of human mesenchymal stem cell constructs. Biomaterials 2015;52:452-62.

Duynstee ML, Verwoerd-Verhoef HL, Verwoerd CD, Van Osch GJ. The dual role of perichondrium in cartilage wound healing. Plast Reconstr Surg 2002;110:1073-9.

Egelman E. Molecular evolution: actin's long lost relative found. Curr Biol 2001;11:R1022-4.

Elder BD, Eleswarapu SV, Athanasiou KA. Extraction techniques for the decellularization of tissue engineered articular cartilage constructs. Biomaterials 2009;30:3749-56.

Elliott MJ, De Coppi P, Speggiorin S, Roebuck D, Butler CR, Samuel E, et al. Stem-cell-based, tissue engineered tracheal replacement in a child: a 2-year follow-up study. Lancet 2012;380:994-1000.

Elliott MJ, Haw MP, Jacobs JP, Bailey CM, Evans JN, Herberhold C. Tracheal reconstruction in children using cadaveric homograft trachea. Eur J Cardiovasc Surg 1996;10:707-12.

Fabre D, Kolb F, Fadel E, Mercier O, Mussot S, Le Chevalier T, Dartevelle P. Successful tracheal replacement in humans using autologous tissues: an 8-year experience. Ann Thorac Surg 2013;96:1146-55.

Faulk DM, Johnson SA, Zhang L, Badylak SF. Role of the extracellular matrix in whole organ engineering. J Cell Physiol 2014;229:984-9.

Fishman JM, De Coppi P, Elliott MJ, Atala A, Brichall MA, Macchiarini P. Airway tissue engineering. Expert Opin Biol Ther 2011;11:1623-35.

Fishman JM, Wiles K, Lowdell MW, De Coppi P, Elliott MJ, Atala A, Birchall MA. Airway tissue engineering: an update. Expert Opin Biol Ther 2014;14:1477-91.

Freed LE, Guilak F, Guo XE, Gray ML, Tranquillo R, Holmes JW, et al. Advanced tools for tissue engineering: scaffolds, bioreactors, and signaling. Tissue Eng 2006;12:3285-305.

Ghosh P, Taylor TK. The knee joint meniscus. A fibrocartilage of some distinction. Clin Orthop Relat Res 1987;224:52-63.

Giannitelli SM, Mozetic P, Trombetta M, Rainer A. Combined additive manufacturing approached in tissue engineering. Acta Biomater 2015;24:1-11.

Gilbert TW, Sellaro TL, Badylak SF. Decellularization of tissues and organs. Biomaterials 2006;27:3675-83.

Gilbert TW, Stewart-Akers AM, Simmons-Byrd A, Badylak SF. Degradation and remodeling of small intestinal submucosa in canine Achilles tendon repair. J Bone Joint Surg Am 2007;89:621-30.

Gilbert TW, Wognum S, Joyce EM, Freytes DO, Sacks MS, Badylak SF. Collagen fiber alignment and biaxial mechanical behavior of porcine urinary bladder derived extracellular matrix. Biomaterials 2008;29:4775-82.

Giordano A, Galderisi U, Marino IR. From the laboratory bench to the patient's bedside: an update on clinical trials with msenchymal stem cells. J Cell Physiol 2007;211:27-35.

Glowacki J, Mizuno S. Collagen scaffolds for tissue engineering. Biopolymers 2008;89:338-44.

Go T, Jungebluth P, Baiguero S, Asnaghi A, Martorell J, Ostertag H, et al. Both epithelial cells and mesenchymal stem cell-derived chondrocytes contribute to the survival of tissue-engineered airway transplants in pigs. J Thorac Cardiovasc Surg 2009;139:437-43.

Gong YY, Xue JX, Zhang WJ, Zhou GD, Liu W, Cao Y. A sandwich model for engineering cartilage with acellular cartilage sheets and chondrocytes. Biomaterials 2011;32:2265-73.

Gorschewsky O, Puetz A, Riechert K, Klakow A, Becker R. Quantitative analysis of biochemical characteristics of bone-patellar tendon-bone allografts. Biomed Mater Eng 2005;15:403-11.

Graham ME, Gratzer PF, Bezuhly M, Hong P. Development and characterization of decellularized human nasoseptal cartilage matrix for use in tissue engineering. Laryngscope 2016 Epub ahead of print.

Gratzer PF, Harrison RD, Woods T. Matrix alteration and not residual sodium dodecyl sulfate cytotoxicity affects the cellular repopulation of a decellularized matrix. Tissue Eng 2006;12:2975-83.

Gray TE, Guzman K, Davis CW, Abdullah LH, Nettesheim P. Mucociliary differentiation of serially passaged normal human tracheobronchial epithelial cells. Am J Respir Cell Mol Biol 1996;14:103-12.

Grayson AC, Voskerician G, Lynn A, Anderson JM, Cima MJ, Langer R. Differential degradation rates in vivo and in vitro of biocompatible poly(lactic acid) and poly(glycolic acid) homo and co-polymers for a polymeric drug-delivery microchip. J Biomaterial Sci Polym Ed 2004;15:1281-304.

Grillo HC, McKhann CF. The acceptance and evolution of dermal homografts freed of viable cells. Transplantation 1964;2:48-59.

Grillo HC. Tracheal replacement: a critical review. Ann Thorac Surg 2002;73:1995-2004.

Harrington WT, Hung WC, Binns PM. Experimental tracheal homografting. J Laryngol Otol 1977;91:101-10.

Haykal S, Solease JP, Salna M, Hofer SO, Waddell TK. Evaluation of the structural integrity and extracellular matrix components of tracheal allografts following cyclical decellularization techniques: comparison of three protocols. Tissue Eng Part C Method 2012;18:614-23.

He M, Callanan A. Comparison of methods for whole-organ decellularization in tissue-engineering of bioartificial organs. Tissue Eng Part B 2013;19:194-208.

Hodde JP, Record RD, Liang HA, Badylak SF. Vascular endothelial growth factor in porcine-derived extracellular matrix. Endothelium 2001;8:11-24.

Hodde JP, Ernst DM, Hiles MC. An investigation of the long-term bioactivity of endogenous growth factor in OASIS Wound Matrix. J Wound Care 2005;14:23-5.

Hodde JP, Record RD, Tullius RS, Badylak SF. Retention of endothelial cell adherence to porcine-derived extracellular matrix after disinfection and sterilization. Tissue Eng 2002;8:225-34.

Hong HJ, Lee JS, Choi JW, Min BH, Lee HB, Kim CH. Transplantation of autologous chondrocytes seeded on a fibrin/hyaluronan composite gel into tracheal cartilage defects in rabbits: preliminary results. Artif Organs 2012;36:998-1006.

Horsfield K. The relation between structure and function in the airways of the lung. Br J Dis Chest 1974;68:145-60.

Iamizumi M, Nomoto Y, Sato Y, Sugino T, Miyake M, Wada I, et al. Evaluation of the use of induced pluripotent stem cells (iPSCs) for the regeneration of tracheal cartilage. Cell Transplant 2013;22:341-53.

Igai H, Chang SS, Gotoh M, Yamamoto Y, Misaki N, Okamoto T, et al. Regeneration of canine tracheal cartilage by slow release of basic fibroblast growth factor from gelatin sponge. ASAIO J 2006;52:86-91.

Igai H, Yamamoto Y, Chang SS, Yamamoto M, Tabata Y, Yokomise H. Tracheal cartilage regeneration by slow release of basic fibroblast growth factor from a gelatin sponge. J Thorac Cardiovasc Surg 2007;134:170-5.

Jacobs IN, Redden RA, Goldberg R, Hast M, Salowe R, Mauck RL, Doolin EJ. Pediatric laryngotracheal reconstruction with tissue-engineered cartilage in a rabbit model. Laryngoscope 2016;S1:S1-21.

Jackson TL, O'Brien EJ, Tuttle W, Meyer J. The experimental use of homogenous tracheal transplants in the restoration of continuity of the tracheobronchial tree. J Thorac Surg 1950;20:598-612.

Ji W, Sun Y, Yang F, van den Beuken JJ, Fan M, Chen Z, Jansen JA. Bioactive electrospun scaffolds delivering growth factors and genes for tissue engineering applications. Pharm Res 2011;28:1259-72.

Jacobs JP, Elliott MJ, Haw MP, et al. Pediatric tracheal homograft reconstruction: a novel approach to complex tracheal stenoses in children. J Thorac Cardiovasc Surg 1996;112:1549-58.

Jones MC, Rueggeberg FA, Faircloth HA, Cunningham AJ, Bush CM, Prosser JD, Waller JL, Postma GN, Weinberger PM. Defining the biomechanical properties of the rabbit trachea. Laryngoscope 2014;124:2352-8.

Jungebluth P, Alici E, Baiguera S, Le Blanc K, Blomberg P, Bozóky B, et al. Tracheobronchial transplantation with a stem-cell-seeded bioartifical nanocomposite: a proof-of-concept study. Lancet 2011;378:1997-2004.

Jungebluth P, Bader A, Baiguera S, Möller S, Jaus M, Lim ML, et al. The concept of in vivo airway tissue engineering. Biomaterials 2012;33:4319-26.

Jungebluth P, Go T, Asnaghi A, Bellini S, Martorell J, Calore C, et al. Structural and morphologic evaluation of a novel detergent-enzymatic tissue-engineering tracheal tubular matrix. J Thorac Cardiovasc Surg 2009;138:586-93.

Junqueira LC, Mones GS, Krisztán RM. The collagen of the vertebrate peripheral nervous system. Cell Tissue Res 1979;202:453-60.

Kajbafzadeh AM, Saketkish S, Sabetkish N, Muhammadnejad S, Akbarzadeh A, Tavangar SM, et al. In-vivo trachea regeneration: fabrication of a tissue-engineered trachea in nude mice using the body as a natural bioreactor. Surg Today 2015;45:1040-8.

Kheir E, Stapleton T, Shaw D, Jin Z, Fisher J, Ingham E. Development and characterization of an acellular porcine cartilage bone matrix for use in tissue engineering. J Biomed Mater Res Part A 2011; 99A:283-94.

Kim K, Doi A, Wen B, Ng K, Zhao R, Cahan P, et al. Epigenetic memory in induced pluripotent stem cells. Nature 2010;467:285-90.

Kleinman HK, Philp D, Hoffman MP. Role of the extracellular matrix in morphogenesis. Curr Opin Biotechnol 2003;14:526-32.

Kojima K, Ignotz RA, Kushibiki T. Tissue-engineered trachea from sheep marrow stromal cells with transforming growth factor B2 released from biodegradable microspheres in a nude rat recipient. J Thorac Cardiovasc Surg 2004;128:147-53.

Komura M, Komura H, Tanaka Y, Kanamori Y, Sugiyama M, Nakahara S, et al. Human tracheal chondrocytes as a cell source for augmenting stenotic tracheal segments: the first feasibility study in an in vivo culture system. Pediatr Surg Int 2008;24:1117-21.

Korossis SA, Booth C, Wilcox HE, Watterson KG, Kearney JN, Fisher J, Ingham E. Tissue engineering of cardiac valve prostheses II: biomechanical characterization of decellularized porcine aortic heart valves. J Heart Valve Dis 2002;11:463-71.

Kunisaki SM, Freedman DA, Fauza DO. Fetal tracheal reconstruction with cartilaginous grafts engineered from mesenchymal amniocytes. J Pediatr Sug 2006;41:675-82.

Lange P, Greco K, Partington L, Carvalho C, Oliani S, Birchall MA, et al. Pilot study of a novel vacuum-assisted method for decellularization of tracheae for clinical tissue engineering applications. J Tissue Eng Regen Med 2015 Epub ahead of print.

Laurance J. British boy received trachea transplant built with his own stem cells. BMJ 2010;340:c1633.

Lee PH, Kim JW, Bang OY, Ahn YH, Joo IS, Huh K. Autologous mesenchymal stem cell therapy delays the progression of neurological deficits in patients with multiple system atrophy. Clin Pharmacol Ther 2008;83:723-30.

Lee W, Miyagawa Y, Long C, Cooper DK, Hara H. A comparison of three methods of decellularization of pig corneas to reduce immunogenicity. Int J Ophthalmol 2014;7:587-93.

Levashov YN, Yablondsky PK, Cherny SM, Orlov SV, Shafirovsky BB, Kuznetzov IM. One-staged allotransplantation of thoracic segment of the trachea in a patient with idiopathic fibrosing mediastinitis, and marked tracheal stenosis. Eur J Cardiothorac Surg 1993;7:383-6.

Li F, Li W, Johnson S, Ingram D, Yoder M, Badylak S. Low-molecular-weight peptides derived from extracellular matrix as chemoattractants for primary endothelial cells. Endothelium 2004;11:199-206.

Li L, Zhou G, Wang Y, Yang G, Ding S, Zhou S. Controlled dual delivery of BMP-2 and dexamethasone by nanoparticle-embedded eletrospun nanofibers for the efficient repair of critical-sized rat calvarial defect. Biomaterials 2015;37:218-29.

Lin CH, Hsu SH, Huang CE, Cheng WT, Su JM. A scaffold-bioreactor system for a tissue-engineered trachea. Biomaterials 2009;30:4117-26.

Lovati AB, Bottagisio M, Moretti M. Decellularized and engineered tendons as biological substitutes: a critical review. Stem Cells Int 2016;1016:7276150.

Ma R, Li M, Luo J, Yu H, Sun Y, Cheng S, Cui P. Structural integrity, ECM components and immunogenicity of decellularized laryngeal scaffold with preserved cartilage. Biomaterials 2013;34:1790-98.

Macchiarini P, Jungebluth P, Go T, Asnaghi MA, Rees LE, Cogan TA, et al. Clinical transplantation of a tissue-engineered airway. Lancet 2008;372:2023-30.

Macchiarini P, Walles T, Biancosino C, Mertsching H. First human transplantation of a bioengineered airway tissue. J Thorac Cardiovasc Surg 2004;128:638-641.

Manoukian JJ, Tan AK. Embryology of the larynx. Tewfik TL. Der Kaloustian VM, eds. Congenital Anomalies of the Ear, Nose, and Throat. New York, NY: Oxford University Press; 1997.

Maresh A, Preciado DA, O'Connell AP, Zalzal GH. A comparative analysis of open surgery vs endoscopic balloon dilation for pediatric subglottic stenosis. JAMA Otolaryngol Head Neck Surg 2014;140:901-5.

Medberry CJ, Tottey S, Jiang H, Johnson SA, Badylak SF. Resistance to infection of five different materials in a rat body wall model. J Surg Res 2012;173:38-44.

Meezan E, Hjelle JT, Brendel K, Carlson EC. A simple, versatile, nondisruptive method for the isolation of morphologically and chemically pure basement membranes from several tissues. Life Sci 1975;17:1721-32.

Miller C, George S, Niklason L. Developing a tissue-engineered model of the human bronchiole. J Tissue Eng Regen Med 2010;4:619-27.

Mitchell JD, Mathisen DJ, Wright CD, Wain JC, Donahue DM, Moncure AC, Grillo HC. Clinical experience with carinal resection. J Thorac Cardiovasc Surg 1999;117:39-52.

Mitchell JD, Mathisen DJ, Wright CD, Wain JC, Donahue DM, Allan JS, et al. Resection for bronchogenic carcinoma involving the carina: Long-term results and effect of nodal status on outcome. J Thorac Cardiovasc Surg 2001;121:465-71.

Mou H, Zhao R, Sherwood R, Ahfeldt T, Lapey A, Wain J, et al. Generation of multipotent lung and airway progenitors from mouse ESCs and patient-specific cystic fibrosis iPSCs. Cell Stem Cell 2012;10:385-97.

Muir H. The chondrocyte, architext of cartilage. Biomechanics, structure, function and molecular biology of cartilage matrix macromolecules. Bioessays 1995;17:1039-48.

Mulliken JB, Grillo HC. The limits of tracheal resection with primary anatomosis: further anatomical studies in man. J Thorac Cardiovasc Surg 1968;55:418-21.

Nagata S, Hanayama R, Kawane K. Autoimmunity and the clearance of dead cells. Cell 2010;140:619-30.

Neville WE, Bolanowski PJ. Tracheal reconstruction. Surg Annu 1979;11:225-47.

Nimeskern L, van Osch GJ, Müller R, Stok KS. Quantitative evaluation of mechanical properties in tissue-engineered auricular cartilage. Tissue Eng Part B Rev 2014;20:17-27.

Nomoto Y, Okano W, Imaizumi M, Tani A, Nomoto M, Omori K. Bioengineered prosthesis with allogenic heterotopic fibroblasts for cricoid regeneration. Laryngoscope 2012;122:805-9.

O'Driscoll SW, Fitzsimmons JS. The role of periosteum in cartilage repair. Clin Orthop Relat Res. 2001;(391Suppl):S190-207.

Okumura N, Nakamura T, Matsume T, Tomihata K, Ikada Y, Shimizu Y. Experimental study on a new tracheal prosthesis made from collagen-conjugated mesh. J Thorac Cardiovasc Surg 1994;108:337-45.

Omori K, Nakamura T, Kanemaru S, Asato R, Yamashita M, Tanaka S, et al. Regenerative medicine of the trachea: the first human case. Ann Otol Rhinol Laryngol 2005;114:429-33.

Omori K, Tada Y, Suzuki T, Nomoto Y, Matsuzuka T, Kobayashi K, et al. Clinical application of in situ tissue engineering using a scaffolding technique for reconstruction of the larynx and trachea. Ann Otol Rhinol Laryngol 2008;117:673-8.

O'Rahilly R, Boyden EA. The timing and sequence of events in the development of the human respiratory system during the embryonic period proper. Z Anat Entwicklungsgesch 1973;141:237-50.

O'Rahilly R, Tucker JA. The early development of the larynx in staged human embryos. I. Embryos of the first five weeks (to stage 15). Ann Otol Rhinol Laryngol 1973;82:1-27.

O'Rahilly R, Müller F. Chevalier Jackson lecture. Respiratory and alimentary relations in staged human embryos. New embryological data and congenital anomalies. Ann Oto Rhinol Laryngol 1984;93:421-9.

Orenstein SB, Qiao Y, Kaur M, Klueh U, Kreutzer DL, Novitsky YW. Human monocyte activation by biologic and biodegradable meshes in vitro. Surg Endosc 2010;24:805-11.

Ott HC, Clippinger B, Conrad C, Schuetz C, Pomerantseva I, Ikonomou L, et al. Regeneration and orthotopic transplantation of a bioartificial lung. Nat Med 2010;16:927-33.

Ott HC, Matthiesen TS, Goh SK, Black LD, Kren SM, Netoff TI, Taylor DA. Perfusion-decellularized matrix: using nature's platform to engineer a bioartificial heart. Nat Med 2008;14:213-21.

Ott LM, Vu CH, Farris AL, Fox KD, Galbraith RA, Weiss ML, et al. Functional reconstruction of tracheal defects by protein-loaded, cell-seeded, fibrous constructs in rabbits. Tissue Eng Part A 2015;21:2390-403.

Pacheco CR, Rivero O, Porter JK. Experimental reconstructive surgery of the trachea. J Thorac Surg 1954;27:554-64.

Peulacher WC, Mooney D, Langer R, Upton J, Vacanti JP, Vacanti CA. Design of nasoseptal cartilage replacements synthesized from biodegradable polymers and chondrocytes. Biomaterials 1994;15:774-8.

Poole CA. Articular cartilage chondrons: form, functin and failure. J Anat 1997;191:1-13.

Prokakis C, Koletsis EN, Dedeilias P, Fligou F, Filos K, Dougenis D. Airway trauma: a review on epidemiology, mechanisms of injury, diagnosis and treatment. J Cardiothorac Surg 2014;9:117.

Qiu QQ, Leamy P, Brittingham J, Pomerleau J, Kabaria N, Connor J. Inactivation of bacterial spores and viruses in biological material using supercritical carbon dioxide with sterilant. J Biomed Mater Res B Appl Biomater 2009;91:572-8.

Reing JE, Brown BN, Daly KA, Freund JM, Gilbert TW, Hsiong SX, et al. The effects of processing methods upon mechanical and biologic properties of porcine dermal extracellular matrix scaffolds. Biomaterials 2010; 31:8626-33.

Remlinger NT, Czajka CA, Juhas ME, Vorp DA, Stolz DB, Badylak SF, et al. Hydrated xenogeneic decellularized tracheal matrix as a scaffold for tracheal reconstruction. Biomaterials 2010;31:3520-6.

Riquet M, Le Pimpec Barthes F, Souilamas R, Hidden G. Thoracic duct tributaries from intrathoracic organs. Ann Thorac Surg 2002;73:892-8.

Roberts N, Hogg D, Whitehouse GH, Dangerfield P. Quantitative analysis of diurnal variation in volume and water content of lumbar intervertebral discs. Clin Anat 1998;11:1-8.

Rose KG, Sesterhenn K, Wustrow F. Tracheal allotransplantation in man. Lancet 1979;1:433.

Ross EA, Williams MJ, Hamazaki T, Terada N, Clapp WL, Adin C, et al. Embryonic stem cells proliferate and differentiate when seeded into kidney scaffolds. J Am Soc Nephrol 2009;20:2338-47.

Rosso F, Giordano A, Barbarisi M, Barbarisi A. From cell-ECM interactions to tissue engineering. J Cell Physiol 2004;199:174-80.

Rubikas R, Matukaityte I, Jelisiejevas JJ, Rackauskas M. Surgical treatment of non-malignant laryngotracheal stenosis. Eur Arch Otorhinolaryngol 2014;271:2481-7.

Rutala WA, Weber DJ. Infection control: the role of disinfection and sterilization. J Hosp Infect 1999;43:S43-55.

Ryu M, Kobayashi T, Kawamukai E, Quan G, Furuta T. Cytotoxicity assessment of residual high-level disinfectants. Biocontrol Sci 2013;18:217-20.

Sachs LA, Finkbeiner WE, Widdicombe JH. Effects of media on differentiation of cultured human tracheal epithelium. In Vitro Cell Dev Biol Anim 2003;39:56-62.

Schwarz S, Koerber L, Elsaesser AF, Goldberg-Bockhorn E, Seitz AM, Dürselen L, et al. Decellularized cartilage matrix as a novel biomatrix for cartilage tissue-engineering applications. Tissue Eng Part A 2012;18:2195-209.

Seddon AM, Curnow P, Booth PJ. Membrane proteins, lipids and detergents: Not just a soap opera. Biochem Biophys Acta 2004;1666:105-117.

Shin YS, Choi JW, Park JK, Kim YS, Yang SS, Min BH, Kim CH. Tissue-engineered tracheal reconstruction using mesenchymal stem cells seeded on a porcine cartilage powder scaffold. Ann Biomed Eng 2015;43:1003-13.

Sittinger M, Reitzel D, Dauner M, et al. Resorbable polyesters in cartilage engineering: affinity and biocompatibility of polymer fiber structures to chondrocytes. J Biomed Mater Res 1996;33:57-63.

Song JJ, Kim SS, Liu Z, Madsen JC, Mathisen DJ, Vacanti JP, Ott HC. Enhanced in vivo function of bioartificial lungs in rats. Ann Thorac Surg 2011;92:998-1005.

Soto-Gutierrez A, Zhang L, Medberry C, Fukumitsu K, Faulk D, Jiang H, et al. A whole organ regenerative medicine approach for liver replacement. Tissue Eng Part C Methods 2011;17:677-86.

Stapleton TW, Ingram J, Katta J, Knight R, Korossis S, Fisher J, Ingham E. Development and characterization of an acellular porcine medial meniscus for use in tissue engineering. Tissue Eng Part A 2008;14:505-18.

Stepanenko AA, Dmitrenko VV. HEK293 in cell biology and cancer research: phenotype, karyotype, tumorigenicity, and stress-induced genome-phenotype evolution. Gene 2015;569:182-90.

Sun WQ, Leung P. Calorimetric study of extracellular tissue matrix degradation and instability after gamma irradiation. Act Biomater 2008;4:817-26.

Sutherland RS, Baskin LS, Hayward SW, Cunha GR. Regeneration of bladder urothelium, smooth muscle, blood vessels and nerves into an acellular tissue matrix. J Urol 1996;156:571-7.

Takahashi K, Yamanaka S. Induction of pluripotent stem cells from mouse embryonic and adult fibroblast cultures by defined factors. Cell 2006;126:663-76.

Tan Q, Steiner R, Hoerstrup SP, Weder W. Tissue-engineered trachea: history, problems and the future. Eur J Cardiothorac Surg 2006;30:782-6.

Tatekawa Y, Kawazoe N Chen GP, Shirasaki Y, Komuro H, Kaneko M. Tracheal defect repair using a PLGA-collagen hybrid scaffold reinforced by a copolymer stent with bFGF-impregnated gelatin hydrogel. Pediatr Surg Int 2010;26:575-80.

ten Hallers EJ, Rakhorst G, Marres HA, Jansen JA, van Kooten TG, Schutte HK, van Loon JP, van der Houwen EB, Verkerke GJ. Animals models for tracheal research. Biomaterials 2004;25:1533-43.

Temenoff JS, Mikos AG. Injectable biodegradable materials for orthopedic tissue engineering. Biomaterials 2000;21:2405-12.

Teng Z, Trabelsi O, Ochoa I, He J, Gillard JH, Doblare M. Anisotropic material behaviours of soft tissues in human trachea: an experimental study. J Biomech 2012;45:1717-23.

Tojo T, Miwaya K, Sawabata N, Kushibe K, Nezu K, Taniguchi S, Kitamura S. Tracheal replacement with cryopreserved tracheal allograft: experiment in dogs. Ann Thorac Surg 1998;66:209-13.

Totonelli G, Maghsoudlou P, Fishman JM, Orlando G, Ansari T, Sibbons P, et al. Esophageal tissue engineering: a new approach for esophageal replacement. World J Gastroenterol 2012;18:6900-7.

Uygun BE, Soto-Gutierrez A, Yagi H, Izamis ML, Guzzardi MA, Shulman C, et al. Organ reengineering through development of transplantable recellularized liver graft using decellularized liver matrix. Nat Med 2010;16:814-20.

Vacanti CA, Cima LG, Ratkowski D, et al. Tissue engineered growth of new cartilage in the shape of a human ear using synthetic polymers seeded with chondrocytes. Mater Res Soc Symp Proc 1992;252:367-73.

Vacanti CA, Paige KT, Kim WS, Sakata J, Upton J, Vacanti JP. Experimental tracheal replacement using tissue-engineered cartilage. J Pediatr Surg 1994;29:201-4.

Vladescu I, Lieleg O, Jang S, Ribbeck K. An adsorption chromatography assay to probe bulk particle transport through hydrogels. J Pharm Sci 2012;101:436-42.

Vunjak-Novakovic G, Martin I, Obradovic B, Treppo S, Grodzinsky AJ, Langer R, Freed LE. Bioreactor cultivation conditions modulate the composition and mechanical properties of tissue-engineered cartilage. J Orthop Res 1999;17:130-8.

Walles T, Giere B, Hofmann M, Schanz J, Hofmann F, Mertsching H, Macchiarini P. Experimental generation of a tissue-engineered fuctional and vascularized trachea. J Thorac Cardiovasc Surg 2004;128:900-6.

Walles T, Giere B, Macchiarini P, Mertsching H. Expansion of chondrocytes in a three-dimensional matrix for tracheal tissue engineering. Ann Thorac Surg 2004;78:444-8.

Wang Z, Du Z, Chan JKY, Teoh SH, Thian ES, Hong M. Direct laser microperforation of bioresponsive surface-patterned films with through-hole arrays for vascular tissue-engineering application. ACS Biomater Sci Eng 2015;1:1239-49.

Wanner A. The role of mucocillary dysfunction in bronchial asthma. Am J Med 1979;67:477-85.

Weidenbecher M, Tucker HM, Awadallah A, Dennis JE. Fabrication of a neotrachea using engineered cartilage. Laryngoscope 2008;118:593-8.

Wong AP, Bear CE, Chin S, Pasceri P, Thompson TO, Huan LJ, et al. Directed differentiation of human pluripotent stem cells into mature airway epithelia expressing functional airway epithelia expressing functional CFTR protein. Nat Biotechnol 2012;30:876-82.

Woods T, Gratzer PF. Effectiveness of three extraction techniques in the development of a decellularized bone-anterior cruciate ligament-bone graft. Biomaterials 2005;26:7339-49.

Wu W, Feng X, Mao T, Feng X, Ouyang HW, Zhao G, Chen F. Engineering of human tracheal tissue with collagen-enforced poly-lactic-glycolic acid non-woven mesh: a preliminary study in nude mice. Br J Oral Maxillofac Surg 2007;45:272-8.

Wurtz A, Hysi I, Kipnis E, Copin MC. Recent advances in circumferential tracheal replacement and transplantation. Am J Transplant 2015; Epub ahead of print.

Yoon JH, Kim KS, Kim SS, Lee JG, Park IY. Secretory differentiation of serially passaged normal human nasal epithelial cells by retinoic acid: expression of mucin and lysozyme. Ann Otol Rhinol Laryngol 2000;109:594-601.

Yu P, Clayman GL, Walsh GL. Long-term outcomes of microsurgical reconstruction for large tracheal defects. Cancer 2011;117:802-8.

Zang M, Zhang Q, Chang EI, Mathur AB, Yu P. Decellularized tracheal matrix scaffold for tissue engineering. Plast Reconstr Surg 2012;130:532-40.

Zhou H, Wu S, Joo JY, Zhu S, Han DW, Lin T, et al. Generation of induced pluripotent stem cells using recombinant proteins. Cell Stem Cell 2009;4:381-4.